ROLE OF THE *Arabidopsis* PEPTIDE TRANSPORTER *AtOPT6* IN HEAVY METAL DETOXIFICATION AND PLANT-PATHOGEN INTERACTION

A Dissertation presented to
the Faculty of the Graduate School
University of Missouri-Columbia

In Partial Fulfillment
of the Requirements for the Degree

Doctor of Philosophy

By

AMI AKSHAY PATEL

Dr. GARY STACEY, Dissertation Supervisor

DECEMBER, 2007

The undersigned, appointed by the dean of the Graduate School, have examined the dissertation entitled:

ROLE OF THE *Arabidopsis* PEPTIDE TRANSPORTER *AtOPT6* IN HEAVY METAL DETOXIFICATION AND PLANT-PATHOGEN INTERACTION

presented by Ami Patel,

a candidate for the degree of doctor of philosophy of Plant Microbiology and Pathology, and hereby certify that, in their opinion, it is worthy of acceptance.

Professor Gary Stacey

Associate Professor Walter Gassmann

Professor John Walker

Professor James Schoelz

Professor Jeanne Mihail

ACKNOWLEDGEMENTS

I would like to thank my major advisor, Dr. Gary Stacey, for his guidance, support and patience during my graduate study. He was a great mentor and has set up an excellent example for me to grow as a scientist. He has always tried to motivate, encourage and challenge me during my research.

I would also like to thank my committee member Dr. Walter Gassmann and ad hoc Dr. Melissa Mitchum for their constant encouragement and valuable advice during my graduate studies. They have selflessly provided me with their valuable time and support without which, I couldn't have achieved accomplishments in my research project. I wouldn't ask for any better collaborators for this research project. I would like to thank my committee members Dr. Jeanne Mihail, Dr. James Schoelz and Dr. John Walker for their valuable advice and encouragement.

I would like to thank Dr. Minviluz Stacey for her help on this project. She taught me valuable techniques in plant biology that has helped me in completion of this research project. I would like to thank Dr. Elizabeth Rogers, who opened up her lab for me to accomplish iron uptake studies in yeast. I would like to thank Sharon Pike for her tireless work on substrate uptake studies for AtOPT6 in *Xenopus*. Her experiments have helped in strengthening characterization of AtOPT6. The collaboration with Dr. David Mendoza and Dr. Julian Schroeder for their ICP-OES work to measure thiols and cadmium content is very much appreciated.

I would like to thank Robert Heinz, Amy Replogle and Dr. Demosthenis Chronis in Dr. Melissa Mitchum's lab for providing nematode eggs, peptides and solutions for the

pathogenesis studies. I would like to thank Dr. Xuecheng Zhang and Dr. Jinrong Wan for their help and advice on bacterial pathogenesis studies. I would like to thank all past and current members of the Stacey lab, especially Brett, Monir, Bill, Kim, Seth, Sandra, Mi-ha, Woo-suk, Andrea, Christine, Sherri and Melanie for their friendship and support. The time spent in Stacey lab will always be remembered with good memories.

Lastly, I would like to thank my family, especially my parents Jash and Sharda Patel, husband Akshay Patel, son Krishang Patel and dear friends who had tremendous faith in me all these years. Their constant and unconditional love, support, belief and encouragement kept me going through hard times and they are the reason I was able to achieve this goal.

TABLE OF CONTENTS

LIST OF TABLES

Page

LIST OF FIGURES

Page

CHAPTER I

CHAPTER II

CHAPTER III

CHAPTER IV

ACADEMIC ABSTRACT

AtOPT6, is a member of oligopeptide transport (*OPT*) gene family. In *Arabidopsis thaliana*, there are nine members in the *OPT* gene family that are thought to be involved in peptide transport. Expression analysis using promoter – GUS transgenic lines showed that AtOPT6 is expressed predominantly in the vascular tissues of vegetative organs including roots, hypocotyl, cotyledons and leaves and in the developing ovules, filament tissues and funiculi in reproductive organs. Spatial and temporal expression of AtOPT6 correlates with transport of peptides in the major sink tissues indicating that this transporter may be involved in long distance transport of peptides to provide organic nitrogen to the developing plant organs.

Over-expression of AtOPT6 leads to cadmium hyper-sensitivity and higher accumulation of cadmium and phytochelatins in root tissues. *opt6* mutant plants exhibited 10-fold less bacterial growth and the leaves showed minimal chlorosis when infected with the bacterial pathogen *Psuedomonas syringae pv. tomato* DC3000 (*Pst* DC3000) as compared with wild-type control plants. This difference in bacterial population was abolished when *opt6* mutant plants were infected with a *Pst* DC3000 strain lacking coronatine biosynthesis. Therefore, AtOPT6 might be involved in the transport of coronatine, a phytotoxin that causes chlorosis in the infected tissue. In addition, the *opt6* mutant plants also showed less susceptibility when infected with both cyst (*Heterodera glycines*) and root-knot (*Melidogyne incognita*) nematode. AtOPT6 mediated transport of various Arabidopsis CLAVATA3/ENDOSPERM SURROUNDING REGION-like (CLE-like) and nematode secreted peptides when expressed in *Xenopus*. Nematode

secreted peptides mimic plant CLEs to induce differentiation of root cells to form the feeding site and assist nematodes in obtaining nutrients for growth and proliferation in infected root tissues. Expression of AtOPT6 increased during the early stages of both cyst and root-knot nematode infection in and around the developing feeding sites. Collectively, these data suggest two possible functions for AtOPT6 during nematode parasitism: AtOPT6 may transport nutrients in the form of peptides into the feeding site developed by the nematodes or AtOPT6 transports plant CLEs or nematode secreted peptides into the infected root cells and these peptides induce root differentiation to form the feeding site.

INTRODUCTION

Plants, immobile and unable to pursue nutrients for sustenance, make use of resident transporters for uptake and distribution of nutrients, vital metals and minerals. Transporters of nutrients, minerals and metals are specific in nature. There are more than one thousand transport proteins in *Arabidopsis* involved in transport of sugars, amino acids, peptides, minerals, metals and other important components required for normal growth and development of plant organs.

PEPTIDE TRANSPORT:

Sequencing of the *Arabidopsis* genome revealed more than 80 families of transport proteins comprising more than 1000 genes, which represent roughly 0.33% of the total genome. These gene families are involved in transport of a large variety of substrates in plants from source to sink tissues (Busch and Saier, 2002). The larger number of transport proteins in plants compared to other organisms may be attributed to the fact that plants have to obtain nutrients and escape from biotic and abiotic stress while remaining stationary. Transport proteins help plants to achieve this goal. Among the diverse nutrients, nitrogen is one of the most crucial elements required by plants. Nitrogen is transported in plants mainly in the form of nitrate or ammonia (Miller et al., 2007) from the soil. Moreover, in plants, reallocation and controlled distribution of organic nitrogen stored in the form of protein reserves is essential during developmental processes such as seed germination, leaf senescence and the formation of reproductive organs (Rentsch et al., 2007). Nitrate transporters are thought to play a role during both

uptake of nitrogen in soil and in distribution of nitrogen during plant development (Tsay et al., 1993; Orsel et al., 2002). Two gene families in *Arabidopsis* were identified that encode transporters responsible for nitrate uptake and distribution within the plant: the peptide transport family (*PTR*; also known at *NTR1*) and (nitrate transport family (*NRT2*) (Tsay et al., 1993; Steiner et al., 1994; Song et al., 1996; Orsel et al., 2002).

Another mechanism by which organic nitrogen is distributed within the plants is by transport of peptides. Peptide transport is a well-studied physiological process in bacteria, fungi, plants and animals. Peptide transporters function in translocating small peptides across the plasma membrane in an energy-dependent manner. In lower eukaryotes, internalized peptides serve primarily as a source of amino acids for protein synthesis or as a nitrogen source (Steiner et al., 1995). In higher eukaryotes, peptide transport is observed during early stages of seed germination and other processes where nitrogen demand is high in the developing tissues (West et al., 1998; Lee and Tageder 2004). Peptide transporters were also found to play roles in cellular processes such as cell wall recycling, quorum sensing and sporulation in bacteria and yeast (Perry et al., 1994; Sato et al., 1994). Recent studies suggested that peptide transporters also play an important role during biotic and abiotic stress (Karim et al., 2005). The three main transporter families discussed below mediate peptide transport in plants.

The ABC family:

Peptide transporters have been classified into different groups based upon their energetic requirements and substrate specificity. In general, the relationship between the transporter and its substrate is very specific. The *ABC* (ATP Binding Cassette) transporter

super family uses energy derived from ATP hydrolysis to translocate substrates across the membrane. Transported substrates include a broad range of compounds such as ions, macromolecules and lipids (Schmitt and Tampe, 2002). ABC transporters are common and well studied in both eukaryotes and prokaryotes. In *Arabidopsis thaliana*, 129 ORFs are predicted to encode transporter proteins belonging to the ABC super family. The ABC super family comprises 13 % of the total number of transporter proteins in Arabidopsis (www.membranetransporter.org, Sanchez et al., 2001). ABC proteins contain one or two ATP-binding cassettes, also termed nucleotide binding folds (NBFs), which share 30-40% identity between family members (Higgins et al., 1992). Each NBFs covers approximately 200 amino acid residues and contains two Walker motifs; where Walker A box and Walker B box are separated by 120 amino acid residues and an ABC signature motif is situated between the two Walker boxes (Sanchez-Fernandez et al., 2001). Walker motifs are known to be nucleotide binding sites. In addition to NBFs, ABC transporters possess two to three hydrophobic integral membrane domains (TMDs) with four to six putative transmembrane α-helices. The NBFs catalyze ATP hydrolysis whereas the TMDs are thought to form the pathway for solute transport across the phospholipid membrane bilayer and contribute to substrate selectivity and specificity. Unlike NBFs, TMDs exhibit no sequence similarity except in the hydrophobic region (Sanchez-Fernandez et al., 2001, Higgins et al., 1992).

The size of ABC proteins range from 250 – 1800 amino acid residues in *Arabidopsis*. Members of the ABC super-family may be divided into 12 subfamilies based on protein size, domain organization and orientation. Of these 12 subfamilies, the prominent sub-families include multidrug resistance proteins (MRPs), multidrug

transport proteins (MDRs), peroxisomal membrane proteins (PMPs), mitochondrial membrane proteins (ATMs) and pleiotropic drug resistance (PDRs) proteins (Sanchez-Fernandez et al., 2001). The first ABC transport gene cloned was *AtMDR1*, a plasma membrane localized protein, involved in light-dependent hypocotyl elongation (Sidler et al., 1998). However, its mode of action in plants remains unclear. *AtMRPs* have orthologs in humans and all MRPs are glutathione S-conjugate (GS-X) pumps that transport a broad range of compounds through conjugation with glutathione (Rea, 1999). The first evidence for the presence of ABC-MRPs in plants was the observation that glutathione-conjugated compounds were transported into vacuoles in an ATP-dependent manner (Martinoia et al., 2002), suggesting that these transporters are an integral part of the plant detoxification mechanism. Since then, five *MRPs* were cloned out of 15 putative *MRPs* from *Arabidopsis* and they encode GS-X pumps with different substrate selectivity and transport capabilities (Rea et al., 1998; Tommasini et al., 1998). Glutathione is a tri-peptide, thought to provide a source of sulphur and peptides during seed development (Cairns et al., 2006). *AtATM3*, a protein localized to the mitochondrial membrane, is the closest homolog to yeast *ATM*. It is ubiquitously expressed in plants and involved in heavy metal tolerance (Kim et al., 2006, Chen et al., 2007). Two other *ATM* members of *Arabidopsis* were localized to the mitochondrial membrane and have a different functional role than *AtATM3*. *AtATM3* was implicated to play a role in the export of mitochondrially synthesized iron/sulphur clusters (Chen et al., 2007). Members of the PDR sub-family, *AtPDR8* and *AtPDR12*, are involved in the transport of heavy metals such as cadmium and lead and function in heavy metal resistance in plants (Lee et al., 2005; Kim et al., 2007). Recent investigations revealed that plant ABC transporters are

not only implicated in detoxification but also in guard cell regulation, chlorophyll biosynthesis and ion fluxes (Gaedeke et al, 2001, Klein et al., 2003 and Martinoia et al., 2002).

While most of the ABC transport proteins are involved in metal detoxification and other cellular mechanisms, some are hypothesized to play a role in providing nutrition in the form of peptides. The transporter associated with the antigen processing (*TAP*) subfamily of ABC transporters in *Arabidopsis* was identified based on sequence similarity to the animal *TAP* gene family (Sanchez-Fernandez et al., 2001). The role of TAP proteins in animals is to transport peptide degradation products into the lumen of the endoplasmic reticulum, which indicates that the function of peptide transport may be extended in the *Arabidopsis TAP* members (Reits et al., 2000). However, experimental evidence is lacking with regard to the function of *TAP* members in plants.

The *PTR* family

The *PTR* (Peptide Transporter) or alternatively *POT* (Proton-coupled Oligopeptide Transporters) family uses the proton motive force to translocate peptides that are two to three amino acids in length (Chiang et al., 2004). These transporters are found in bacteria, archaea, plants and animals. PTR proteins contain twelve putative transmembrane (TM) domains and are 450-600 amino acid residues in length in bacteria and 600-750 amino acid residues in length in eukaryotes (Steiner et al., 1995, Hauser et al., 2001). There is a hydrophilic loop between transmembrane domains 6 and 7; the function of which is still unclear (Tsay et al., 2007). Members of the *PTR* gene family function as proton symporters, but the substrate:H+ stoichiometry is variable and

depends upon the peptide charge (Chiang et al., 2004). The generalized transport stoichiometry is as follows: substrate (out) + nH^+ (out) → substrate (in) + nH^+ (in) (http://www.tcdb.org/tcdb/). PTR proteins possess a unique signature motif FING (Steiner et al., 1995), and two other conserved motifs (Hauser et al., 2001). The FING motif is required for peptide transport. A mutation at amino acid 167 in *hPepT1* (human PTR type peptide transporter) resulted in the loss of protein activity (Yeung et al., 1998).

Members of the *PTR* family were shown to transport a wide range of nitrogen-containing substrates including amino acids, peptides and nitrate (Tsay et al., 1993; Frommer et al., 1994; Stacey et al., 2002; Chiang et al., 2004). The *PTR* gene family in *Arabidopsis* consists of 53 genes, while rice (*Oryza sativa*) has more than 80 putative *PTR* members (Tsay et al., 2007). Most of the characterized PTR proteins transport di-peptides. The first *PTR* gene isolated from *Arabidopsis* was defined through study of chlorate resistant mutant 1 (*CHL1*). This gene is also known as *AtNRT1.1* (Tsay et al., 1993). Chlorate is a homolog of nitrate and is transported into plants *via* the nitrate uptake system and then it is converted into chlorite, which is toxic to plants. Mutants defective in nitrate uptake showed resistance to chlorate treatment. A nitrate uptake mutant, *chl1* was isolated by screening plants for chlorate resistance and the *CHL1* gene was subsequently isolated using this *T-DNA* tagged mutant. Transport studies in *Xenopus laevis* oocytes indicated that CHL1 is a proton-coupled nitrate transporter (Tsay et al., 1993). Another *PTR* protein, *NTR1,* was shown to transport histidine in addition to peptides (Frommer et al., 1994). However, histidine uptake assays by *AtPTR2-B*, which is identical to *NTR1*, showed that there was no difference in the growth of yeast cells (a histidine auxotroph requiring the peptide histidine for growth) expressing or lacking the

AtPTR2-B gene. The data suggest that *AtPTR2-B* (*NTR1*) is not an amino acid transporter (Song et al., 1996). *AtPTR2B* (now referred to as *AtPTR2*) was expressed in germinating seedlings, roots, leaves, stem and floral organs. Antisense expression of *AtPTR2* cDNA in *Arabidopsis* resulted in an enlargement of rosette leaves, delay in flowering, and a partial degree of abortion in developing seeds (Song et al., 1997). *AtPTR2* was localized to the embryo around the heart stage during seed development, correlating with the seed abortion phenotype (Rentsch et al., 1995). Functional characterization of *AtPTR2* and another fungal *PTR2* in *Xenopus* revealed that these peptide transporters did not exhibit any nitrate transport activity (Chiang et al., 2004). Moreover, both *AtPTR2* and *fPTR2* showed transport of di- and tri-peptides but not tetra-peptides. Both transporters showed high affinity towards di- and tri-peptides with neutral and positively charged amino acids. However, they differed in transport containing negatively charged peptides. Negatively charged di-peptides evoked larger currents in *AtPTR2*-injected oocytes but smaller currents in *fPTR2*-injected oocytes (Chiang et al. 2004).

So far, the best characterized peptide transporter is *HvPTR1*. Expression of *HvPTR1* is highly specific to the scutellum of germinating barley grain and is not expressed in the roots or leaves of mature plants. The temporal and spatial expression pattern correlates with a peptide transport mechanism during barley germination (West et al., 1998; Higgins and Payne, 1977). *HvPTR1* was cloned based on sequence similarity with *AtPTR2* and *PEPT1*, and it mediates transport of di-peptides in *Xenopus* (Waterworth et al., 2000). It is localized to the plasma membrane of scutellar epithelial cells only during germination and is phosphorylated in response to a high levels of amino acids present in germinating barely (Waterworth et al., 2000; Waterworth et al., 2005).

The phosphorylation of *HvPTR1* in response to rising levels of amino acids reflect post transcriptional regulation of this protein and suggest a balance in flux of organic nitrogen in the endosperm during germination mediated by transport protein activity (Waterworth et al., 2005).

The general function of PTR family members is thought to be transport of di- and tri-peptides and provision of nitrogen and amino acids to sink tissues during plant growth and development (Stacey et al., 2002; Chiang et al., 2004). However, recent studies indicate that some members of the *PTR* family also contribute to biotic and abiotic stress tolerance in plants and are implicated to play a role during plant defense (Dietrich et al., 2004 and Karim et al., 2007). For example, AtPTR2 was shown to transport phaseolotoxin when expressed in yeast (Dietrich et al., 2004). However, the speficic role of *AtPTR2* during bacterial pathogenesis remains to be determined. *AtPTR3*, another member of the *PTR* family, was shown to be induced when exposed to higher salt concentrations and *Atptr3* mutant seedlings were unable to grow on high salt concentrations (Karim et al., 2005). In addition, *Atptr3* mutants were also more susceptible to bacterial pathogens *Pseudomonas syringae* pv. *syringae* and *Erwinia corotivora* species (Karim et al., 2007) suggesting a role of *AtPTR3* during abiotic stress and in plant defense.

The OPT family:

The *OPT* super-family (Oligo-Peptide Transporters) of peptide transporters use proton coupling to drive transport (Osawa et al., 2006). Members vary in the length of substrates transported, ranging from peptides that are three to thirteen amino acids in

length (Osawa et al., 2006; Reuss and Morschhauser, 2006; Sharon Pike, personal communication). The *OPT* family is found in bacteria, fungi and plants but not in animals (Lubkowitz et al., 1997; Stacey et al., 2002; Weinberg and Maier, 2007). Hydropathy plots reveal that the OPT proteins contain 12-14 putative transmembrane domains (Stacey et al., 2002). The first identified OPT member was the yeast *CaOpt1p* in *Candida albicans* (Lubkowitz et al., 1997), followed by *Isp4* in *S. pombe* (Sato et al., 1994; Lubkowitz et al., 1998) and *ScOPT1*, ORF YPR194c and ORF YGL114w in *S. cerevisiae* (Lubkowitz et al., 1998; Hauser et al., 2001). Heterologous studies of *CaOpt1p* expressed in *S. cerevisiae* demonstrated that it transports tetra- and penta-peptides and, to a lesser extent, tri-peptides. Transcription is regulated by nitrogen (Lubkowitz et al., 1997). The *OPT1* gene of *S. cerevisiae* (ORF YJL212c), also known as *Hgt1p*, was shown to transport the endogenous opioids, Met-enkephalin (YGGFM) and Leu-enkephalin (YGGFL) into yeast cells when expressed under the control of a constitutive promoter (ADH) in a high copy number vector (Hauser et al., 2000). The *Hgt1p* (*ScOPT1*) protein also mediates specific uptake of reduced and oxidized glutathione (GSH and GSSG, respectively) in yeast. This uptake is not affected by an excess of L-amino acids or by various di- and tri-peptides and the Δ *hgt1* mutant also accumulates amino acids such as proline at a normal rate (Bourbouloux et al., 2000). The *S. pombe Isp4p* gene, a close homologue of *Hgt1p* (38% identity and 57% similarity), is induced during sporulation and transports tetra- and penta-peptides (Sato et al., 1994, Bourbouloux et al., 2000).

Members of the *OPT* gene family from *Arabidopsis* were identified based on sequence similarity with the yeast *OPT* (*CaOPT1p*) (Koh et al., 2002). The *OPT* super-family in *Arabidopsis* comprises 17 genes that can be divided in two sub-clades based on

sequence similarity and putative function (Koh et al., 2002; Yen et al., 2001;http://www.cbs.umn.edu/arabidopsis). The oligo-peptide transporter sub-clade consists of nine *OPT* members that are likely involved in transport of tetra- and penta-peptides (Koh et al., 2002). Hereafter, we refer to this sub-clade as the *OPT* gene family, to distinguish it from the *OPT* super-family. The yellow stripe-like (*YSL*) gene sub-clade contains eight *OPT* members that appear to function in the transport of chelated transition metals, such as iron and copper (Curie et al., 2001). Hereafter, we refer to this sub-clade as the *YSL* gene family. The plant *OPT* family is relatively small when compared to the ABC super-family and the *PTR* family. Sequence comparison of nine *AtOPTs* revealed a highly conserved NPG motif (NPG[P/A]F[N/T/S]XKEH[V/T/A][L/I/V][I/V]I[T/S/V][I/V/M] [F/M][A/S][N/S/A]) with an invariant glutamic acid residue and a KIPPR motif (K[L/F][G/A][H/M/T]YMK[I/V/L][P/D/S] PR) (Koh et al., 2002). Transport uptake studies in heterologous systems of yeast and *Xenopus* suggested that plant *OPTs* can mediate transport of tetra- and penta-peptides, indicating that these OPTs are functional peptide transporters (Koh et al., 2002; Osawa et al., 2006). Expression analysis using RT-PCR and promoter – GUS constructs revealed that AtOPTs are preferentially expressed in the vascular tissues of root, leaves, flower and seeds (Koh et al., 2002; Stacey et al., 2006). The characterization of *AtOPTs* is described in detail in Chapter I.

Besides the *Arabidopsis OPTs*, *OPTs* from other plant sources have also been characterized. *BjGT1* was isolated from *Brassica juncea* based on sequence similarity to *AtOPT3* and *ScHGT1* (Bogs et al., 2003). Heterologous expression of *BjGT1* in yeast mutants deficient in glutathione transport could complement and rescue the yeast growth

when supplied with GSH as the only source of sulfur, suggesting *BjGT1* could mediate transport of glutathione in yeast (Bogs et al., 2003). Another *OPT* homologs, *OsGT1* from *Oryza sativa*, also conveyed transport of glutathione and its conjugates when expressed in yeast (Zhang et al., 2004).

The evidence that various yeast and plant *OPTs* are regulated by nitrogen and are involved in uptake of tetra- and penta-peptides, enkephalin and glutathione suggests that *OPTs* play an important role not only in nutrient transport but also during other cellular processes.

THE FUNCTION OF PEPTIDE TRANSPORTERS DURING PLANT GROWTH AND DEVELOPMENT

Peptide transporters play significant roles during plant development. Reallocation of nitrogen is essential during seed germination, leaf senescence and seed loading and is aided by peptide transporters (West et al., 1998, Miranda et al., 2003). The first evidence of active peptide transport in plants was shown in barley embryos (Higgins and Payne 1977a; Higgins and Payne 1977b). Later, it was observed that transport of peptides was faster than that of amino acids during seed germination in barley (Higgins and Payne, 1978). Transport of peptides is more efficient than transport of amino acids in terms of nitrogen transporter per energy used. During pollen development, seed germination, and accumulation of storage proteins in seeds, when nitrogen is required in greater amounts, peptide transporters are able to transport nitrogen and carbon more efficiently than amino acid transporters. During seed germination, protein storage reserves are partially hydrolyzed into smaller peptides. These peptides are then transported into the developing

embryo where they are completely hydrolyzed and serve as a source of carbon and nitrogen. One of the best characterized peptide transporters is *HvPTR1,* which is expressed in the scutellum of germinating barley (West et al., 1998). The temporal and spatial pattern of *HvPTR1* expression suggests that it plays a role in transport of peptides in the germinating barley grain. Expression analysis of *AtOPT* gene family members, based on studies of promoter – GUS fusions, also indicates that they are involved in transport of peptides during seed germination and seedling development (Stacey et al., 2006). Thus, several lines of evidence indicate that peptide transport provides a significant source of organic nitrogen during germination and growth processes associated with the early stages of seedling development. In plants, about 8,000 different peptides are produced as a result of protein degradation (Dietrich et al., 2004). The possible substrates for peptide transporters can vary broadly, ranging from several hundred hydrolyzed peptides to signaling molecules. These peptides are produced by protein degradation or synthetic biosynthesis and are found to be present during plant development.

Stacey et al. (2002) showed that *AtOPT3* is required for proper embryo development. An *AtOPT3* T-DNA insertional knock-out mutant line (T-DNA insertion was in exon 4; referred to as the *Atopt3-1* mutant) showed an arrest in embryo development at the eight-cell stage. An *AtOPT3* promoter::GUS fusion showed expression in maternal tissue during embryo development. *AtOPT3* promoter::GUS fusions also showed *AtOPT3* expression in vascular tissues of root, stem and leaf (Stacey et al., 2002). Yeast complementation experiments in a rich nutrient medium showed that *AtOPT3* can rescue a yeast mutant deficient in metal transporters and was possibly

involved in copper, manganese and iron transport (Wintz et al., 2003). A two-three fold increase in GUS activity was observed in roots and shoots when *AtOPT3* promoter::GUS plants were grown under iron starvation (Stacey et al., 2006), suggesting a role for *AtOPT3* in iron transport. A second T-DNA knock-out insertion mutant with an insertion in the 5` UTR region of *AtOPT3* (referred as the *Atopt3-2* mutant) resulted in shorter plants compared with the wild-type control. *Atopt-2* showed significantly lower expression of *AtOPT3* transcripts. Also, the *Atopt3-2* mutant had much lower iron content and higher Cu, Zn and Mn content compared with wild-type control plants (Stacey et al., 2007). Cross-sections of *Atopt3-1* leaves showed defects in the chloroplast development. This likely explains the embryo lethal phenotype since other mutants that affect plastid development are also embryo lethal (Yu et al., 2004; Stacey et al., 2007 – In press). The iron distribution in roots and shoots of the *Atopt3-2* mutant was very different from that of the wild-type plants. Iron distribution was mainly in the vascular tissue in the *Atopt3-2* mutant; whereas it was distributed throughout the roots in wild-type plants (Stacey et al., 2007). The difference in iron distribution between the mutant and wild-type plants is indicative of disruption in iron mobilization in *Atopt3-2* mutant plants. Thus, all of the above data suggest that *AtOPT3* could play an important role in long distance transport of iron.

THE FUNCTION OF TRANSPORTERS IN HEAVY METAL DETOXIFICATION

Plants, being rooted in soil, are unable to escape toxicity resulting from the presence of heavy metals in the soil. During the acquisition of essential transition metals such as iron, zinc, copper, and manganese from soil, plants inevitably take up heavy metals such as cadmium, mercury and lead. Moreover, accumulated transition metals can also be harmful to plants. Plants have developed homeostatic mechanisms to ensure proper concentrations of transition metals and to minimize the damage from exposure to toxic heavy metals. This homeostatis requires a regulated network of transport, mobilization and sequestration processes to maintain uptake, distribution and detoxification of metal ions. There are two known mechanisms that plants utilize to remove excess metal ions from the cytoplasm; efflux into the apoplastic space and compartmentalization (Kim et al., 2006). The main storage compartment for toxic metals is the vacuole in plant cells. The known proteins that mediate transport and detoxification of heavy metals in plants belong to the following families: the cation diffusion facilitator (*CDF*) family (Blaudez et al., 2003), the heavy metal transporting P_{1B} -ATPases (*HMA*) family (Hammond et al., 2006), the natural resistance associated macrophage protein (*NRAMP*) family (Weber et al., 2004) and the *ABC* family (Lee et al., 2005).

Transporters of the *CDF* family mediate cytoplasmic efflux of metals such as zinc, cobalt, cadmium and nickel and have been termed metal tolerance proteins (*MTP*) (Becher et al., 2004; van de Mortal et al., 2006; Talke et al., 2006). Three genes of the *CDF* family: *MTP1*, *MTP8* and *MTP11* are highly expressed in *Arabidopsis halleri* and *Thlaspi caerulescens*, and are accumulators of heavy metals. *MTP1* most likely transports

zinc as it was identified in a screen for proteins that were able to complement a Zn-sensitive yeast mutant and was shown to contribute to basal zinc tolerance and accumulation in leaves (Drager et al., 2004). *MTP8* and *MTP11* are close homologs to *Stylosanthes hamata MTP8* (*ShMTP8*), which conferred manganese tolerance when expressed in yeast and *Arabidopsis* (Delhaize et al., 2003). *MTP8* was also shown to be up-regulated in response to cadmium and copper exposure in roots and shoots in *A. halleri* (Talke et al., 2006; van de Mortel et al., 2006). Higher transcript levels of these genes during heavy metal exposure suggest a role in adjustment of metal homeostasis in the hyper-accumulator plants.

The *HMA* family members are involved in pumping cations across the membranes and out of the cytoplasm using hydrolyzed ATP as an energy source. Two genes, *HMA3* and *HMA4* contribute to partial zinc tolerance in a zinc sensitive yeast mutant and are highly expressed in hyper-accumulator plants *A. halleri* and *T. caerulescens* (Becher et al., 2004; Talke et al., 2006; van de Mortel et al., 2006). *HMA4* was also shown to mediate efflux of cadmium from yeast cells (Talke et al., 2004). In both hyper-accumulator species, *HMA4* was expressed 2-3 fold higher in roots than in shoots and its transcript levels showed increases in response to elevated cadmium concentrations and zinc deficiency (Bernard et al., 2004; Papoyan and Kochian, 2004). In *A. thaliana*, *HMA2* and *HMA4* were suggested to play roles in root-to-shoot mobilization of zinc *via* xylem loading and are thought to be plasma-membrane localized. Moreover, over-expression of *HMA4* confered cadmium tolerance in *Arabidopsis* (Verret et al., 2004). It may be possible that *HMA4* causes cadmium hyper-accumulation and contributes to cadmium

tolerance by mediating cytoplasmic cadmium efflux in root and leaf cells (Verret et al., 2004).

The *NRAMP* gene family also plays a role in metal homeostatis. *NRAMP3*, for example, is highly expressed in roots and shoots, and is implicated in iron homeostasis. Heterologous expression of *NRAMP1*, *NRAMP3* and *NRAMP4* in yeast can mediate iron, manganese and cadmium uptake (Curie et al., 2000). An *A. thaliana nramp3-1* mutant was shown to accumulate manganese and zinc in roots under iron deficiency (Thomine et al., 2003). However, a direct role of the NRAMP transporters in cadmium hyper-accumulation or tolerance has not been demonstrated.

AtPDR12, a member of the pleiotrophic drug resistance (PDR) sub-family of the *ABC* transporter super-family, is a plasma-membrane localized protein shown to confer lead resistance in *Arabidopsis*. *Atpdr12* mutant plants showed higher lead content and plants over-expressing *AtPDR12* showed lower lead content and were more resistant as compared to wild type plants, suggesting a function as an efflux pump to exclude lead or lead containing toxic compounds from the cytoplasm (Lee et al., 2005). In yeast, *HMT1* is involved in vacuolar sequestration of cadmium (Cd). The *HMT1* gene encodes an ABC membrane transport protein (Ortiz et al., 1995). *hmt1* is a cadmium-sensitive mutant, and unable to form GSH-Cd complexes upon exposure to cadmium. The HMT1 protein is localized in the vacuolar membrane where it mediates MgATP-energized transport. *YCF1* is another ABC-type vacuolar transporter in yeast, which was shown to confer tolerance to cadmium by vacuolar sequestration of a GSH-Cd complex (Li et al., 1997).

AtOPT6, another member of the *OPT* gene family, was able to mediate uptake of both reduced (GSH) and oxidized (GSSG) forms of glutathione in yeast strains deficient

in the endogenous glutathione transporter (*HGT1*; also called *ScOPT1*) (Cagnac et al., 2004). The authors also reported that *AtOPT6* expression was induced in the presence of herbicide, primisulfuron (Cagnac et al., 2004). Uptake studies in *Xenopus laevis* oocytes indicated that *AtOPT6* was able to transport GSH supporting earlier data (Sharon Pike – personnal communication). Identification and characterization of transporters in metal homeostasis has shed light on possible entry pathways into the plant and the mechanism of metal tolerance for toxic metals such as cadmium and lead. Heavy metal treatment of plants induces the transcription of many genes (Weber et al., 2004). However, the mechanism by which the heavy metal is sensed and the downstream signaling pathways leading to gene induction have yet to be elucidated. Heavy metal detoxification mechanisms are also mediated by phytochelatin (PC), which can bind heavy metals. The role of *AtOPT6* in heavy metal detoxification is discussed in detail in Chapter II.

THE FUNCTION OF TRANSPORTERS DURING PLANT DEFENSE

Plants are sessile organisms and cannot escape when attacked and are continuously threatened by potential pathogens. Unlike animals, plants do not possess an adaptive immune system. Instead, plants have developed a number of defense mechanisms that facilitate defense against pathogens. They make use of pre-existing physical and chemical barriers, as well as inducible defense mechanisms that become activated upon attack. The primary line of defense is composed of pre-existing physical and chemical barriers preventing pathogen entry. Physical barriers such as the plant cuticle may inhibit fungal infection by reducing spore germination or hyphal penetration (Jarosz et al., 1982). Chemical barriers such as secretion of cell wall phenolics,

phytoalexin production (Kauss et al., 1992), and elicitation of an oxidative burst (Kauss and Jeblick 1995) provide an initial level of defense (Mur et al., 1996). In addition to preexisting barriers, plants can mount a systemic response, which establishes an enhanced defensive capacity in tissues adjacent to and distant from the site of primary attack. There are active plant defense mechanisms that enable systemic responses. During basal plant defense, plants use salicyclic acid (SA) and jasmonic acid (JA) / ethylene-induced signaling pathways that restrict the invasion and subsequent growth of a pathogen (Metraux et al., 1990; Doares et al., 1995). Basal plant defense also involve recognition of effector proteins released by the invading pathogen by specific resistance genes (R) encoded in plants. This mechanism is termed gene-for-gene resistance, since resistance requires the presence of an avirulence gene (encoding the effector protein) in the pathogen and the corresponding resistance gene in the host plant (Flor 1971).

Several transport proteins play a role during plant defense. Upon entry into the plant, pathogens modify host cellular mechanisms promoting virulence and facilitating their own proliferation within various plant tissues. In order to propagate within plant tissues, pathogens need transporters to send signals to modify plant development and obtain nutrients to support their growth. Several proteins transporting sugars, amino acids and peptides are induced upon and during pathogen attack and, therefore, are implicated to play a role in the host-pathogen interaction (Meyer et al., 2004, Hammes et al., 2006, Karim et al., 2005 and Campbell et al., 2003). *AtPTR1*, a plasma-membrane localized di- and tri-peptide transporter, also mediates transport of phaseolotoxin when expressed in yeast (Dietrich et al., 2004). Phaseolotoxin is a bacterial phytotoxin produced by *Pseudomonas syringae pv phaseolicola*, which causes halo blight on legumes and

bacterial canker on kiwifruit (Bender et al., 1999). However, *Atptr1* mutants have not been characterized and the relation between phaseolotoxin transport and the function of AtPTR1 during pathogenesis is unclear. Penetration 3 (*PEN3*), an ABC transporter protein, was suggested to play a role in exporting toxic material to attempted invasion sites by biotrophic fungal pathogens (Stein et al., 2006). *pen3* mutants were highly susceptible to biotrophic and necrotrophic fungal pathogens and Pen3 was localized to the plasma-membrane (Stein et al., 2006). A full discussion of the role of transporters in plant defense can be found in Chapter III and Chapter IV.

CHAPTER I: EXPRESSION ANALYSIS OF THE *AtOPT* GENE FAMILY IN *ARABIDOPSIS*

INTRODUCTION

The OPT gene family in *Arabidopsis* is composed of nine members (*AtOPT1-AtOPT9*) that are thought to play a role in nitrogen transport to sink tissues during vegetative growth, seed germination, pollen and ovule development, and seed formation. There is also evidence supporting a role of *AtOPT3* in mobilization of iron during plant development (Stacey et al., 2006; Stacey et al., 2007). A total of nine Arabidopsis *OPT* orthologs were identified based on sequence similarity (49% - 53%) to the yeast OPT, *CaOPT1p* (Koh et al., 2002). Within the family, OPTs share 61% to 85% sequence similarity. Moreover, there is no significant sequence similarity of these OPTs with either ABC or PTR transporters. The size of OPT proteins ranges between 737 – 767 amino acids and hydropathy plots suggest 12 – 15 putative transmembrane domains (Koh et al., 2002,; www.rarge.gsc.riken.jp). Heterologous expression of *AtOPTs* in yeast showed that *AtOPT1, 4, 5, 6* and *7* were able to transport a penta-peptide (KLLLG) and *AtOPT4* was able to transport additional tetra-peptides KLGL and KLLG (but not di- and tri-peptides), suggesting that *AtOPTs* are functional peptide transporters and *AtOPT4* demonstrates a less stringent substrate specificity (Koh et al. 2002).

A detailed electrophysiological study of *AtOPT4* was carried out in *Xenopus laevis* oocytes by cloning *AtOPT4* behind the 5` UTR of *ScOPT1* to improve expression efficiency (Osawa et al., 2006). Studies using KLGL as a substrate, indicated that *AtOPT4* is a proton-coupled transporter with high affinity for the tetra-peptide substrate (Km=15μM) (Osawa et al., 2006). Expression analysis of AtOPTs during plant growth and development was carried out using *AtOPT* promoter – GUS constructs to observe the role of *AtOPTs* during germination, seedling development, vegetative growth and flower and seed development. Preferential expression of all *AtOPTs* (*AtOPT1*, *AtOPT3*, *AtOPT4*, *AtOPT6*, *AtOPT7* and *AtOPT8*) was observed during early stages of plant growth with all OPTs expressed in vascular tissues (Stacey et al., 2006). The expression analysis conducted using promoter – GUS constructs also correlated with the RT-PCR expression profile of the *AtOPTs* carried out earlier by Koh et al. (2002). During germination, higher expression levels were observed for *AtOPT3*, *AtOPT6* and *AtOPT7* in the cotyledons and hypocotyl tissues, whereas other OPTs showed weaker expression levels in those tissues. During seedling growth, the expression of all OPTs was limited to developing vascular tissues of roots, cotyledons and true leaves with varied degrees of expression among the OPTs. No GUS activity was detected in the root epidermis, root hairs or root tips of any of the OPTs indicating that OPTs do not play any role in acquisition of nutrients from soil or other medium. The expression pattern differed during the reproductive stage of development among all the OPTs with AtOPT1 expressed in sepals, anthers, pollen grains and pollen tubes; *AtOPT3* in anthers, pollen grains and the developing embryo; *AtOPT4* with weaker expression in sepals; *AtOPT7* was expressed in pollen grains and *AtOPT8* was expressed in anthers, pollen grains and during early stages of seed

development (Stacey et al., 2006). *AtOPT1* was the only member that showed expression in the pollen tube. These data were strengthened by performing reciprocal crosses between wild-type control plants and transgenic plants expressing the *AtOPT1* promoter – GUS construct (Stacey et al., 2006). *AtOPT8* was expressed in the integument and endosperm tissues of the embryo immediately after embryo development (Stacey et al., 2006). Thus, the differential expression patterns of *OPTs* during flower and seed development suggest a possible role for *OPTs* in flower development, pollen tube growth and seed development. However, single knock-out mutant lines of specific *AtOPTs* do not exhibit any visible phenotype likely reflecting functional redundancy among different members of the family. One exception is *Atopt3* mutant lines, which are embryo lethal (Stacey et al., 2002a). In this Chapter, I will discuss in detail the expression analysis of *AtOPT6* and *AtOPT9*, comparing these results to the published expression patterns of *AtOPT7* and *AtOPT8* (Stacey et al., 2006).

METHODS AND MATERIALS

Bacterial Strains and Plasmids

Bacterial strains and plasmids are listed in Table 1. When necessary, the construction of various strains and plasmids is described in the text.

Bacterial Culture Medium and Growth Conditions

All strains of *Escherichia coli* were grown and maintained on LB medium; pH- 7.0 at 37 °C (Sambrook et al., 1989). Transformed *Escherichia coli* strains were routinely maintained on LB medium supplemented with appropriate antibiotics or streaked from frozen stock prepared for a particular strain as indicated in the text.

Plasmid DNA Isolation

Plasmid DNA was isolated from *E. coli* using the standard alkaline lysis method (Sambrook, et al, 1989) or using a QIAprep Spin Miniprep Kit (Qiagen, Valencia, CA) according to the manufacturer's instructions. DNA concentration was determined using a ND-1000 spectrophotometer (NanoDrop, Wilmington, DE).

Enzymes and DNA Primers

Restriction enzymes used in this study were purchased from Promega (Madison, WI) and New England Biolabs (Ipswich, MA), whereas enzymes used in various other molecular biology techniques were used as specified in the text. DNA primers used in this study

were ordered from Integrated DNA Technologies (IDT, Coralville, IA) or Sigma Genosys (Sigma, St. Louis, MO).

Cloning Plant Constructs

AtOPT promoter sequences were PCR amplified from *Arabidopsis thaliana* ecotype Col-O genomic DNA using Turbo Pfu DNA Polymerase (Stratagene, La Jolla, CA) and cloned upstream of the promoterless β-glucoronidase (*GUS*) gene encoded in the binary vector pCambia1391Z (Hajdukiewicz et al. 1994). Gene specific primers and their sequences are listed in Table 2. Restriction sites engineered in the primer sequences are underlined. Promoter regions were 2.0 kb for *AtOPT6*, 2.2 kb for *AtOPT7*, 2.2 kb for *AtOPT8* and 3.0 kb for *AtOPT9*.

Plant Germination and Growth Conditions

Arabidopsis thaliana seeds were surface sterilized in a solution containing 35% chlorox and 0.05% Tween-20 for 15 minutes, washed five-times with sterile distilled water and re-suspended in 300 µl sterile distilled water. Seeds were then vernalized at 4°C for 3 days in the dark and germinated on half-strength Murashige and Skoog salts (Murashige and Skoog, 1968, Sigma, St. Louis, MO), 1 % Sucrose (w/v), 0.1 % Murashige and Skoog Vitamin solution (Sigma, St. Louis, MO), 0.05 % MES (Fisher Scientific) and 0.8% agar, pH: 5.7 and supplemented as required with 25 µg/mL hygromycin (Sigma, St. Louis, MO). Seedlings were grown for up to 3 weeks or as required. Plants were grown in a model CU-32L plant growth chamber (Percival Scientific Inc., Boone, Iowa).

Table 1: Bacterial strains and plasmids

Strain / Plasmid	Genotype / Relevant Characteristics	Source
Escherichia coli		
DH10B	F$^-$ *mcr*A Δ(*mrr-hsd*RMS-*mcr*BC) ϕ80*lac*ZΔM15 Δ*lac*X74 *rec*A1 *end*A1 *ara*D139 Δ (*ara*, *leu*) 7697 *gal*U *gal*K λ$^-$ *rps*L *nup*G /pMON14272 / pMON7124	Invitrogen, Carlsbad, CA
DH5α	F$^-$ ϕ80*lac*ZΔM15 Δ(*lac*ZYA-*arg*F) U169 *rec*A1 *end*A1 *hsd*R17 (r_k-, m_k+) *pho*A *sup*E44 λ$^-$ thi$^-$1 *gyr*A96 *rel*A1	Invitrogen, Carlsbad, CA
Agrobacterium tumefaciens		
EHA105	pTiBo452 ΔT-DNA, bar/GUS	Hood et al., 1993
Ag11	pAL154/156, C58, RecA, pTiBo452 ΔT-DNA, bar/GUS	Jones et al., 2005
Promoter::GUS plasmid constructs:		
AtOPT6-ProGUS	A 2.0 kb genomic DNA amplified from *AtOPT6* promoter region cloned into HindIII- AvrII site in pCAMBIA1391z	This study
AtOPT7-ProGUS	A 2.2 kb genomic DNA amplified from *AtOPT7* promoter region cloned into BamHI-EcoRI site in pCAMBIA1391z	Stacey et al., 2006

Table 1: *Continued*

AtOPT8-ProGUS	A 2.2 kb genomic DNA amplified from *AtOPT8* promoter region cloned into BamHI-AvrII site in pCAMBIA1391z	Stacey et al., 2006
AtOPT9-ProGUS	A 3.0 kb genomic DNA amplified from *AtOPT9* promoter region cloned into BamHI site in pCAMBIA1391z	This study

under 16 hour day/ 8 hour night cycle or continuous light at 22 °C with 60 % relative humidity. For seed amplification and analysis of mature plants, 14-day-old seedlings were transferred to Pro-mix soil (Premier Horticulture, Red Hill, PA) and grown at 22 °C under continuous fluorescent white light in either a plant growth chamber with 60 % relative humidity or in the green house.

Plant Transformation and Selection of Transgenic Plants

Stable transformation of *Arabidopsis* was performed by the vacuum infiltration protocol for *Agrobacterium tumefaciens*- mediated T-DNA gene transfer as described (Bechtold and Pelletier, 1993) with slight modification. *Arabidopsis thaliana* (ecotype Columbia) plants were grown as described above until first bolts emerged. To facilitate growth of multiple bolts, emerging bolts were clipped off and multiple bolts were grown to an approximate length of 15 cm. *Agrobacterium tumefecians* (EHA105) cultures were started 24-48 hours prior to infiltration and grown to an $O.D_{600\ nm}$ of 0.8 at 30°C in LB medium with appropriate antibiotics. Cells were centrifuged at 4000 rpm in a J2-MC centrifuge (Beckman Coulter, Inc., Fullerton, CA) for 5 minutes and re-suspended in infiltration medium (1X MS salts, 1X B5 Vitamins, 5 % Sucrose and 10 μg of benzyl aminopurine, pH: 5.7). Silwet L-77 (0.05 %, OSi Specialities Inc., Danbury, CT) was added to promote better infiltration. Plants were inverted in an *Agrobacterium* culture solution to submerge the flowers and a vacuum of approximately 0.05 bars was applied for 5 minutes. Plants were then laid on their sides to remove excess *Agrobacterium* culture, covered with a plastic dome for 24 hours at room-temperature and later transferred to a growth chamber until the seeds were ready to harvest.

Table 2: Sequences of DNA primers used in this study

Application	Sequence	Tm (°C)
Promoter-GUS cloning		
AtOPT6 ProG-F	5` - CTC AAG CTT AAA GGA GCC GAT GAA GTG ATA TTC TT - 3`	65.5
AtOPT6 ProG-R	5` - CTG CCT AGG GTT TTA GAA GAG TGA GTG TTC CGT TCT TT - 3`	66.8
AtOPT9 ProG-F	5` - CTA GGA TCC AAA CTA GCA ATG AAG AGT GAC CGT GTA GA - 3`	66.1
AtOPT9 ProG-R	5` - CTA GGA TCC GTG GTG AAT CTT TTA TAG GGT TAA GGG TG - 3`	65.3

Tm = Annealing temperature of the primer.

To select transgenic plants, transgenic seeds were surface sterilized and grown on half-strength MS medium containing 12.5 μgm/ml hygromycin. 18-day-old transgenic seedlings were transferred to soil for further propagation. Homozygous seeds, verified by growth on appropriate antibiotics, of the T3 generation of transgenic plants were used for expression analysis. For each construct, four to six independent transgenic lines were selected for further characterization.

Histochemical Staining with X-Glucuronidase (X-Gluc)

X-Gluc staining was carried out according to Stacey et al. (2006) with slight modifications. Plant tissues at different development stages including germinating seeds, seedlings, rosette leaves, flower and siliques were picked using clean forceps and immersed in a X-Gluc stain solution (100 mM Sodium phosphate, pH 7.0; 1 mM EDTA; 1% TritonX-100; 5mM Potassium ferricyanide, 1mg/ml X-Gluc) overnight at 37 °C. Samples were washed once with wash solution (i.e., X-Gluc staining solution without X-Gluc and Potassium ferricyanide) and fixed in a formaldehyde, acetic acid and alcohol (FAA) solution (50% ethanol, 5% acetic acid and 3.7% formaldehyde) for 30 minutes. Samples were rinsed once with potassium phosphate buffer pH 7.0 and washed with 30%, 50% and 70% ethanol for 30 minutes each followed by incubation in 70% ethanol for 16 hours or overnight to dissolve the chloroform present in leaves, flowers and siliques. Samples were again passed through a series of alcohol washes of 70%, 50%, 30% and 0% and stored in 100mM potassium phosphate buffer pH 7.0. GUS patterns were observed with an Olympus SZX12 microscope.

DNA and amino acid sequence comparisons

Amino-acid sequences of plant OPTs were obtained from the following databases: *Arabidopsis* (*Arabidopsis thaliana*; www.arabidopsis.org), rice (*Oryza sativa*; http://www.tigr.org/tdb/e2k1/osa1) and Aramemnon plant membrane protein database (http://aramemnon.botanik.uni-koeln.de) for AtOPT, AtYSL, OsOPT and BjGT1 sequences. Yeast OPT sequences were obtained from NCBI sequence viewer v2.0 by submitting a query for *Candida albicans* and *Saccharomyces cerevisiae* OPT genes. Sequence alignments were performed using ClustalX 1.83 (Thompson et al., 1997) with PHYLIP output format. Dendrograms of OPT sequences were generated using the program PHYLIP (Felsenstein, 2000) and trees were viewed and rooted using Tree Viewer (Zmasek and Eddy, 2001).

Public microarray data analysis

Microarray data were collected from the GENEVESTIGATOR website (www.genevestigator.eth.chhttps://www.genevestigator.ethz.ch). A 22K array of Arabidopsis genes and collective dataset from NASCArrays, ArrayExpress, and AtGeneExpress was used for data mining. Where possible, normalized data were used and experiments with low signal value were eliminated due to the difficulty of differentiating real expression from background. Digital northerns were performed at the Genevestigator website to assess the reliability of the data.

RESULTS

Phylogenetic analysis of *Arabidopsis* OPTs: Comparison with OPT transporters from fungi and plants

A phylogenetic tree was generated for all OPT transporters to identify close homologues of AtOPTs and shed light on possible functions of *Arabidopsis* OPTs based on the known function of OPTs from other species (Fig 1). OPT transporters from *S. cerevisiae*, *C. albicans*, *S. pombe*, *B. juncea*, *O. sativa* and YSL transporters from *Arabidopsis* were selected for phylogenetic comparison since OPTs from these species have been identified and some are well characterized. The amino acid sequences of Arabidopsis OPTs do not show strong similarity to Arabidopsis *YSLs* and fall into two separate sub-families of the OPT super-family. This analysis suggests that *Arabidopsis* OPTs and YSLs likely carry out distincut functions. The exception is OPT3 which, although it clearly groups with the OPT sub-family, was recently shown to be involved in iron transport (Wintz et al., 2003; Stacey et al., 2007). A recent publication suggested that AtYSL2 mediates transport of a Fe-phytosiderophore complex in yeast implicating a role of YSLs in iron transport (Schaff et al., 2005). The major iron chelator in plants, nicotianamine, which is transported by YSLs, is a modified peptide. Therefore, both YSL and OPT are known to transport peptide-like substrates. Rice and *Arabidopsis* OPTs are highly similar and fall into the same clade, along with OsGT1, a known rice glutathione transport protein (Zhang et al., 2004). Among Arabidopsis OPTs, ATOPT6 was shown to mediate transport of glutathione. Therefore, OsGT1 and AtOPT6 appear to be related orthologs.

Figure 1: Phylogenetic relationship of *A.thaliana* OPT transporters with several paralogs and orthologs from plants and fungi.

Amino acid sequences from *A. thaliana*, *O. sativa*, *B. juncea*, *S.* cerevisia*, S. pombe* and *C. albicans* were used for comparison. The branch lengths are proportional to the degree of divergence, with the scale of "0.1" representing 10% change.

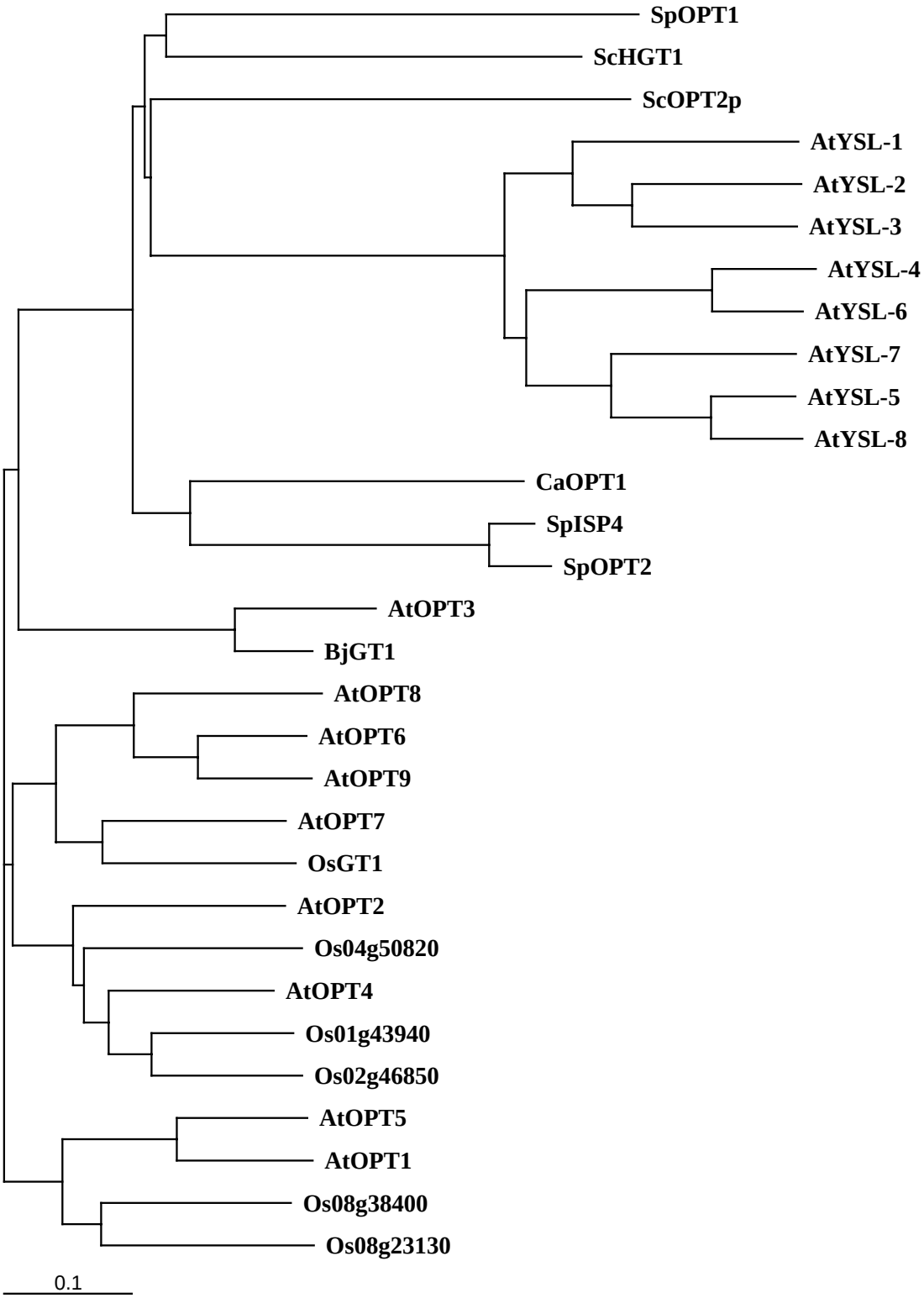
SpOPT1
ScHGT1
ScOPT2p
AtYSL-1
AtYSL-2
AtYSL-3
AtYSL-4
AtYSL-6
AtYSL-7
AtYSL-5
AtYSL-8
CaOPT1
SpISP4
SpOPT2
AtOPT3
BjGT1
AtOPT8
AtOPT6
AtOPT9
AtOPT7
OsGT1
AtOPT2
Os04g50820
AtOPT4
Os01g43940
Os02g46850
AtOPT5
AtOPT1
Os08g38400
Os08g23130
0.1

The transport properties of AtOPT7, the closest homologue of OsGT1, have not been characterized. It is also interesting to note that ScHGT1, which is known to mediate glutathione transport (Osawa et al., 2006) does not fall into the same cluster as AtOPT6 and OsGT1. Since the selectivity filter of transporters can be defined by only a few amino acids, overall sequence similarity is not a good predictor of substrate specificity.

Expression analysis of *AtOPT6* and *AtOPT9* during seed germination and vegetative growth

Storage proteins are degraded into smaller peptides by proteases during seed germination, which can serve as a nitrogen source to actively growing cells. *AtOPT6* and *AtOPT9* promoter – GUS lines were analyzed during seed germination, seedling growth and vegetative growth stages to elucidate a possible role of these OPTs in peptide mobilization and distribution to actively dividing cells. *AtOPT6* showed a strong expression pattern in pre-vascular tissue of cotyledons from newly germinated seeds, as compared to a weaker expression pattern of *AtOPT9*. During seedling growth (3-5 days post germination), expression of *AtOPT6* was localized in the developing vascular tissue of cotyledons and hypocotyls (Fig 2A). Expression of *AtOPT9* was limited only to developing vascular tissue of cotyledons (Fig 2D). No expression was observed for *AtOPT9* in vascular tissue of developing hypocotyls. The expression pattern of *OPTs* in germinating seedlings is suggestive of a role in peptide mobilization and redistribution in developing tissues after storage proteins are broken down by peptidases during initial germination.

Both *AtOPT6* and *AtOPT9* are not expressed in the developing root tissues at this stage (Fig 2A and 2D). *AtOPT7* and *AtOPT8* showed a similar expression pattern in developing seedling to *AtOPT6* (Fig 2B and 2C). Seedlings with the first two true leaves and seedlings at the 6-7 leaf stage were observed to see if any changes occurred in the expression patterns of *AtOPT6* and *AtOPT9*. As shown in Fig 2E-2L, expression of *AtOPT6* was consistently higher than AtOPT8 and AtOPT9 in vascular tissues of cotyledons, hypocotyl and true leaves (Fig 2E, 2I). *AtOPT7* showed expression similar to *AtOPT6* (Fig 2F, 2J). *AtOPT8* (Fig 2G, 2K) and *AtOPT9* (Fig 2H, 2L) showed similar, although weaker, expression in the vascular tissues of cotyledons, hypocotyls and true leaves. In roots, the strongest OPT expression was in *AtOPT6* promoter – GUS lines (Fig 2M), followed by *AtOPT7* (Fig 2O), *AtOPT9* (Fig 2S) and weakest in *AtOPT8* (Fig 2Q). The expression was detectable in the stele tissue of the roots including pericycle and vascular tissue. However, in *AtOPT8* and *AtOPT9* promoter – GUS lines, the expression seemed to be restricted to vascular tissues. None of the OPTs were expressed in the root hairs. No detectable expression of any of the OPTs was observed in root tips (Fig 2N (*AtOPT6*), 2P (*AtOPT7*), 2R (*AtOPT8*) and 2T (*AtOPT9*)). In rosette leaves, *AtOPT6* (Fig 2U) was predominantly expressed in primary veins and also in the secondary and tertiary veins as was *AtOPT7* (Fig 2V) However, the expression of *AtOPT7* may be the result of GUS diffusion into other tissues. The diffusion may be the result of longer exposure to the GUS substrate. *AtOPT8* (2W) and *AtOPT9* (2X) were not expressed as strongly as the other OPTs in rosette leaves. Interestingly, expression of *AtOPT9* in rosette leaves was limited to primary and tertiary veins. There was no detectable GUS expression in secondary veins.

Figure 2: GUS expression patterns for promoter::GUS lines of *AtOPT6*, *AtOPT7*, *AtOPT8* and *AtOPT9* in various plant organs.

(A-D) Staining of vascular tissue in developing cotyledons and hypocotyls in germinating seeds.

(E-H) Vascular tissues of roots, cotyledons, leaves and hypocotyls were stained similarly in developing seedlings.

(I-L) Vascular tissues of roots, cotyledons, leaves and hypocotyls were stained in a similar pattern in 3-week-old seedlings. Staining was strong in roots of *AtOPT6* (I) and *AtOPT7* (K) promoter GUS lines.

(M-T) GUS staining in the roots and root-tips: Note the strong staining in *AtOPT6* (M) and *AtOPT7* (O) promoter GUS lines in roots. None of the promoter GUS lines were expressed in root-tips.

(U-X) Similar GUS staining pattern in rosette leaves. All promoter - GUS lines are expressed in vascular tissue, however the expression pattern is strongest in *AtOPT7* (V) and weakest in *AtOPT9* (X) promoter - GUS line.

(A, E, I, M, N, U) – *AtOPT6* promoter - GUS lines

(B, F, J, O, P, V) – *AtOPT7* promoter - GUS lines

(C, G, K, Q, R, W) – *AtOPT8* promoter - GUS lines

(D, H, L, S, T, X) – *AtOPT9* promoter - GUS lines

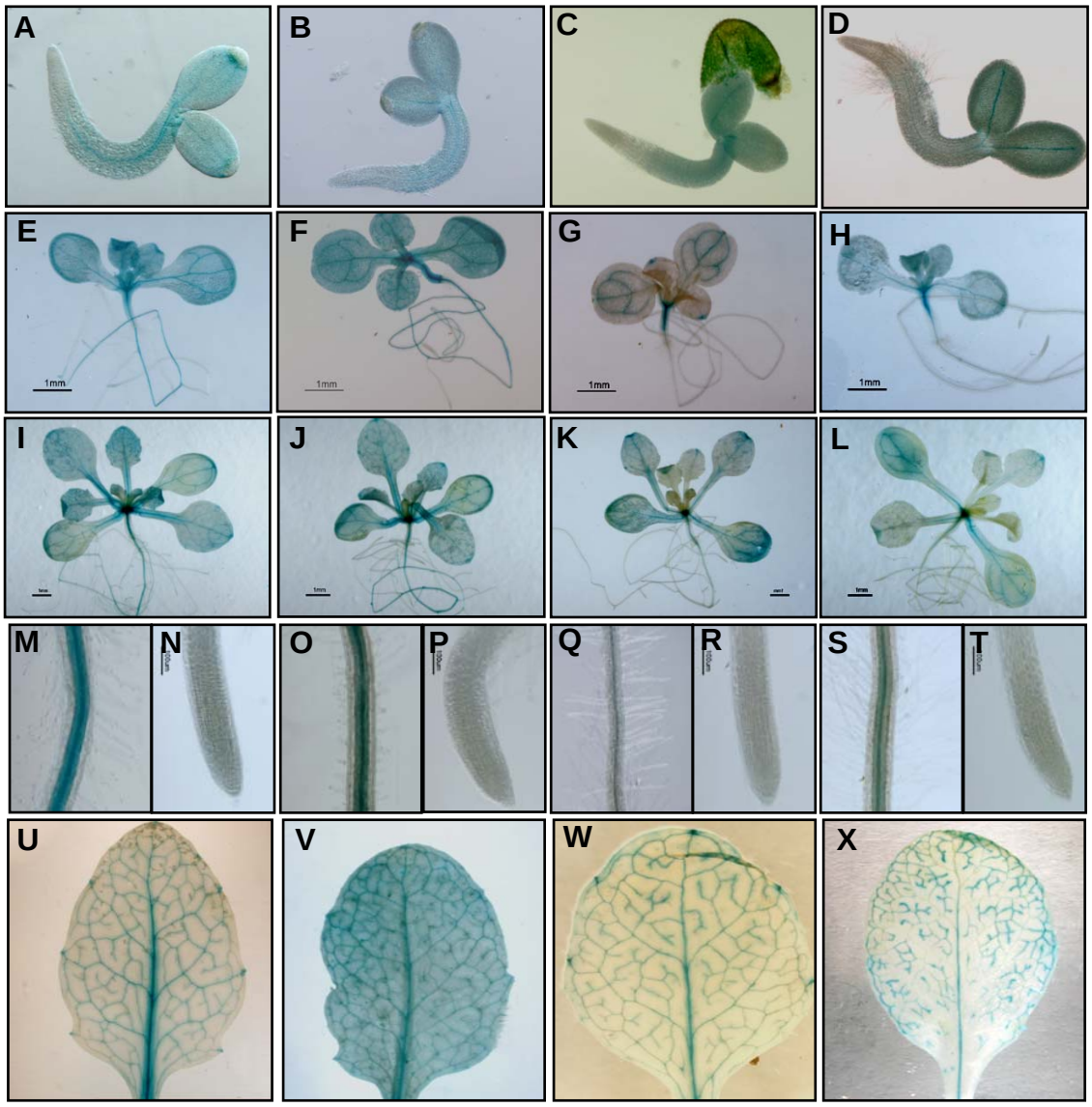
A
B
C
D
E
1mm
F
1mm
G
1mm
H
1mm
I
J
1mm
K
L
1mm
M
N
O
P
Q
R
S
T
U
V
W
X

Expression patterns in roots and seedling tissues suggest that *OPTs* do not play a role in acquisition of nutrients from soil or medium, rather they may be involved in mobilization of nutrients *in planta*.

Expression analysis of *AtOPT6* and *AtOPT9* during flower and seed development

AtOPT6 showed very high expression levels in the filament of stamens, vascular tissue of sepals and developing ovules during early stages of flower development (Fig 3A). Post-fertilization, the expression of *AtOPT6* was still strongest in the filament of stamens and vascular tissue of sepals. However, there was no detectable expression in the fertilized ovules (Fig 3B). There was no expression in petals at any stage during flower development. During flower development the demand of nitrogen is high in sink tissues such as developing ovules and anthers that produce a large amount of pollen. The expression in developing ovules and vascular tissues of filaments suggest that *AtOPT6* might be involved in providing nitrogen in the form of small oligopeptides. In contrast to *AtOPT6*, *AtOPT9* was expressed only in anthers and pollen grains during flower development (Fig 3C and 3D). There was no difference in the expression level of *AtOPT9* pre- or post-fertilization in anthers and pollen grains. During seed development, both *AtOPT6* (Fig 3E and 3G) and *AtOPT9* (Fig 3F) were expressed in the vascular tissue of funiculi, which provide nutrition to developing maternal tissues of the embryo at the onset of heart stage of embryo development. *AtOPT9* promoter – GUS lines were stained for a longer period of time to observe the expression pattern. *AtOPT6* and *AtOPT9* were still expressed in vascular tissues of funiculi during later stages of seed development. There were differences in the expression patterns of *AtOPT6* and *AtOPT9* during flower

development. *AtOPT6* was expressed in sepals, filaments of stamens and developing ovules. *AtOPT9* was expressed only in anthers and pollen grains. The data clearly show differences in the tissue-specific expression of the OPTs during flower development, suggesting different or overlapping roles in providing nutrition to selective sink tissues during times of higher nutrient demand. The expression pattern and the timing of the GUS expression during seed development indicate that OPTs might be involved in supplying nitrogen to rapidly developing seed tissue. There is selective and distinct tissue specific expression of *AtOPT6*, *AtOPT7*, *AtOPT8* and *AtOPT9* during various stages of plant growth and development (Table 3). Microarray expression analysis (Fig 4) also supports the *AtOPT* promoter – GUS expression data.

Figure 3: Expression analysis of *AtOPT6* and *AtOPT9* during flower and seed development.

(A-B) *AtOPT6* promoter – GUS expression during pre- and post fertilization stage in floral tissues.

(C-D) *AtOPT9* promoter – GUS expression during pre- and post fertilization stage in floral tissues.

(E and G) Expression of *AtOPT6* promoter – GUS lines during seed development.

(F) Expression of *AtOPT9* promoter – GUS lines during seed development.

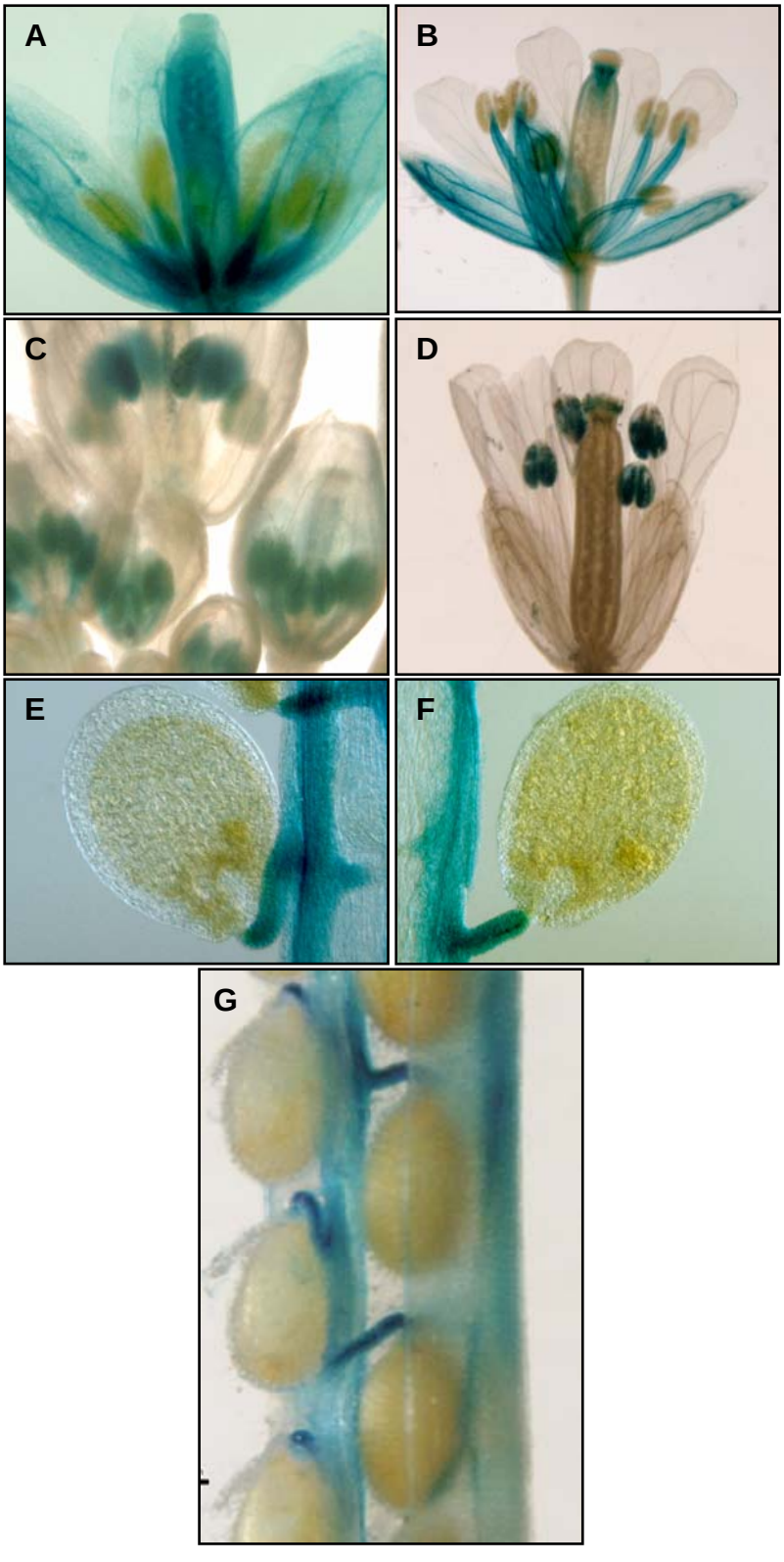
A
B
C
D
E
F
G

Table 3: Comparative analysis of expression patterns of *AtOPT* Promoter-GUS lines at different stages of plant growth and development.

Plant tissues	***AtOPT* Promoter-GUS lines**						
	AtOPT1	***AtOPT3***	***AtOPT4***	***AtOPT6***	***AtOPT7***	***AtOPT8***	***AtOPT9***
Germinating seeds	**Vascular**	**Vascular**	**Vascular**	**Vascular**	**Vascular**	**Vascular (weak)**	**Vascular (weak)**
Seedling	**Vascular**	**Vascular**	**Vascular**	**Vascular**	**Vascular**	**Vascular (weak)**	**Vascular (weak)**
Root	**Vascular**	**Vascular**	**Vascular**	**Vascular**	**Vascular**	**Vascular (very weak)**	**Vascular (weak)**
Rosette leaf	**Vascular**	**Vascular**	**Vascular**	**Vascular**	**Vascular**	**Vascular**	**Vascular (weak)**
Sepal	**Vascular**	**Vascular**	**Vascular (Stigma)**	**Vascular**	**Vascular**	**None**	**None**
Petal	**Vascular**	**Vascular**	**Vascular**	**None**	**None**	**Vascular**	**None**
Stamen	**Filament/ Pollen**	**Pollen**	**Filament**	**Filament**	**Filament**	**Filament/ Pollen**	**Pollen**
Carpel	**Pollen-tube**	**Style**	**Style**	**Developing Ovules**	**Style Stigma**	**None**	**None**
Silique	**Funiculi**	**Funiculi**	**Funiculi**	**Funiculi**	**Funiculi**	**Funiculi**	**Funiculi**
Seed	**None**	**Endosperm Integument Embryo**	**None**	**None**	**None**	**Endosperm/ Integument**	**None**

Figure 4: Development map of AtOPT expression.

This graph was generated using public micro-array data, of tissue specific expression of *AtOPT* Promoter-GUS fusions at various growth stages during plant development. Values below 200 are inconclusive due to background hybridization noise in microarray experiments. (This data was obtained from www.genevestigator.ethz.ch).

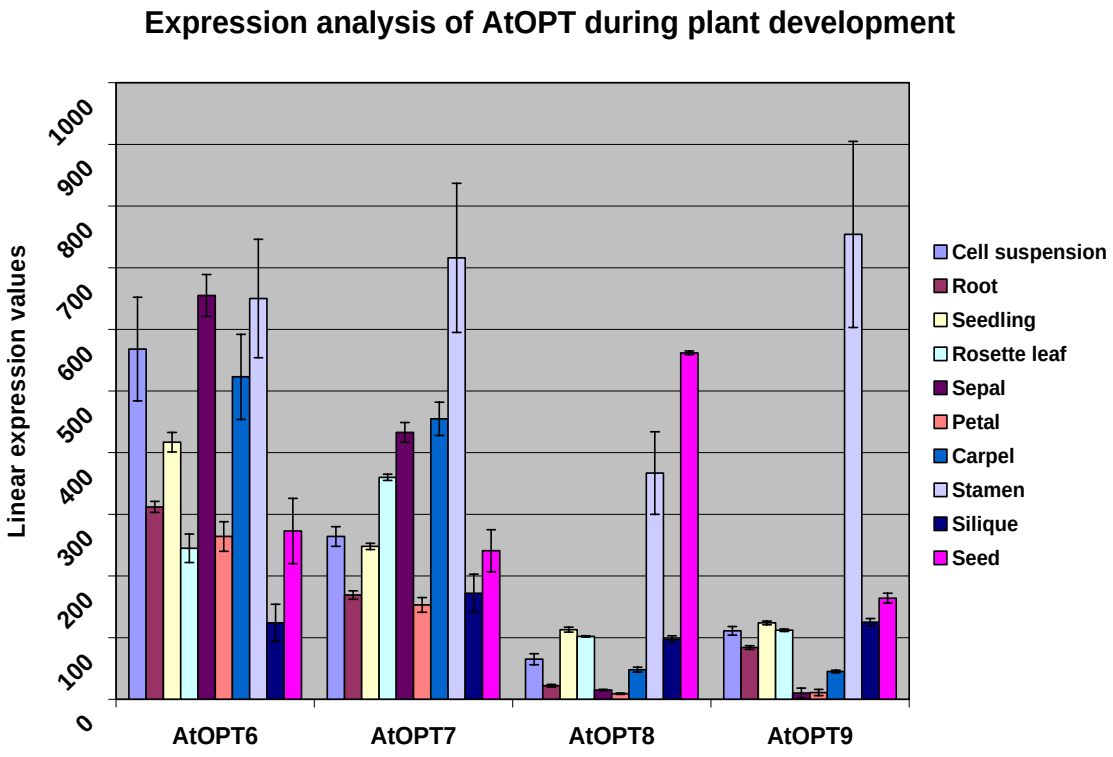

DISCUSSION

AtOPTs as a gene family may play a role in peptide transport during seed germination and vegetative development

Peptide transporters are thought to transport peptides during germination. Storage proteins, the reservoirs of nitrogen, are known to be hydrolyzed into smaller peptides by proteases present during seed germination (Muntz et al., 2001). These small peptides were shown to be transported across the scutellum into the differentiating embryo (cotyledons and hypocotyl) by peptide transporters (Higgins and Payne, 1977a and Higgins and Payne, 1982). The spatial and temporal expression patterns of *AtOPT6* and other *AtOPTs* seem to overlap with the timing of protein degradation during early seedling germination. Also, the expression of *AtOPT6* and *AtOPT9* in the vascular tissue of developing cotyledons and the expression of *AtOPT6* in the vascular tissue of developing hypocotyls provides evidence that these *OPTs* are involved in transport and redistribution of peptides derived from hydrolyzed storage proteins in cotyledons, providing nitrogen transport to cells rapidly undergoing division and differentiation. Expression of *AtOPT6* and *AtOPT9* in the vascular tissue of rosette leaves, even after bolting, suggests that they are involved in the long distance transport of peptides from source tissues to sink tissues, such as developing floral organs. Stacey et al (2006) suggested a role of *AtOPTs* in senescence based on the spatial and temporal expression pattern in rosette leaves. This suggestion was based on the observation that the onset of senescence begins immediately after rosette leaves fully expand (with *OPTs* being expressed in vascular tissue of leaves) and the plants redistribute nitrogen rapidly from

rosette leaves to other tissues with the aid of *OPTs*. The absence of expression of all *AtOPTs* in root epidermis, root hairs and root tips indicates that *OPTs* are not involved in the uptake of nutrients from soil or medium but rather mobilization, transport and redistribution within the plant.

AtOPT6 and *AtOPT9* play distinct roles during flower and seed development

AtOPT6, *AtOPT9* and all other members of the *AtOPT* gene family showed distinct tissue specific expression during flower development. The temporal and spatial expression patterns were different for each *AtOPT*, with some overlap. *AtOPT6* was the only *AtOPT* gene family member that showed unique expression in developing ovules. *AtOPT1*, *AtOPT3* and *AtOPT8* were the only members of the family that showed unique expression in pollen tubes and the developing embryo, respectively (Stacey et al., 2006). *AtOPT6* expression is strong in ovules during early stages of inflorescence development but is completely abolished as the flower reaches maturity. Female gametophyte development, megagametogenesis and megasporogenesis, occur during this stage of inflorescence development and require high amounts of nitrogen and carbon for developing ovules (reviewed in Drews et al., 1998). The expression of *AtOPT6* coincides with female gametophyte development implying that *AtOPT6* may be transporting peptides from source tissues, such as rosette leaves, to sink tissues of ovules. Also, *AtOPT6* shows very strong expression in stamen filaments in the early stages of inflorescence and the expression remains strong throughout inflorescence development. Stamens consist of filaments, anthers and pollen grains. The tapetum cells are part of the anther and are sites of intense metabolic activity during microsporogenesis (Lee and

Tegeder, 2004). Nitrogen and carbon demands in those tissues are higher during microsporogenesis. Expression of *AtOPT6* and *AtOPT9* in the filaments during microsporogenesis indicates that both are involved in mobilization of nitrogen in the form of peptides to these actively developing cells. *AtLHT2*, an amino acid transporter with high affinity for neutral and acidic amino acids was shown to localize in tapetum cells and was implicated in the import of amino acids into the tapetum cells (Lee and Tegeder, 2004). In order for amino acids to be imported to tapetum cells they need to be transported from source tissues to filaments and anthers. It is possible that amino acid transporters and peptide transporters are working together to achieve import of nitrogen to sink tissues.

The chalazal is a specialized maternal tissue formed in vascular tissues of the funiculi and is thought to promote transfer of nutrients across the plasmalemma between the developing endosperm and maternal tissues of the embryo (Olsen, 2004) during the heart stage of embryo development. The onset of expression of *AtOPT6*, *AtOPT9* and other *AtOPTs* in vascular tissue of the funiculi and the rest of the silique overlap with the heart stage of embryo development, indicating a functional role of *OPTs* in peptide transport to developing seeds.

The synopsis of the expression analysis of *AtOPT6* and *AtOPT9*, along with other *AtOPTs* (Stacey et al., 2006), at seed germination, vegetative growth, flower and seed development stages indicates a functional role of these oligo-peptide transporters in the import of nitrogen into rapidly differentiating tissues and other sink tissues. Overlapping expression in rosette leaves, stem and sink tissues of floral organs reveals a role in long distance mobilization of protein reserves. Single knock-out mutant lines of specific

AtOPTs did not show any visible phenotypes during plant growth and development with the exception of in *Atopt3-1*, where one-fourth of the seeds were aborted in the heterozygous mutant lines indicating a seed lethality phenotype (Stacey et al., 2002). Other peptide transporters were also proposed to play similar role in peptide or amino acid mobilization, including the amino acid transporter *AtLHT2* (Lee and Tegeder, 2004), peptide transporters *HvPTR1* (West et al., 1998) and *AtPTR1* (Dietrich et al., 2004). This indicates that different transporters transporting various forms of petides may have overlapping functions in mobilization and transport of nitrogen in form of peptides.

CHAPTER II: THE FUNCTION OF *AtOPT6* IN HEAVY METAL DETOXIFICATION

INTRODUCTION

Heavy metals such as cadmium (Cd) and lead (Pb) are widespread environmental pollutants that are toxic to plant growth. Plants take up these toxic metals when essential transient metals such as zinc (Zn), manganese (Mn), copper (Cu) and cobalt (Co) are transported from soil to plant cells by specific transport proteins. The tolerance to heavy metals is achieved by sequestration of ions, after their uptake, in metabolically inactive compartments, such as vacuoles and the apoplastic space (Clemens, 2000). Excess cadmium can have a negative impact on various metabolic enzymes and transcription factors by substituting for zinc (Qu and Zhu, 2006). Cellular mechanisms for sequestration of Cd during high Cd exposure are thought to include sequestration of this toxic metal in the cytosol via glutathione (GSH) and phytochelatins (PCs). Cd sequestration in the vacuole is carried out by tonoplast Cd/H antiporters, ABC transporters and NRAMPs (Clemens, 2000; Hall and Williams, 2003; Martinoia et al., 2007). Metal binding peptide ligands such as metallothioneins (MTs), which are small gene-encoded, cysteine-rich polypeptides, also play a role in heavy metal tolerance (Cobbett, 2000). The role of GSH and PCs in Cd tolerance has been extensively studied in yeast and plants.

GSH is a tri-peptide consisting of the amino acids Glu, Cys and Gly with Glu and Cys residues linked through a γ-carboxylamide bond and Gly linked with Glu and Cys residues (Cobbett, 2000). There is evidence that GSH binds with Cd and this results in compartmentalization to avoid toxicity (Adamis et al., 2007). PCs are synthesized from GSH where repetitions of a γ-Glu-Cys dipeptide are followed by a terminal Gly; $(\gamma\text{-Glu-Cys})_n$ – Gly, n is typically 2-5 residues but can be as many as 11. The main enzyme catalyzing the reaction is phytochelatin synthase (PCS) (Cobbett, 2000). Expression of *AtPCS1* mediated an increase in Cd accumulation, indicating it was probably involved in chelation of the PC-Cd complex (Vatamaniuk et al., 1999). *AtPCS1* was isolated through the cloning of the *CAD1* gene of *Arabidopsis* (Howden et al., 1995). Mutants at the *cad1* locus in *Arabidopsis* are Cd sensitive and deficient in the formation of Cd-binding complexes and in PC biosynthesis. In particular, PCs are undetectable in the *cad1-3* mutant after prolonged exposure to Cd (Howden et al., 1995). PC-Cd complexes are sequestered in the vacuole as demonstrated through studies of Cd-sensitive mutant *hmt1* in yeast (Ortiz et al., 1995). The *Hmt1* gene encodes an ABC transport protein localized to the vacuole membrane and *hmt1* mutants were unable to form PC-Cd complexes and export the complex into the vacuole upon exposure to Cd and, therefore, were sensitive to Cd (Ortiz et al., 1995).

Distinct from the PC-Cd transport activity, an alternative mechanism, identified in yeast and oat tonoplast vesicles, is a Cd/H antiporter activity dependent upon the proton gradient (Salt and Wagner, 1993; Ortiz et al., 1995). Cd/H antiporters such as *CAX4* (cation exchanger) are involved in root-to-shoot partitioning of Cd and contribute to increased tolerance to high Cd, Zn and Mn ions (Korenkov et al., 2007). Another gene

family involved in heavy metal detoxification is the ABC transporter family. AtATM3 over-expressing plants showed increased Cd resistance, whereas *Atatm3* mutant plants were sensitive to Cd, compared to wild-type controls. Also, the closest homolog of *AtATM3* was *HMT1* suggesting *AtATM3*, like *HMT1*, may be involved in sequestration of PC-Cd complexes in plant cells (Kim et al., 2006). Similar to AtATM3, AtPDR8 also enhanced resistance to Cd and Pb when over-expressed and *Atpdr8* mutants were sensitive to Cd and Pb. However, unlike AtATM3, which is localized in the mitochondrial membrane, AtPDR8 was localized in the plasma-membrane suggesting it may be an efflux pump that drives Cd or Cd-conjugates out of the cytoplasm and into the apoplastic space (Kim et al., 2006; Kim et al., 2007).

From the preceding discussion it is apparent that the mechanism of Cd detoxification is more complex than simply chelation of Cd-PC and sequestration to the vacuole or apoplastic space. Additional experiments are needed to address the long distance transport of PC-Cd and the proteins involved in this process. In this chapter, I will discuss a possible role of *AtOPT6* in mobilization of Cd and PC-Cd conjugates. Over-expression of AtOPT6 resulted in hypersensitivity to Cd whereas *Atopt6* mutant and wild-type control plants did not display hypersensitivity as seen in over-expressing lines. More experiments will be discussed in detail to address the possible involvement of *AtOPT6* in long distance transport of GSH-Cd and PC-Cd complexes.

METHODS AND MATERIALS

Bacterial strains and plasmids

Bacterial strains and plasmids used are listed in Table 1 of Chapter I.

Bacterial culture media and growth conditions

Refer to Chapter I for strains of *Escherichia coli*. *Agrobacterium tumefaciens* was grown and maintained on LB medium; pH- 7.0 at 30 °C.

Plasmid DNA isolation

Refer to methods and materials in Chapter I.

Enzymes and DNA primers

Refer to methods and materials section of Chapter I.

Generation of *AtOPT6* over-expression transgenic lines

A 2.4 kb genomic DNA of *AtOPT6* (At4g27730) was PCR amplified from genomic DNA of *Arabidopsis thaliana* ecotype Col-O using Turbo Pfu DNA Polymerase (Stratagene, La Jolla, CA) and cloned downstream of the CaMV 35S promoter region in the modified binary vector pCAMBIA1200 (+S) between the *Eco*RI-*Bam*HI restriction sites (Dr. Minviluz Stacey – personal communication). Primers and sequences are listed in Table I.

Plant transformation and selection of transgenic plants

Refer to methods and materials section of Chapter I.

Total RNA isolation and reverse transcription polymerase chain reaction (RT-PCR)

Total RNA was isolated from 2 to 3-week old seedlings of *Arabidopsis thaliana* (ColO) using the Trizol® reagent (Invitrogen, Carlsbad, CA). Where necessary, the roots and shoots were separated prior to RNA isolation. The quantity of RNA was measured using a ND-1000 spectrophotometer. The quality of RNA was determined by agarose gel electrophoresis. RNA samples were purified using the Qiagen RNeasy Mini Kit (Qiagen, Valencia, CA) according to manufacturer's protocol. To remove genomic DNA contamination, total RNA was treated with TURBO DNase (Ambion Inc., Houston TX) according to manufacturer's protocol. RNA was reverse transcribed to synthesize single-stranded cDNA using Superscript III reverse transcriptase (Invitrogen, Carlsbad CA), oligo(dT), 10mM dNTP and 0.1M DTT at 50° C for 2 hours in a 25 μl reaction. The reaction was inactivated by heating at 70° C for 15 minutes. 2 μl of this reaction was used in a polymerase chain reaction (PCR) including 2.5 mM $MgCl_2$, 1mM dNTPs, 0.5 units of Ex-Taq DNA Polymerase (Takara, Madison WI) and gene specific primers as listed in Table I. As an internal control, gene specific primers of *Actin2* were used in each PCR reaction. To analyze expression of specific genes, 4 μl of the PCR reaction was used for agarose gel electrophoresis.

Quantitative RT-PCR

Total RNA was isolated according to the above protocol. A total of 2 μg of RNA was used with 5μl of SYBR green (Applied Biosystems, Foster City, CA) and a 2mM final primer concentration in a 10μl reaction volume. Relative quantification analysis was run on a 7500 Real Time PCR system (Applied Biosystems, Foster City, CA) for total of 40 cycles. Data analysis was performed according to manufacturer's protocol. A list of gene specific primers and sequences is given in Table I.

Plant germination and growth conditions

Refer to methods and materials in Chapter I. All plants described in this section are from *Arabidopsis thaliana* (ecotype – ColO).

Root inhibition and root growth assay

Wildtype (ecotype – ColO), *opt6* mutant plants (Rosso et al., 2003) and *AtOPT6* over-expression transgenic plants were sterilized, vernalized and germinated on half-strength MS and half-strength MS medium containing 50 μM cadmium chloride ($CdCl_2$) for 18 days under continuous light at 22°C with 60% relative humidity in a model CU-32L plant growth chamber (Percival Scientific Inc., Boone, Iowa). The plates were placed vertically in the growth chamber. Root measurement was carried out and recorded for each plant line grown on MS and MS medium supplied with 50 μM $CdCl_2$.

Table 1: Sequences of DNA primers used in this study

Application	Sequence	Tm (°C)
Generation of over-expressions transgenic lines		
AtOPT6Oex-A	5`- CAG GAA TTC ATG GGA GAG ATA GCA ACA GAG TTC AC - 3`	64.8
AtOPT6Oex-B	5` - CAG GGA TCC CTA GAA GAC GGG ACA GCC TTT GAC - 3`	70.9
Quantitative and semi-quantitative RT-PCR		
AtOPT6OexRT-L	5` - ATG AGC TAG AAG ACG GGA CAG CCT TT - 3`	61.5
AtOPT6OexRT-R	5` - TAC TTG CTT GTG CCA TTG CCA TCA - 3`	59.6
Actin2-F	5` - GTT GGT GAT GAA GCA CAA TCC AAG - 3`	56.7
Actin2-R	5`- CTG GAA CAA GAC TTC TGG GCA TCT - 3`	58.9
AtOPT6 qRT-F	5` - CAA CCA AAT CCA AGA ATC TAA ACA C - 3`	58.1
AtOPT6 qRT-R	5` - GTC ATG ATC ACC ACT CAG GTA CTC - 3`	57.9
At2g28390-F	5` - AAC TCT ATG CAG CAT TTG ATC CAC T - 3`	59.6
At2g28390-F	5` - TGA TTG CAT ATC TTT ATC GCC ATC - 3`	58.9

Tm = Annealing temperature of the primers.

Root inhibition was calculated based on the root length of seedlings grown on MS medium (100%) vs. root length of seedlings grown on MS medium supplied with cadmium (100-X %). To measure fresh tissue weight, seedlings were removed from the plates, washed twice with sterile water and blotted dry with tissue paper to remove excess water. Fresh tissue weight was measured in milligrams and plotted on the graph.

Inductively coupled plasma optical emission spectroscopy (ICP-OES) measurements of thiols (GSH and PCs) and cadmium

Sample preparation

Arabidopsis seedlings of wild-type and *AtOPT6* over-expressing transgenic lines were germinated on ¼ strength MS agar medium until the first true leaves appeared. Seedlings were transferred to hydroponic culture and 4-week-old seedlings were exposed to 20 μM $CdCl_2$ for 72 hours. Roots and shoots were separated from seedlings and frozen in liquid nitrogen. The tissues were ground in a chilled mortar and then placed in micro centrifuge tube. The thiols were extracted by adding 1 ml of extraction buffer (6.3mM Diethylenetriamine-pentaacetic acid (DTPA) in 0.1% trifluroacetic acid) per 1 gram of fresh ground tissue weight. Samples were vortexed and centrifuged at 10,000 x g for 10 minutes at 4 °C. The resulting supernatant was used for thiol-labeling with monobromobimane (mBBr). To avoid oxidation of thiols, all buffers used in this study were bubbled with nitrogen for at least 10 minutes prior to use in the extraction procedure.

Fluorescence high pressure liquid chromatography (HPLC)

65 µl of the extracted sample was mixed with 115 µl of the labeling solution (200 mM Heppes buffer, 6.3mM DTPA, 0.5mM mBBr; pH 8.0) and incubated for 30 minutes at 45 °C in the dark. Post incubation the labeling procedure was terminated by acidifying the medium with 20 µl of 30% v/v perchloric acid (PCA). The samples were vortexed and centrifuged for 10 minutes at 10,000 x g at 4 °C. The supernatant was filtered using 0.22 µm membrane filter (Millipore, Billerica, MA). Before HPLC analysis, the supernatant was precipitated by adding 30% PCA to achieve a 3% final concentration. Samples were vortexed for 1 minute and centrifuged at 10,000 x g for 10 minutes at 4 °C. A total of 50-150 µl of sample was injected into the HPLC for analysis.

ICP-OES measurement of cadmium

Arabidopsis seedlings from wild-type and *AtOPT6* over expressing lines were grown on ¼ strength MS agar plates until the first true leaves appeared. Seedlings were then transferred to hydroponic culture. 4-week-old seedlings were exposed to 20 µM $CdCl_2$ for 72 hours. Roots and shoots were separated, dried and digested in nitric acid for cadmium quantification by ICP-OES (Lee et al., 2003).

Substrate uptake studies

Plasmid constructs

To increase the expression efficiency of *AtOPT6* cDNA when expressed in *Xenopus laevis* oocytes, a 17 bp sequence of 5` UTR of *ScOPT1* (ATAACGTCACAGAACAC) was introduced at the 5` end of the *AtOPT6* cDNA (Osawa et al., 2006). A *Bam*HI restriction site and a 5` UTR sequence was engineered at the 5` end of a *AtOPT6* forward

primer and was used to amplify a 600 bp sequence of *AtOPT6* cDNA using Turbo Pfu DNA polymerase (Stratagene, CA). The resulting PCR product was purified using QIAquick PCR Purification Kit. The *AtOPT6* reverse primer contained a *Bse*RI restriction site in the primer sequence. A partial 600 bp product of *AtOPT6* cDNA cloned in pGEM-HE was digested with *Bam*HI-*Bse*RI (600 bp) and was replaced with the modified PCR product containing the 5` UTR of *ScOPT1* and partial *AtOPT6* cDNA. The absence of amplification errors in the PCR product was confirmed by sequencing and restriction digestion.

cRNA synthesis

For expression in oocytes, the *AtOPT6* 5` UTR vector was linearized by digestion with a *Nhe*I restriction enzyme and purified using a QIAquick PCR Purification Kit (Qiagen, Valencia, CA). Capped cRNA was transcribed *in vitro* using the T7 mMessage mMachine RNA transcription kit (Ambion, Austin, TX) according to manufacturer's protocol.

Two-electrode voltage clamping and substrate uptake studies

Two-electrode voltage clamping was performed as described in Osawa et al. (2006). For glutathione and phytochelatin uptake studies, these peptides were dissolved in water and uptake was measured at various peptide concentrations.

RESULTS

Construction of transgenic *Arabidopsis* over-expressing AtOPT6

AtOPT gene family members show 61%-85% sequence similarity within the family and single knock-out mutants of the various *AtOPTs,* with the exception of *AtOPT3*, do not display visible phenotypes. To address the function of *AtOPT6* by gain-of-function, transgenic lines over-expressing a 2.4 kb genomic DNA coding sequence of *AtOPT6* expressed from the CaMV35 S promoter were generated. Four independent transgenic lines, termed 6Oex-1, 6Oex-11, 6Oex-27 and 6Oex-31, were selected for further analysis from a total of 32 independent transgenic lines tested for their expression level. Transcript levels of *AtOPT6* assessed by semi-quantitative RT-PCR analysis revealed that these four independent transgenic lines expressed 2.25 – 4.25 fold higher transcript levels than the wild-type control (Fig 1). Further analysis of the transcript by quantitative PCR showed that 6Oex-1, 6Oex-27 and 6Oex-31 transgenic lines showed 2-3 fold higher expression that the wild type, whereas 6Oex-11 showed almost 8-fold higher *AtOPT6* RNA levels (Fig 2). The transcript level of *AtOPT6* in 6Oex-1, 6Oex-27 and 6oex-31 fell in a similar range with each other. Therefore, 6Oex-1, 6Oex-27 and 6Oex-31 transgenic lines were selected for further analysis.

AtOPT6 mediates glutathione and phytochelatin transport in *Xenopus laevis* oocytes

Cagnac et al., 2004, showed that *AtOPT6* could transport glutathione (GSH) in yeast cells. Later, transport studies of *AtOPT6* in *Xenopus* gave no inward currents when studied for glutathione uptake (Osawa et al., 2006).

Figure 1: Semi-quantitative RT-PCR analysis of *AtOPT6* over-expressing transgenic lines.

Four independent transgenic lines were included for RT-PCR analysis and each analysis was performed twice per transgenic line to determine the folds increase of *AtOPT6* transcript in each transgenic line. Error bars represent standard error.

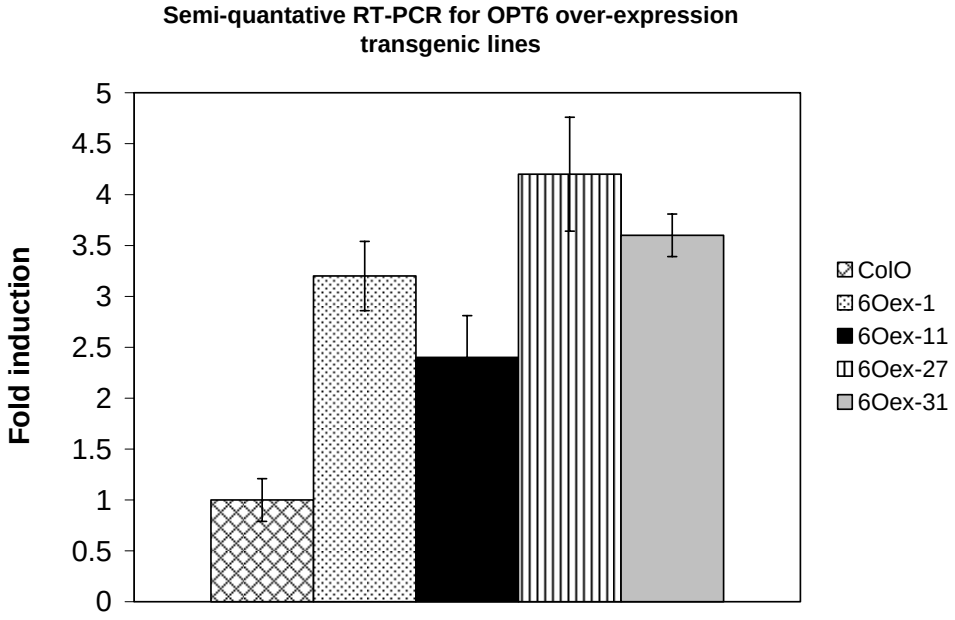

Figure 2: Quantitative real time PCR data for *AtOPT6* over-expressing transgenic lines. Four independent transgenic lines were included for quantitative real time PCR analysis and each analysis was performed in duplicate per transgenic line to determine the relative level of *AtOPT6* expression relative to the wild type. Error bars represent standard error.

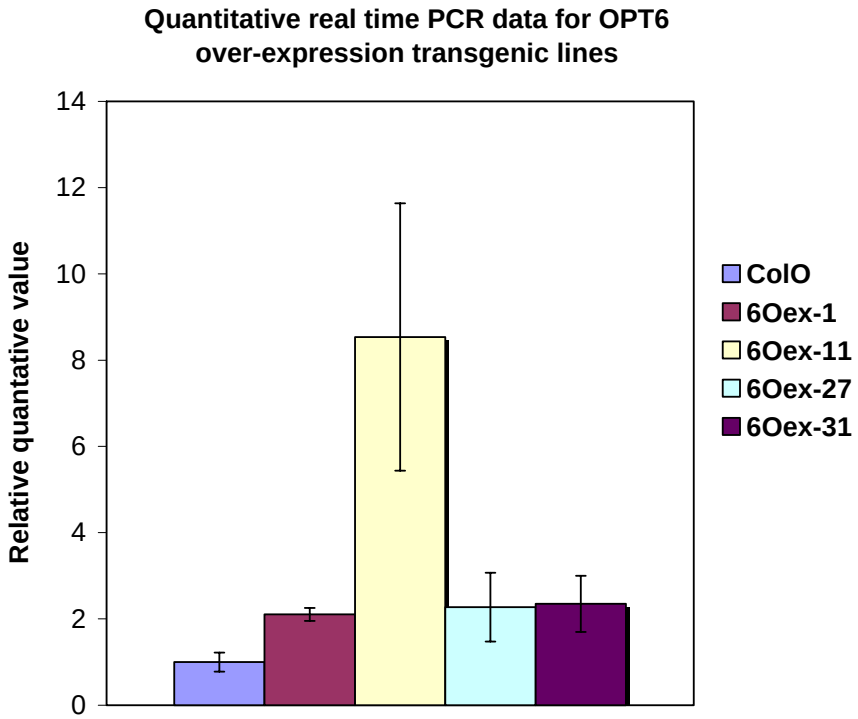

Another member of the *AtOPT* gene family, *AtOPT4*, showed improved expression in oocytes when the 5` UTR of *ScOPT1* was cloned upstream of the *AtOPT4* start codon (Osawa et al., 2006). Therefore, to improve expression of *AtOPT6* in oocytes, a similar approach was used. The 5` UTR region from *ScOPT1* was cloned upstream of the start codon of *AtOPT6* cDNA. This construct was expressed in Xenopus oocytes to examine transport of GSH, GGFL, KLLLG and GGFM was tested for *AtOPT6*. In addition, transport of PC_2 and PC + Cd transport in oocytes was also tested with two-electrode voltage clamping technique. Phytochelatins (PCs) are oligopeptides, synthesized from glutathione (GSH), with (γGlu-Cys)n-Gly (where n = 2 to 11) (Cobbett, 2000). As shown in Fig 3A, oocytes injected with *AtOPT6* cRNA showed an inward current in the presence of GSH, GGFL, GGFM and KLLLG. Surprisingly, there was no change in inward current when GLLLK was added to bath solution containing oocytes injected with *AtOPT6* cRNA. The difference in transport of KLLLG vs. GLLLK by *AtOPT6* demonstrates the substrate specificity of this transport protein.

Addition of PC_2 and PC+Cd to the bath solution showed relatively low inward current in oocytes when compared with the inward currents exhibited by GSH, GGFL, GGFM and KLLLG. There is evidence of transport of PC-Cd complex in oat roots with stochiometry of 3 Cd molecules to 1 PC_3 molecule (Salt et al., 1995). Therefore, it is possible that *AtOPT6* mediates transport of PC_3 or higher PCs and PC+Cd complex may not be well formed *in vitro* at pH 5.0, resulting in low inward currents. AtOPT6 mediated GSH transport in a dose-dependent manner (Fig 3B) with highest inward current

Figure 3: Uptake studies of glutathione and phytochelatins in *Xenopus* oocytes by *AtOPT6*.

A. AtOPT6 mediates transport of tri-, tetra- and penta-peptides in *Xenopus* oocytes.

B. AtOPT6 mediates transport of glutathione in a dose-dependent manner.

Three independent trials were carried out for each experiment and error bars indicate standard deviation.

A

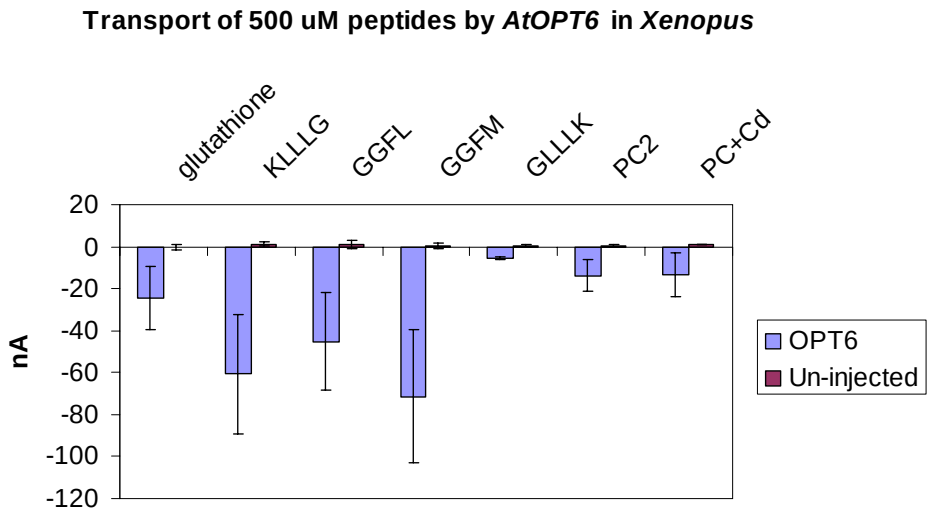

B

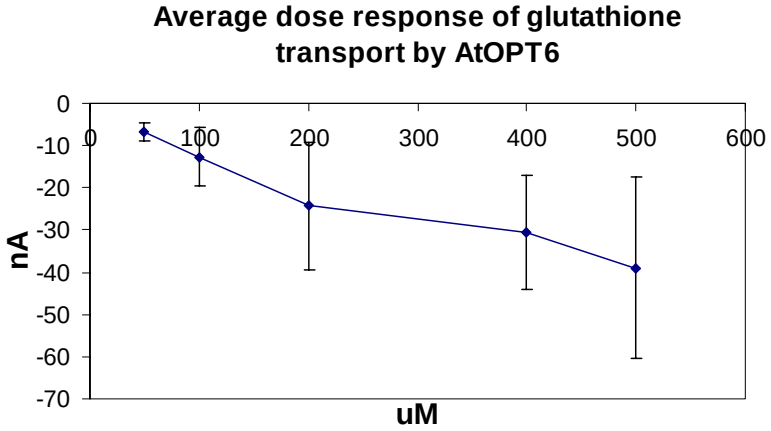

The above data was kindly provided by Sharon Pike in Dr. Walter Gassmann's laboratory.

exhibited at 500mM concentration of GSH. However, the currents were too low to calculate V_{max} amd K_m values for GSH transport.

AtOPT6 over-expressing transgenic lines are hypersensitive to cadmium

Glutathione and phytochelatins are known to complex with Cd and subsequently are sequestered into the vacuolar compartment or pumped out of the cytoplasm into the apoplastic space (Ortiz et al., 1995; Kim et al., 2007). Besides sequestration of GSH-Cd or PC-Cd complexes, long distance transport of PC-Cd from root-to-shoot and shoot-to-root was also demonstrated (Gong et al., 2003; Chen et al., 2006). However, the mechanism of this long distance transport is unknown. Three independent *AtOPT6* over-expressing transgenic lines and one wild-type control plant line were germinated and grown on ½ strength MS salt medium as a control and ½ strength MS salt medium supplied with 15μM, 20μM, 30μM, 40μM, 50μM, 75μM and 100μM $CdCl_2$ to observe the effect of cadmium on the root and shoot growth. While higher concentrations of 75μM and 100μM $CdCl_2$ completely abolished growth of both wild-type and *AtOPT6* over-expressing transgenic plants (data not shown), growth in the presence of 50μM $CdCl_2$ clearly distinguished the wild-type plants from those over-expressing AtOPT6. As shown in Fig 4A, wild-type and AtOPT6 over-expressing transgenic lines showed no difference in root or shoot growth when grown on ½ strength MS. When grown on MS supplied with 50μM $CdCl_2$, AtOPT6 over-expressing transgenic lines showed relatively higher root growth inhibition compared to wild-type plants (Fig 4B). The root growth of *opt6* mutant lines was similar to the wild-type control in both MS and MS supplied with 50μM $CdCl_2$. The root length of AtOPT6 over-expressing transgenic lines was 1 cm as

Figure 4: Root inhibition assay of wild-type (Col-O), *opt6* mutant and AtOPT6 over-expressing seedlings.

Three independent transgenic lines over expressing AtOPT6 were used in this study. This figure is representative of all three independent AtOPT6 over-expressing transgenic lines. This figure is represents a single experiment. Root inhibition assay was performed four times with similar results.

(A) *AtOPT6* Oex, *opt6* mutant and wild type seedlings were grown on ½ strength MS medium. Seedling growth was similar in all three lines.

(B) *AtOPT6* Oex, *opt6* mutant and wild type seedlings were grown on ½ strength MS medium supplied with 50 μM $CdCl_2$. *AtOPT6* Oex seedlings were hypersensitive to cadmium and showed higher root growth inhibition compared to wild-type and *opt6* mutant plants.

A

OPT6Oex *opt6* Wild-type

B

OPT6Oex *opt6* Wild-type

compared with the 3 cm root length of wild- type plants and *opt6* mutant lines (Fig 5). When root inhibition was calculated based on root length of these three lines, AtOPT6 over-expressing transgenic lines showed 85% root inhibition and wild-type control and *opt6* mutant lines showed around 65% root inhibition (Fig 6). Similarly, fresh seedling weight of AtOPT6 over-expressing transgenic lines was half (~ 80 mg) that of the wild-type control (~ 180 mg) and *opt6* mutant lines (~ 160 mg) in seedlings grown on 50μM $CdCl_2$. Fresh weight of all three independent lines was similar when seedlings were grown on MS salts only (Fig 7).

The data on root inhibition and fresh weight clearly show that the AtOPT6 over-expressing lines are hypersensitive to cadmium. The data suggested that AtOPT6 over-expressing plants accumulated higher Cd levels, than the wild-type or *opt6* mutant plants. Interestingly, *opt6* mutant and wild-type plants showed very similar levels of cadmium tolerance on 50μM $CdCl_2$. The similar level of cadmium tolerance of *opt6* mutant and wild-type plants may be due to gene redundancy among the *AtOPT* gene family members. It is possible that one or more members of the *OPT* family is transporting cadmium and, therefore, we were unable to observe a different phenotype for the *opt6* mutant line. Three independent *AtOPT6* over-expressing transgenic lines were used in the root inhibition assays and all three independent lines gave similar results, indicating that the phenotype was due to gain-of-function of *AtOPT6*.

Figure 5: Root-length comparison for wild-type, *opt6* mutant and *AtOPT6* over-expressing transgenic seedlings.

Three independent transgenic lines over expressing *AtOPT6* were used in this study. Wild-type, *opt6* and *AtOPT6* Oex transgenic seedlings were grown on ½ strength MS and ½ strength MS medium supplied with 50µM $CdCl_2$ to determine the difference in root length in the presence and absence of cadmium. The graph is representative of a single trial and error bars represent standard error. This experiment was performed four times with similar results with n = 20.

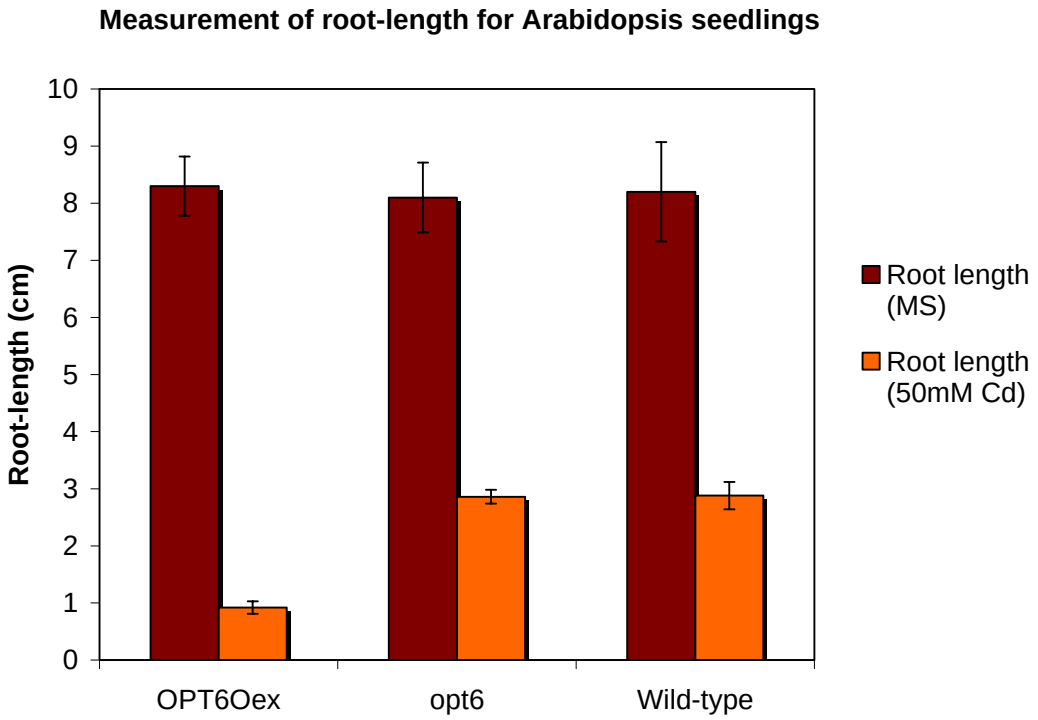

Figure 6: Root inhibition assay for wild-type, *opt6* mutant and *AtOPT6* over-expressing transgenic lines.

Three independent transgenic lines over expressing *AtOPT6* were used in this study. Seedlings were grown on ½ strength MS and ½ strength MS medium supplied with 50µM $CdCl_2$. Root length for each seedling (n=20) per treatment was measured. Root inhibition was calculated based on the root length of seedlings grown on MS (m; 100%) vs. root length of seedlings grown on MS medium supplied with cadmium (n; 100-X %); m-n/m * 100 and plotted on the graph. The graph is representative of a single trial and error bars represent standard error. This experiment was performed four times with similar results with n = 20.

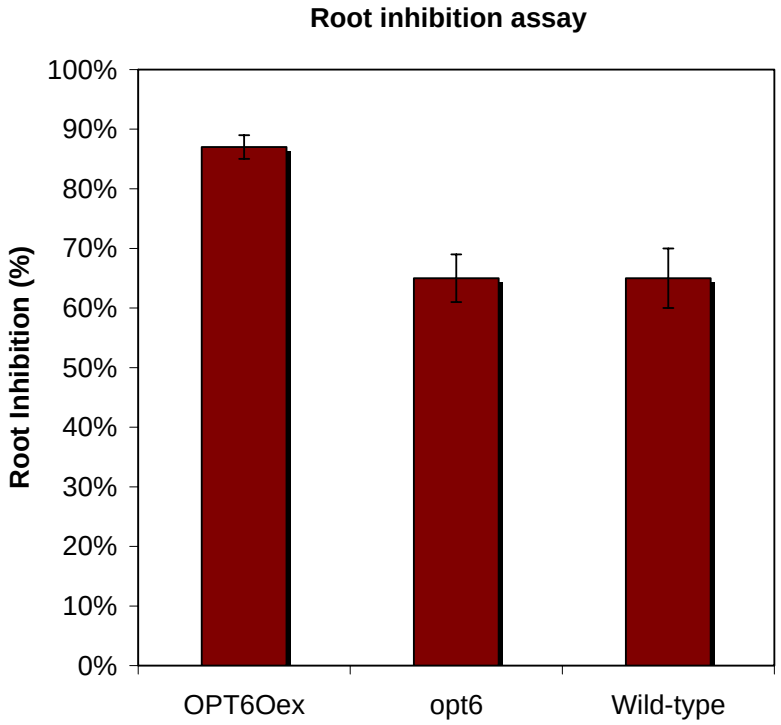

Figure 7: Fresh tissue weight of wild-type, *opt6* mutant and *AtOPT6* over-expressing transgenic seedlings.

Thre independent transgenic lines over expressing *AtOPT6* were used in this study. Plants were grown on ½ strength MS and ½ strength MS medium supplied with 50µM $CdCl_2$, tissues were harvested and their fresh weight was measured. The graph is representative of a single trial and error bars represent standard error. This experiment was performed two times with similar results with n = 20.

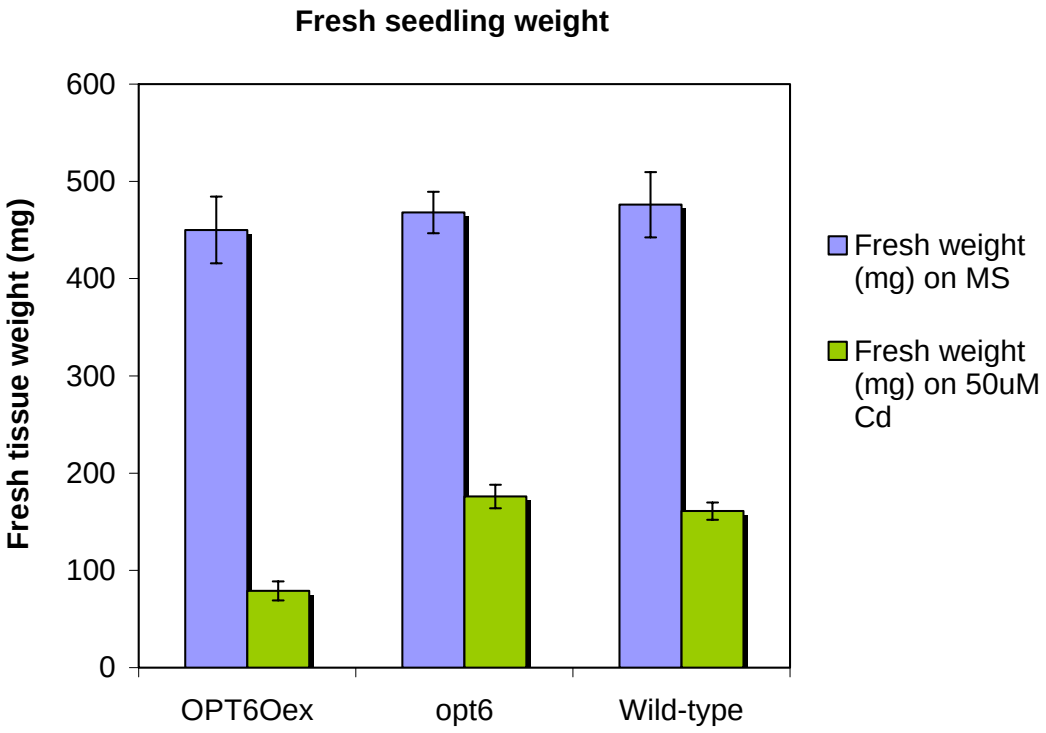

AtOPT6 over-expressing transgenic lines accumulate higher level of cadmium, GSH and PCs in roots and lower levels of cadmium and PCs in shoots

To demonstrate that the cadmium hypersensitivity phenotype and root inhibition was indeed due to accumulation of cadmium, we carried out ICP-MS analysis of Cd and thiols (GSH and PCs) that bind Cd in *AtOPT6* over-expressing transgenic lines and wild-type controls. Overall, the Cd content for both root and shoot fell in similar ranges for wild-type controls (1200 μg – 1800 μg Cd/g dry-weight) (Fig 8A-8B) However, the Cd content of *AtOPT6* over-expressing transgenic lines in roots was significantly higher at 2500 μg/g (Fig 8A). In contrast, the Cd content in shoots of *AtOPT6* over-expressing transgenic lines was approximately 900 μg/g (Fig 8B), a significantly lower value than the Cd content in roots of over-expressing lines and in the roots and shoots of wild-type plants. These data suggest that *AtOPT6* over-expressing lines do accumulate more Cd in roots, consistent with a higher degree of root inhibition and cadmium hypersensitivity than the wild-type control.

As indicated earlier, Cd is sequestered when conjugated with GSH or PCs. To determine whether Cd was transported via a GSH-Cd conjugate, we checked the levels of GSH in root and shoot tissues of both *AtOPT6* over-expressing lines and wild-type plants. As shown in Fig 9, the GSH content of wild-type roots and shoots differed greatly within lines. However, *AtOPT6* over-expressing lines showed higher levels of GSH (Fig 9A) in roots than wild-type plants and there was no difference in GSH content of *AtOPT6* over-expressing lines or wild-type plants in shoots (Fig 9B). These data suggest that Cd may be conjugated with GSH for long distance transport.

Figure 8: Cadmium accumulation data of wild-type and *AtOPT6* over-expressing plants. Three independent transgenic lines over expressing *AtOPT6* were used in this study. This graph is representation of one independent experiment. Error bars represent standard error.

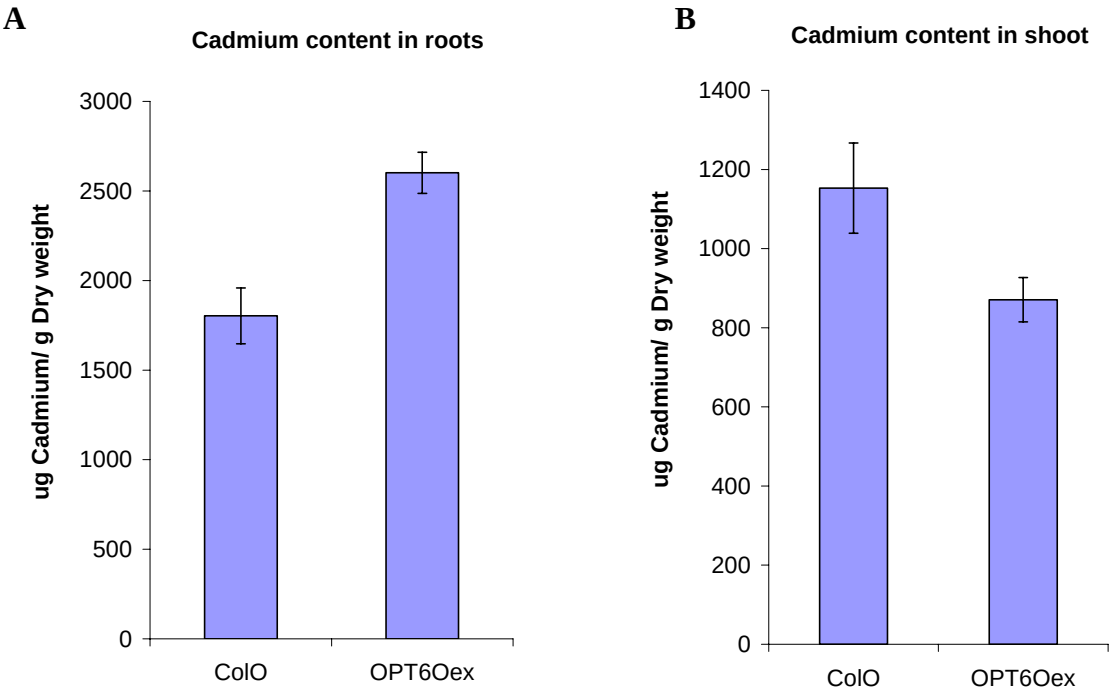

The above data was kindly provided by Dr David Mendoza in Dr. Julian Schroeder's laboratory.

Figure 9: Glutathione levels in wild-type, *opt6* and *AtOPT6* over-expressing plants. Three independent transgenic lines over expressing *AtOPT6* were used in this study. This graph is representation of one independent experiment. Error bars represent standard error.

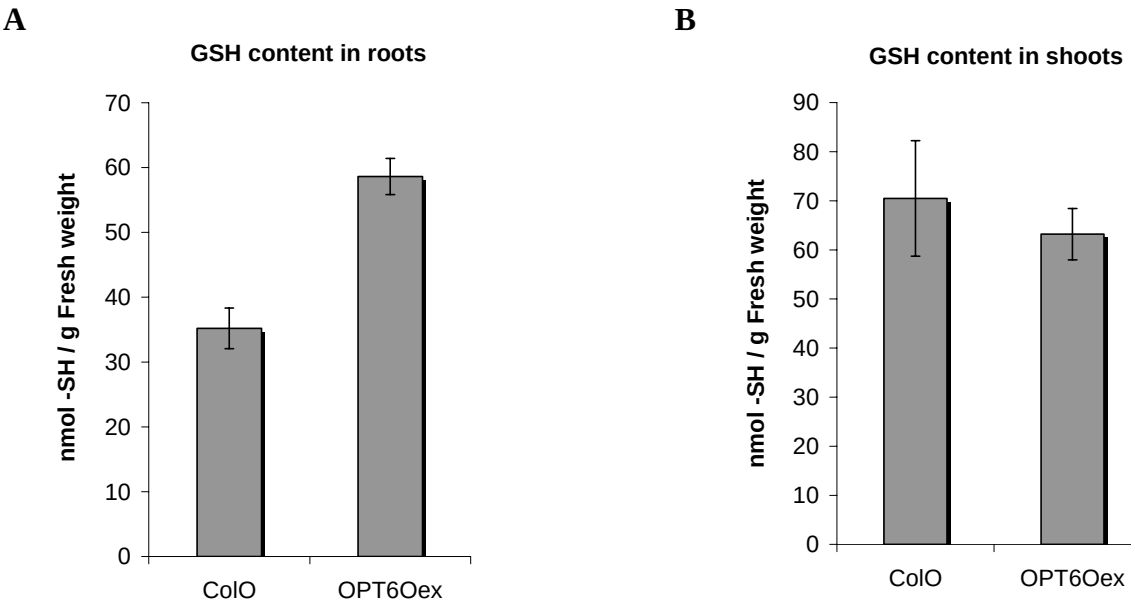

The above data was kindly provided by Dr David Mendoza in Dr. Julian Schroeder's laboratory.

Figure 10: Phytochelatin content of wild-type and *AtOPT6* over-expressing plants. Three independent transgenic lines over expressing *AtOPT6* were used in this study. This graph is representation of one independent experiment. Error bars represent standard error.

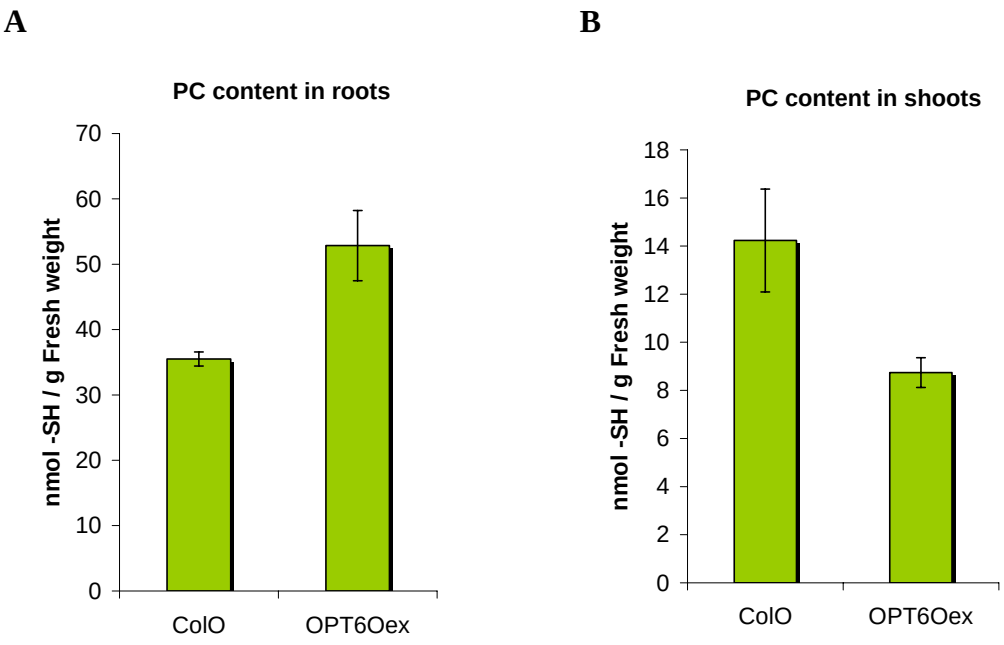

The above data was kindly provided by Dr David Mendoza in Dr. Julian Schroeder's laboratory.

The PC content in roots of *AtOPT6* over-expressing lines was considerably higher than the overall PC content of roots and shoots in wild-type controls (Fig 10A-10B). The accumulation of PCs in roots of over-expressing lines was almost two-fold higher at 55 nmols/g, as compared with 35 nmols/g of PCs in the roots of wild-type controls (Fig 10A). Accumulation of PCs in shoots of *AtOPT6* over-expressing lines was almost 10 times lower than PCs in shoots of over-expressing lines and half that of PCs in the shoots of wild-type control. Notably, this suggests that Cd in the *AtOPT6* over-expressing transgenic plants is primarily in the form of a PC-Cd complex. The accumulation in roots is consistent with the greater inhibition of root growth in the *AtOPT6* over-expressing transgenic plants.

DISCUSSION

AtOPT6 mediates glutathione and peptide transport in the heterologous system

To improve the expression of *AtOPT6* in oocytes, the 5` UTR of *ScOPT1* was cloned upstream of *AtOPT6* cDNA and transport properties were examined in oocytes using two-electrode voltage clamping. Transport studies in oocytes demonstrated that *AtOPT6* transports various peptides including GGFM, GGFL and KLLLG. Surprisingly, *AtOPT6* was unable to transport GLLLK, KG or KLG (Fig 3A and data not shown; Sharon Pike – personal communication) indicating that *AtOPT6* possesses very distinct substrate specificity for various peptides. GSH, a tri-peptide is also transported by *AtOPT6*, supporting the previous data of GSH transport in yeast (Cagnac et al., 2004). Dose-dependent transport studies demonstrated that *AtOPT6* mediates GSH uptake in a concentration dependent manner. However, the inward currents were too small to calculate kinetic parameters for GSH transport. The inward currents and dose-dependent GSH uptake suggests that *AtOPT6* is a low-affinity GSH transporter. The ability of *AtOPT6* to transport PC_2 and PC+Cd at very low levels indicates that the choice of PCs may be different for *AtOPT6*. Also, it is not known whether PCs can form a complex with Cd *in vitro*. It is possible that *AtOPT6* mediates PC_3, PC_4 or PC_5 transport. It is difficult to chemically synthesize and dissolve longer PCs and therefore transport of longer PCs by *AtOPT6* in oocytes was not tested.

AtOPT6 over-expressing lines contain higher amount of PCs in roots

In addition to Cd, the root PC content of the *AtOPT6* over-expressing lines was also notably higher than the level in shoots. The combined data of higher Cd and higher PC in roots supports the notion that PC-Cd complex is formed in *AtOPT6* over-expressing plants. It was surprising that the shoot Cd content of the over-expressing lines was lower than the root Cd levels. It was shown that PCs can be transported from roots to shoots and over-expression of the phytochelatin synthase (PCS) gene increased long-distance, root-to-shoot transport of Cd, suggesting that Cd is transported as a PC-Cd complex (Gong et al., 2003). It is possible that *AtOPT6* mediates long distance transport of PC-Cd complex from shoot-to-root, where PC-Cd is sequestered in the vacuole in shoot tissue or stored in the apoplastic space. However, PC_2-Cd complex failed to induce inward currents in oocytes expressing *AtOPT6* cRNA (Sharon Pike – personal communication). It may be possible that the PC-Cd complex contains PC_3 or higher PCs and therefore PC2-Cd did not show any inward currents in *Xenopus*. There is evidence for the transport of PC_3-Cd in the oat roots (Salt et al., 1995).

In conclusion, the over-expression of *AtOPT6* results in hypersensitivity to Cd, as manifested by root growth inhibition and accumulation of Cd and thiols, mainly PCs, in roots relative to the wild-type control. Heavy metals such as Cd, Pb, and Ni pose a threat to the environment and are among the contaminants that need to be removed from soil, a process broadly known as phytoremediation. Plants have the ability to hyper accumulate various heavy metals by action of phytochelatins forming a complex with heavy metals and sequester them into vacuole (Suresh and Ravishankar, 2004). Various strategies are used to generate plants capable of phytoremediation such as construction of transgenic

plants with higher PC levels to enhance uptake of heavy metals, testing multiple genes of hyper-accumulator species (e.g. *Arabidopsis halleri*) involved in phytoremediation and expressing them in plants with greater biomass (e.g. poplar) (Chang et al., 2005). *AtOPT6* over-expression may become a part of various strategies for cadmium phytoremediation.

CHAPTER III: ROLE OF *AtOPT6* DURING BACTERIAL PATHOGENESIS IN PLANTS

INTRODUCTION

Plants possess a battery of mechanisms to defend themselves from potential pathogens. These mechanisms range from pre-existing resistance to induced resistance. Pre-existing resistance includes the cuticle and plant cell wall, which act as barriers preventing entry of pathogens into host cells. Induced resistance includes basal defense and gene-for-gene resistance. To evade bacterial pathogens, the basal defense responds to complex pathogen-associated molecular patterns (PAMPs) (Nurnberger and Brunner, 2002), whose recognition induces various defense responses. In gene-for-gene resistance, plants employ resident disease-resistance (R) proteins that recognize the effector proteins (avirulence proteins) secreted by pathogens. This recognition results in an acceleration and amplification of the defense response (Kim et al., 2005). *RPS2* was the first plant *R* gene cloned from *Arabidopsis* and confers resistance against the bacterial pathogen *Pseudomonas syringae* expressing the avrRpt2 effector protein (Bent et al., 1994; Mindrinos et al., 1994). A plethora of genes encoding transcription factors, receptor kinases, protein kinases and transport proteins play a variety of roles during plant defense triggered upon recognition of bacterial effector proteins (Li et al., 2004, Kim et al., 2005, Campbell et al., 2003).

There are also low molecular weight compounds, such as β-aminobutyric acid (BABA), phytoalexins and defensins, which protect plants against pathogens, either through their direct anti-microbial effects or through activation of other defense mechanisms (Zimmerli et al., 2000, Darvill and Albersheim, 1984, Hilpert et al., 2001). BABA is a non-protein derived amino acid implicated in protection of Arabidopsis against fungal pathogens through activation of defense mechanisms, such as callose deposition and the hypersensitive response (HR) (Zimmerli et al., 2000). Phytoalexins are antimicrobial compounds synthesized by plants upon infection. Accumulation of phytoalexins was shown to be instrumental in disease resistance (Darvill and Albersheim, 1984).

For successful pathogen colonization, the key step is suppression of host defenses. Besides the effector proteins, plant pathogenic bacteria are also equipped with an arsenal of non-host specific toxins that contribute to virulence. These non-host specific toxins contribute to virulence but are not required for pathogenicity and their production aids in bacterial fitness. Most pathovars of the bacterial pathogen *Pseudomomas syringae* produce a family of structurally diverse phytotoxins, some of which are peptide in nature (Gross et al., 1991). These toxins include coronatine, tabtoxin, phaseolotoxin, syringomycins and syringopeptins. Coronatine, phaseolotoxin and tabtoxin generally induce chlorosis whereas syringomycin and syringopeptins induce necrosis in host tissue (Gross et al., 1991).

Coronatine (COR) is composed of two distinct components: coronafacic acid (CFA) and coronamic acid (CMA). CFA is a polyketide and CMA is an α-amino acid derived moiety. CMA and CFA moieties are synthesized via different biochemical

pathways but are coupled together in the final step of COR biosynthesis by an amide linkage to the polyketide moiety (Ichihara et al., 1977). COR is the most toxic of all phytotoxins and the primary symptom in host tissue is chlorosis. COR also causes cell wall thickening, changes in chloroplast structure, hypertrophy, inhibition of root elongation and stimulation of ethylene production (Palmer and Bender, 1995; Kenyon and Turner, 1992). There is a strong structural and functional similarity between COR and methyl jasmonate (MeJA), a plant defense signaling molecule derived from the octadecanoid pathway involved in JA biosynthesis, which is elicited by biological stress (Figure 1; Wasternack and Parthier, 1997). Both COR and MeJA induce similar biological responses in tomato cells and potato tissues, suggesting that COR might function as a molecular mimic of the octadecanoid signaling molecules upon entry into the host cell (Greulich et al., 1995). Moreover, a *coronatine-insensitive* (*coi1*) mutant in *Arabidopsis* showed insensitivity to both COR and MeJA, suggesting a similar mode of action (Feys et al., 1994). However, jasmonic acid and COR induced production of different volatile compounds in lima bean tissues (Krumm et al., 1995) indicating that COR does not necessarily function as a direct molecular mimic of MeJA. It may be possible that COR interacts with a plant receptor to activate downstream signaling or is transported into the cytoplasm where it activates the octadecanoid-signaling pathway. The mechanism of COR function will remain unclear until putative receptors or transporters for this toxin are discovered in plant species.

Syringomycin is a cyclic lipodepsinonapeptide composed of a polar peptide and hydrophobic 3-hydroxy fatty acid tail (Fukuchi et al., 1992). Plasma membranes of the host cells are the primary target. The lipopeptide promotes insertion of syringomycin into

the lipid bilayer forming pores resulting in an increase in transmembrane fluxes of calcium, potassium and protons that are deadly to host cells (Bidwai and Takemoto, 1987). Syringopeptins are lipodepsipeptides consisting of 22-25 amino acids (Ballio et al., 1991). They exhibit close similarity to syringomycin in phytotoxic activity and also cause electrolyte leakage of plant cells, thus leading to necrosis (Iacobellis et al., 1992). Tabtoxin is a monocyclic β-lactam compound. This dipeptide toxin contains the unusual amino acid tabtoxinine-β-lactam linked by a peptide bond to form tabtoxin. Tabtoxin inhibits glutamine synthetase, a key enzyme for nitrogen assimilation and the only enzyme that can detoxify ammonia, which otherwise causes a variety of harmful effects in host cells (Turner and Debbage, 1982). Phaseolotoxin consists of sulfodiaminophosphinyl moiety linked to a tripeptide consisting of ornithine, alanine and homoarginine (Mitchell 1976). Phaseolotoxin inhibits ornithine carbamoyl transferase (OCTase), which converts ornithine and carbamoyl phosphate to citrulline. Inhibition of OCTase in plant cells causes an accumulation of ornithine and a deficiency in the intracellular pool of arginine leading to chlorosis (Mitchell and Bieleski, 1977). Phytotoxin biosynthesis, regulation and modes of action are well characterized. However, the mode of transport of tabtoxin, phaseolotoxin and coronatine into the host cytoplasm is yet to be elucidated.

Multiple transport proteins belonging to the ABC, sugar and peptide transporter families have been implicated in bacterial pathogenesis. A member of the peptide transport family, *AtPTR3*, had elevated transcripts levels upon wounding (Karim et al., 2005). *Atptr3* mutants were more susceptible to *P. syringae* and *Erwinia caratovora* pathogens and produced more reactive oxygen species (Karim et al., 2007).

Figure 1: Structure of coronatine and MeJA for comparison.

The coronafacic acid (CFA) moiety closely resembles MeJA structure. This figure is taken from Uppalapati et al., 2005.

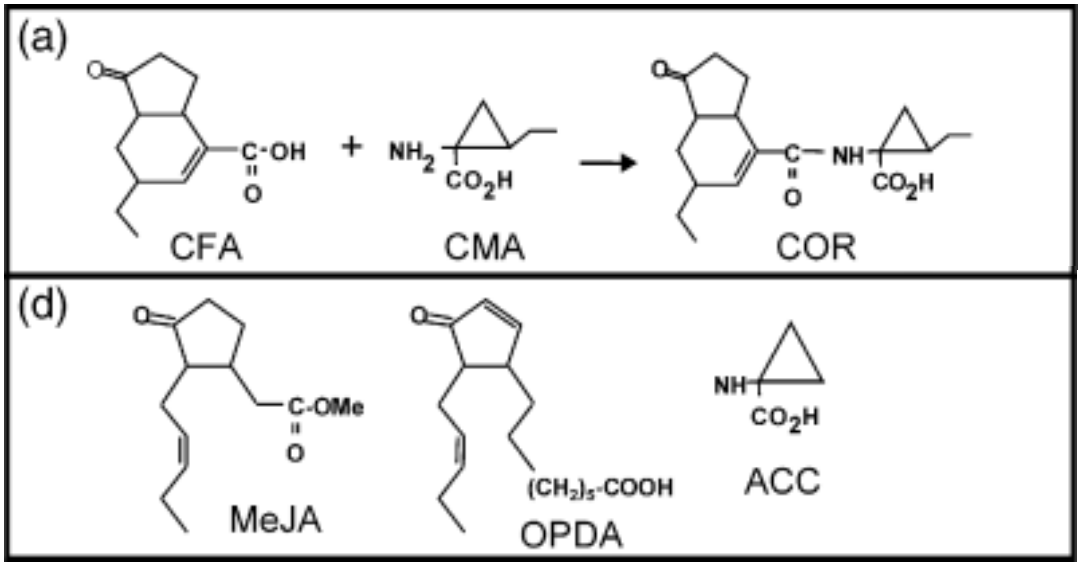

The increase in susceptibility to bacterial pathogens in *Atptr3* mutant plants and the level of transcript accumulation upon wounding suggests that *AtPTR3* may be involved in protecting plants against biotic and abiotic stress (Karim et al., 2007). A sugar transport protein, *AtSTP4*, is induced in leaves infected with a fungal pathogen and the induction coincides with glucose uptake in host tissue after fungal infection (Fotopoulos et al., 2003). There is also coordinated expression of *AtSTP4* and a cell wall invertase, *Atβfruct1*, during the host response to fungal infection suggesting a functional connection to supply sugars to infected host cells (Fotopoulos et al., 2003). Thus, evidence exists that transport proteins play a secondary role during plant defense and are also a target for pathogenicity, possibly providing nutrition to the proliferating pathogen or directing accumulation of phytotoxins at infection sites. In this chapter, I will discuss the role of AtOPT6 during bacterial pathogenesis.

METHODS AND MATERIALS

Bacterial strains

The bacterial pathogen *Pseudomonas syringae* pv. *Tomato* (*Pst*) strain DC3000 was used in this study. A bacterial strain defective in coronotine synthesis (COR^-) was kindly provided by Dr. Barbara Kunkel from Washington University (Brooks et al., 2004).

Plant material and growth conditions

Arabidopsis thaliana ecotype ColO was used in this study. All transgenic lines mentioned in this study were of the ColO background. All plants used in this study were maintained in growth chambers under an 8 hour light/ 16 hour dark photoperiod at 22 °C, 70% relative humidity and 130 EC m^{-1} s^{-2} light intensity.

Inoculation and disease assay

Disease growth assays were carried out on 5-6 week-old plants. All bacterial strains were freshly grown on NYG (0.5% Bacto-peptone, 0.3% yeast extract, 2% glycerol and 1.5% bacto agar; pH 7.0 with 1M NaOH) plates containing appropriate antibiotics. Bacterial suspensions were made in 10mM $MgCl_2$. Fully grown leaves were selected to perform disease assays and individual leaves were syringe-inoculated with 1 x 10^6 CFU/ml of bacterial suspension. Disease assays were scored at 0 and 3 days by bacterial counting. Four leaf punches (0.45 μm in diameter) were collected in triplicate for each bacterial strain per *Arabidopsis* line and ground in 100 μl of 10mM $MgCl_2$. Appropriate dilutions were made and the diluted suspension was spread on NYG plates containing appropriate

antibiotics. All plates for bacterial counts were incubated at 28 °C for 2 days and the total number of bacterial colonies was counted. Calculations for bacterial assay were performed as below:

$$\text{Day 0 }_{\text{CFU/ml}} = N * \frac{[V_{TO} / V_{TS}]}{Y * LDA}$$

N = number of colonies

Y = number of leaf discs used

V_{TO} = Volume of original suspension

V_{TS} = volume spread per plate

LDA = Leaf disc area

$$\text{Day 3 CFU/ml} = N * DF * \frac{[V_F / V_{TS}]}{Y * LDA}$$

Where symbols are noted above except:

Df = dilution factor

V_F = final volume

For graph, average CFU/ml was calculated for each inoculum/time point and the averages were converted into a log scale. Triplicate samples were averaged for each time point.

RESULTS

The *opt6* mutants exhibited less susceptibility to *Pseudomonas syringae* pv. *tomato* DC3000

Public microarray data revealed that *AtOPT6* transcripts were up-regulated 24 hours post infection with *Pst* DC3000. The microarray data suggested a possible involvement of *AtOPT6* during the plant defense response. Therefore, to investigate the role of *AtOPT6* during bacterial infection, wild-type (Col-0) plants, *AtOPT6* over-expressing transgenic lines (two independent lines were used in this study) and *opt6* mutant plants were infected with virulent *Pst* DC3000. Experiments with *Pst* DC3000 revealed that *opt6* mutant plants had reduced susceptibility and developed mild to no chlorosis in the infected leaves 3 days post infection (Fig 2). In contrast, the wild-type control plants and *AtOPT6* over-expressing plants developed chlorosis and displayed higher susceptibility to *Pst* DC3000.

To determine whether the decreased chlorosis symptoms in *opt6* mutant plants was correlated with decreased bacterial growth in plant leaves, levels of *Pst* DC3000 were measured over the course of infection (Fig 3). When compared in all three lines infected with *Pst* DC3000, *opt6* mutant plants supported one order of magnitude fewer bacteria than wild-type control plants. In AtOPT6 over-expressing lines, the bacteria multiplied to similar orders of magnitude as the wild-type control. At 3 days post infection, bacterial numbers were approximately 10-fold lower in *opt6* mutant plants when compared to wild-type controls or AtOPT6 over-expressing plants.

Figure 2: Chlorosis observed in wild-type, *opt6* mutant and *AtOPT6* over-expressing transgenic plants in response to bacterial infection.

Leaves from wild-type, *opt6* mutant and *AtOPT6* over-expressing lines showed variable amounts of chlorosis 3 days post infection with *Pst* DC3000 at a concentration of $1 * 10^6$ CFU/ml. Note the amount of chlorosis in the *opt6* mutant leaves as compared with wild-type and *AtOPT6* over expressing lines. Similar results were observed in all three independent biological experiments.

Wild-type *opt6 mutant* OPT6 Oex

Pst DC3000

Figure 3: Bacterial growth assay for wild-type, *opt6* mutant and *AtOPT6* over-expressing lines using *Pst* DC3000.

Two independent transgenic lines over expressing AtOPT6 were used in this study and both gave similar results. However, data for only one AtOPT6 over expressing line is included in this graph. This graph is representative of 3 independent biological experiments. Bacterial growth assays were done in triplicate for each plant line and each strain and the average of the triplicate of a single experiment is plotted. Error bars represent standard deviation.

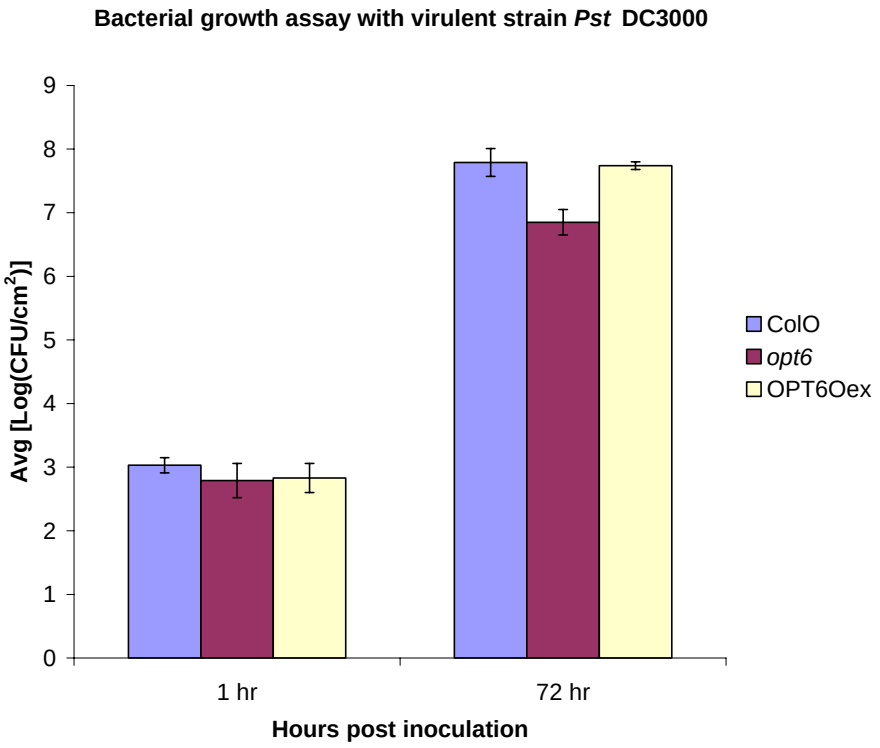

Thus, *opt6* mutant plants exhibited reduced bacterial growth levels compared to wild-type and *AtOPT6* over-expressing plants. This difference in bacterial growth also correlated well with the milder chlorotic symptoms observed in *opt6* mutant plants compared with wild-type plants.

opt6 mutant plants exhibited similar sensitivity to the wild-type control and _AtOPT6_ over-expressing plants when infected with a _Pst_ DC3000 strain deficient in coronatine production

During successful infection in host plants, chlorosis is often associated with the release of coronatine into host cells by virulent *Pst* DC3000 (Gross, 1991). During infection with *Pst* DC3000, *opt6* mutant plants displayed mild to no chlorosis and reduced susceptibility and bacterial growth. To explore the possibility that the reduced chlorosis in *opt6* mutant plants was due to lack of movement of coronatine into host cells, wild-type control plants, *opt6* mutant plants and *AtOPT6* over-expressing plants were infected with a *Pst* DC3000 strain deficient in coronatine (COR^-) production and bacterial growth was observed over the course of infection. The COR^- strain has a Tn5 insertion in the *cfa* and *cma* genes, encoding enzymes responsible for the synthesis of coronafacic acid (CFA) and coronamic acid (CMA), respectively, two well defined intermediates in COR biosynthesis. COR^- mutants are impaired in their ability to multiply at higher levels and to elicit disease symptoms on *A. thaliana* (Brooks et al., 2004). As shown in Fig 4, when infected with COR^- strain, all three plants showed similar levels of bacterial growth.

Figure 4: Bacterial growth assay with *Pst DC3000* and COR$^-$ bacterial strains.

This graph is representative of 2 independent biological experiments. Bacterial growth assays were done in triplicate per each plant line per each strain and the average of a single experiment is plotted. Error bars represent standard deviation.

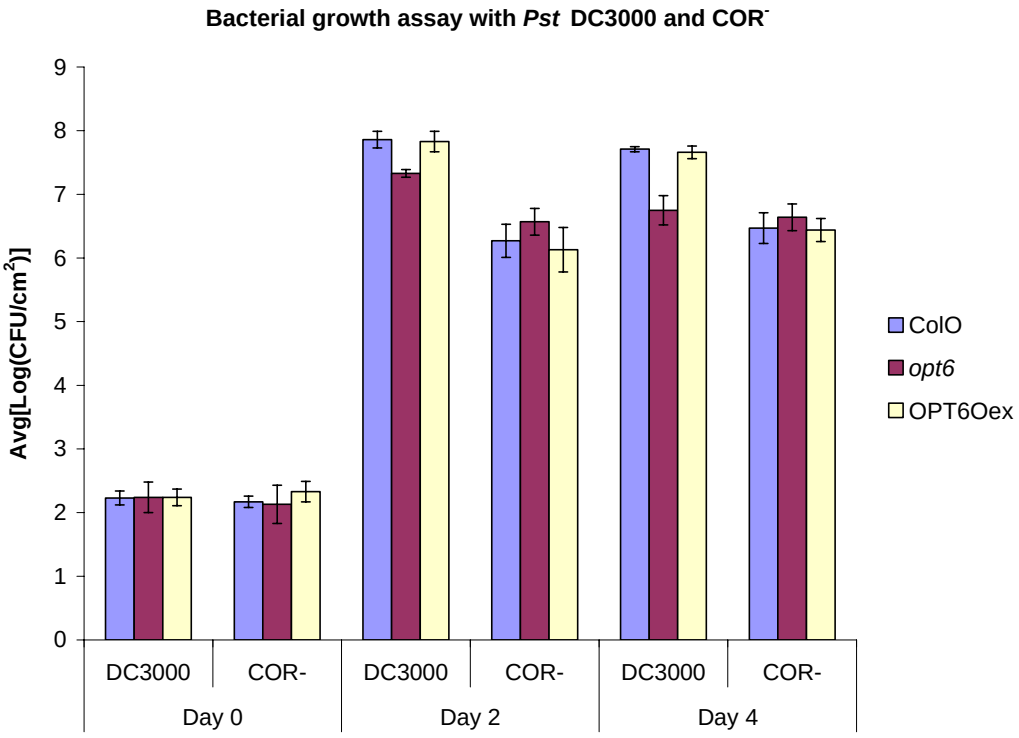

In all three lines, bacteria multiplied approximately four orders of magnitude in the first two days following infection and reached stable population levels at day four with no subsequent increase in bacterial growth. Infection with *Pst* DC3000, in contrast elicited similar responses with *opt6* mutant plants exhibiting one order of magnitude lower bacterial growth than wild-type and *AtOPT6* over-expressing plants within the first two days (compare Fig 3 and Fig 4). However, over the next two days, bacterial populations failed to increase and rather declined in *opt6* mutant plants (Fig 4).

Thus, the *opt6* mutant plants exhibited one order of magnitude lower bacterial growth when infected with virulent strain *Pst* DC3000 and displayed no difference in bacterial population when infected with the *Pst* DC3000 strain deficient in COR production. Moreover, very mild to no chlorosis was observed in all three lines when infected with the COR^- strain. Taken together, these data indicate that coronatine plays a role in developing chlorosis in infected host tissues and a lack of coronatine in host plant cells impairs the ability of pathogen to obtain peak population levels. It also suggests that *AtOPT6* may be involved in transport of coronatine into host cells. Transport of coronatine by *AtOPT6* still remains to be studied.

DISCUSSION

Virulent bacterial pathogen *Pst* DC3000 manipulates *AtOPT6* during pathogenesis to promote bacterial proliferation in host cells

The reduced susceptibility of *opt6* mutant plants to the virulent bacterial pathogen *Pst* DC3000 supports microarray data indicating up-regulation of *AtOPT6* transcripts 24 hours post infection. *opt6* mutant plants exhibited one order of magnitude lower bacterial multiplication *in planta* than wild-type control plants and were less susceptible to the pathogen. Interestingly, *AtOPT6* over-expressing plants did not show an increase in susceptibility and bacterial multiplication was similar to wild-type plants. Multiple players and pathways are involved in plant defense during bacterial infection. The role of transport proteins may be limited to providing nutrition for bacterial growth or delivery of small molecules such as phytotoxins into host cells. Therefore, the difference in bacterial populations is not as substantial as when primary players of plant defense are involved, such as R genes. One cannot rule out functional redundancy among the various AtOPT transporters, which exhibit up to 85% sequence similarity. It is possible that mutant plants defective in two or more AtOPT transporters could show a much more pronounced bacterial infection phenotype.

A few transport proteins have been suggested to play a role in plant defense during bacterial invasion. *AtPTR1*, a di- and tri-peptide transport protein, was shown to mediate transport of the bacterial phytotoxin phaseolotoxin in addition to transporting several acidic, neutral and basic amino acids (Dietrich et al., 2004). However, the importance of *AtPTR1* during bacterial pathogenesis is still unknown. Mutant plants

defective in another member of the *PTR* super-family, *AtPTR3*, showed increased susceptibility to bacterial pathogens. The suggestion was made that *AtPTR3* is probably one of the defense-related genes involved in protecting plants against biotic and abiotic stresses (Karim et al., 2007). The type of substrate transported by *AtPTR3* is still unknown. In this study, the absence of *AtOPT6* results in reduced bacterial populations *in planta*. These data suggest that *AtOPT6* is somehow utilized by successful pathogens to deliver phytotoxins or other signaling molecules essential during successful invasion and subsequent pathogenesis.

AtOPT6 may be involved in transport of bacterial phytotoxins

The number of transport proteins implicated to play a role during plant defense is growing. *AtOPT6*, a member of *OPT* gene family, was shown to have an impact on bacterial growth during a compatible interaction with the pathogen. However, the mode of action by which *AtOPT6* functions during bacterial invasion is still unclear. However, preliminary data with a COR $^{-}$ strain suggests that *ATOPT6* might be involved in transport of phytotoxins such as coronatine. *opt6* mutant plants exhibited mild to no chlorosis when infected with *Pst* DC3000. Moreover, bacterial growth assays with a COR $^{-}$ strain showed no substantial difference in bacterial populations among wild-type, *opt6* mutant and *AtOPT6* over-expressing lines. Conversely, infection with *Pst* DC3000 showed one order of magnitude lower bacterial multiplication in *opt6* mutant plants. Taken together, these data suggest that *AtOPT6* might be involved in transport of a phytotoxin like coronatine, which is known to contribute to *Pst* DC3000 growth and colonization of host tissues. However, this phytotoxin is not the primary virulence factor

responsible for disease and it was shown that disease and bacterial proliferation occurs even in the absence of coronatine production (Brooks et al., 2004), which can explain the lower difference of bacterial growth in *opt6* mutant plants as compared with wild-type controls. COR, especially the CFA moiety, shares structural and functional relatedness with methyl jasmonate (MeJA), a plant growth regulator and defense signaling molecule produced under wounding (Wasternack and Parthier, 1997). It is also known that *Pst* DC3000 takes advantage of COR to manipulate jasmonate signaling within the host to support bacterial growth and disease development (Laurie-Berry et al., 2006). Transport studies of MeJA by *AtOPT6* in *Xenopus* oocytes did not reveal uptake of MeJA by *AtOPT6* ruling out the possibility that *AtOPT6* is involved in transport of this signaling molecule (Sharon Pike, personal communication). To provide solid evidence in support of the hypothesis that *AtOPT6* transports COR, the uptake of COR by *AtOPT6* needs to be tested.

CHAPTER IV: THE ROLE OF *AtOPT6* DURING PLANT-NEMATODE INTERACTIONS

INTRODUCTION

Plant parasitic nematodes can infect a wide range of crop plant species and are known to cause billions of dollars of loss each year in terms of agricultural yield (Koenning et al., 1999). Several species of nematodes are plant parasites. The most economically important plant-parasitic nematodes are the root-knot nematodes (RKNs; *Meloidogyne* spp.) and the cyst nematodes (*Heterodera* and *Globodera* spp.). Both cyst and root-knot nematodes are obligate parasites and they feed solely on the cytoplasm of living host cells (Williamson and Gleason, 2003). They are sedentary endoparasites and have complex interactions with their host plants but demonstrate distinct differences in their migration pattern, development of feeding site and parasitic life cycle (Davis et al., 2000). Both cyst nematodes and root-knot nematodes have wide host range and these plant parasites can infect thousands of plant species in a similar manner, probably by altering fundamental elements of plant cell development (Vanholme et al., 2004).

During compatible interactions, the infective second-stage juveniles (J2) of RKN penetrate behind the root tip and migrate between cells to invade the vascular cylinder. J2 cyst nematodes can enter the host cells at any point and migrate intracellularly towards the vasculature of the root. Once inside the root, both RKN and cyst nematodes form complex multinucleate feeding cells, which provide nutrients to the parasite. Cyst

nematodes form feeding cells called syncytia by dissolution of cell walls and fusion of neighboring cells. The syncytia increase in volume by integrating adjacent cells (Jones, 1981). RKNs dedifferentiate 5-7 parenchymatic root cells around its head into multinucleate and hypertrophied giant-cells (Fig. 1). These giant-cells are formed by repeated cycles of mitosis without cytokinesis (Jones, 1981). Both syncytia and giant-cells are multinucleate cells with thickened cell walls that form elaborate ingrowths and contain dense granular cytoplasm, numerous mitochondria, plastids, ribosomes, well developed Golgi apparatus, endoplasmic reticulum and a number of small vacuoles (Wiggers et al., 1990). During early stages of cyst nematode infection, there is no symplastic connection between the syncytia and phloem, thus requiring active transport of nutrients into developing syncytia. At later stages when the syncytia expand and reach the phloem cells, a symplastic connection is established between syncytia and phloem via functional plasmodesmata allowing nutrient transport into the syncytia (Hoth et al., 2005; Hoffmann and Grundler, 2006; Hoffmann et al., 2007).

For successful invasion and establishment of feeding sites, secretions are released during penetration, migration and feeding cell formation. These parasitic nematodes use a stylet, a hollow, protrusible feeding structure, to penetrate the plant cell wall. Upon penetration into the plant cell wall, stylet secretions are released from adjacent glands into the cell and are then used to extract nutrients from the host cytoplasm (Davis et al., 2000). Gland secretions contain a variety of parasitism proteins that are known to induce morphological, physiological and molecular changes in the host root cells. These secreted proteins alter host gene expression and aid in modification of specific host root cells into syncytia and giant-cells, which act as a continuous source of nutrients for the nematode

(Bird, 1996). Several nematode parasitism genes encoding the stylet-secreted proteins have been identified. Parasitism genes encode stylet secretions that are protein in nature and are synthesized in the esophageal gland cells of the nematode. These proteins are secreted into the host during parasitic stages of nematode infection and act as primary signaling molecules during plant-nematode interaction to help the nematode during migration within plant tissues, feedling cell formation and nematode feeding activity (Davis et al., 2000).

β-1,4-endoglucanase genes from cyst nematodes were successfully isolated using an esophageal gland-specific monoclonal antibody (Smant et al., 1998). These endoglucanases facilitate cell wall degradation during intracellular migration of nematodes through plant roots. Several other β-1,4-endoglucanase genes have since been cloned from cyst and RKN by homology-based cloning or EST analysis. These genes were up-regulated upon infection in both *Arabidopsis* and tobacco roots (Rosso et al., 1999; Goellner et al., 2000; Goellner et al., 2001). Several other genes encoding cell wall modifying proteins, such as pectate lyase, β-1,4-endoxylanase and a cellulose-binding protein, were also identified from gland secretions of cyst and RKN (Doyle and Lambert, 2002; Dautova et al., 2001; Ding et al., 1998). Nematode β-1, 4-endoglucanase genes have similarity with bacterial genes suggesting a horizontal gene transfer from bacteria (Davis et al., 2000).

After becoming established in the host root tissues, both cyst and RKN likely need to evade plant defenses in order to form feeding cells to support their growth and reproduction. These plant-parasitic nematodes are known to secrete proteins that may play a role in suppressing plant defense. Chorismate mutase, an RKN esophageal gland-

Figure 1: Life cycle of cyst and root-knot nematodes.

A. Life cycle of cyst nematode (*Heterodera* and *Globodera* spp.)

B. Life cycle of root-knot nematode (*Meloidogyne* spp.)

This figure is taken from Williamson and Gleason, 2003.

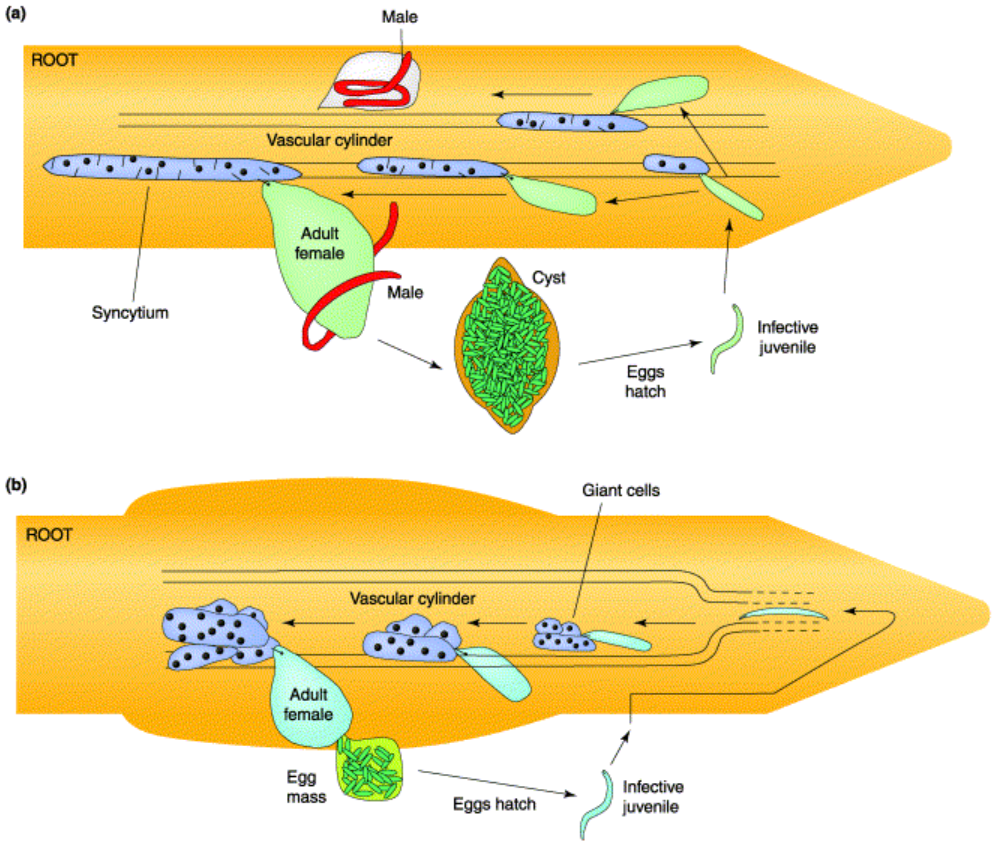

specific protein was implicated in the suppression of plant defense. Plant chorismate mutases are the main enzymes in the shikimic acid pathway involved in the synthesis of cellular amino acids, phytohormones and plant defense compounds. It was proposed that nematode chorismate mutase may alter the synthesis of chorismate-dependent compounds, which are involved in formation of the cell wall, as well as the biosynthesis of hormones and defense compounds (Doyle and Lambert, 2002). A second RKN effector protein involved in modulating plant defense is calreticulin. Calreticulin is secreted into the feeding site via the stylet and accumulates in cell walls of giant cells and is thought to be involved in calcium signaling and cell cycle regulation during giant cell formation (Borisjuk et al., 1998).

Recently, a 13-amino acid peptide, 16D10, secreted from esophageal glands of RKN parasitic juveniles into host cells, was shown to interact with two SCARECROW-like transcription factors *in vivo*. Transgenic expression of 16D10 in tobacco hairy roots stimulates root growth and generates extensive lateral roots (Huang et al., 2006a). *In vivo* RNAi silencing of parasitism gene 16D10 in *Arabidopsis* resulted in higher resistance against 4 RKN species (Huang et al., 2006b), suggesting a clear role for this peptide in RKN parasitism. Another nematode parasitism gene involved in modification of host plant cells is *Hg-SYV46*. *Hg-SYV46* was characterized from soybean cyst nematode (SCN, *Heterodera glycines)* and encodes a secretory protein with a conserved C-terminal domain of the CLAVATA3/ENDOSPERM SURROUNDING REGION (ESR)-related (CLE) family of *Arabidopsis* (Wang et al., 2005). *Arabidopsis thaliana* has 31 members in the CLE family and majority of the members have an N-terminal secretory signal peptide and a conserved 14-amino acid domain at the C-terminus called the CLE motif

(Cock and McCormick, 2001). The *Arabidopsis* CLV3 peptide is known to direct shoot meristem organization by binding with the CLV1/CLV2 receptor complex to activate downstream signaling and negatively regulating WUSCHEL expression to restrict stem cell population size in the shoot (Rojo et al., 2002; Schoof et al., 2000). *clv3* mutants display higher numbers of floral organs. This phenotype is reversed by transgenic expression of *Hg-SYV46* in *Arabidopsis* (Wang et al., 2005). Therefore, the nematode secreted peptide is functionally similar to the plant CLV3 peptide. Several CLE peptides including *Arabidopsis* CLE19 and CLE40 have been implicated in maintenance of the root meristem based on the observation that over expression of these peptides caused a short root phenotype, in which the primary root meristem was fully differentiated (Fiers et al., 2004; Hobe et al., 2003). A similar short root phenotype was observed when CLE19 and CLE40 peptides, corresponding to the conserved CLE motif were applied exogenously to *Arabidopsis* roots (Fiers et al., 2005) confirming earlier results. Evidence based on these findings suggests that CLE19 and CLE40 peptides are involved in the suppression or maintenance of root differentiation, probably by interacting with membrane-bound proteins.

Recent findings that the SCN gene *Hg-SYV46* can mimic the plant CLE-peptide phenotype when expressed ectopically in plants indicates that these plant parasites have evolved a mechanism to modulate fundamental developmental processes within the plant cells to their advantage (Huang et al., 2006a; Wang et al., 2005). One possibility is that these secreted nematode peptides may compete with plant peptides and mimic the CLE-peptide-receptor interaction; thereby, promoting differentiation of root cells to establish and maintain the feeding site. The mechanism by which nematode peptides or plant

peptides are processed and modified, their movement *in planta*, their delivery into the plant cells, their mode of action and their interaction with membrane-bound receptors or proteins remains unclear. The only evidence is that CLV3 is localized to the extracellular space and signals a stem-cell restricting pathway presumably through the CLV1/CLV2 receptor complex (Rojo et al., 2003).

Only a handful of transport proteins have been shown to respond during nematode infection. The syncytia are known to undergo dramatic changes in anatomy, gene expression and physiology during cyst nematode development. The juveniles induce syncytial cells 24 hours post infection and start feeding to promote nematode development. During early stages of infection, syncytia are symplastically isolated from the phloem and the plasmodesmata in the cell walls of syncytia are not-functional (Hoth et al., 2005). Due to symplastic isolation, there is a need for active transport of nutrients from phloem into the developing syncytia. AtSUC4, a sucrose transporter, was implicated in transport of sucrose into feeding cells during cyst nematode development when syncytium was symplastically isolated from phloem during early stages of nematode development (Hoffmann et al., 2007). During later stages of cyst development, when the syncytia expand and reach the vascular tissues around 12 days post infection, syncytia and phloem are symplastically connected through a functional plasmodesmata (Hoffmann and Grundler, 2006; Hoffmann et al., 2007) allowing the transport of nutrients through plasmodesmatal connections. AtSUC2, another sucrose transporter, is expressed in companion cells (CCs) of root phloem and was suggested to play a role in unloading of sucrose into cyst nematode-induced syncytia. The study of GFP movement, expressed from an *AtSUC2* promoter in root cells, revealed a symplastic connection between root

phloem and syncytia large enough to allow cell-to-cell movement of molecules up to 27 kDa (Hoth et al., 2005) at later stages of cyst nematode development.

AtCAT6, an amino acid transporter, was up-regulated during root-knot nematode infection in giant cells indicating that *AtCAT6* might be involved in the transport of amino acids as nutrients in feeding sites (Hammes et al., 2006). In a study of nematode-induced changes of transporter genes in *Arabidopsis*, expression of several sugar transporters, amino acid transporters, aquaporins and peptide transporters was altered in giant cells upon nematode infection (Hammes et al., 2005). An additional study using promoter – GUS analysis of the amino acid transport protein *AtAAP6* and aquaporin *AtPIP2.5* revealed that expression of these genes was higher in the feeding cells during nematode infection, suggesting a role in transport of nutrients and water to the developing root-knot nematodes (Hammes et al., 2005). In the current studies, a role for AtOPT6 during cyst and root-knot infection of *Arabidopsis* was investigated. Expression analysis of *AtOPT6* using promoter – GUS lines and infection assays using *opt6* mutant lines indicated that *AtOPT6* plays a role during nematode parasitism of plants.

METHODS AND MATERIALS

Plant growth and germination

Seeds of *AtOPT6* promoter-GUS lines, wild-type (Col-O) and the *opt6* mutant line were surface sterilized with 30% bleach, re-suspended in 0.1% agarose and stratified at 4° C for 2 days. Seeds were germinated on modified Knop's nutrient agar medium (10X macronutrient stock: 3g/L calcium nitrate, 0.68g/L potassium phosphate-monobasic, 0.49g/L magnesium sulfate; 10000X micronutrient stock: 13.5g/L potassium chloride, 5.56g/L boric acid, 1.2g/L sodium chloride, 3.56g/L manganese chloride; 5000X zinc chloride-0.099g/L; 1000X ferric sodium EDTA 8g/L; 100000X: 1.45g/L sodium molybdate, 0.571g/L cobalt chloride, 1.02 g/L cupric chloride; 100X potassium phosphate dibasic 17.4g/L; 1% sucrose; 0.8% Daishin Agar; pH 6.4), plated one seed per well in a 12 well plate (Corning Inc., NY) and incubated in the growth chamber at 23° C with a photoperiod of 14 hour light and 10 hour dark. After approximately 8-10 days, when the roots were 1.5 – 2 cm long, 10 μl of 0.1% agarose containing an appropriate amount of parasitic juveniles was applied at the base of each seedling. As a mock treatment, negative control, 0.1% agarose was applied to seedlings. Both infected and uninfected seedlings were incubated in a growth chamber at 22 °C, 60% relative humidity and 14 hour dark/10 hour light period and samples were collected 3, 10, 14 and 21 days post infection to follow the life cycle of the nematode at the J2, J3 and J4 stages.

Nematode egg hatching

Sugar beet cyst nematode (SBCN) *Heterodera schachtii* was maintained by mass selection on susceptible Monohikari (Sugar beet) in green house. SBCN were extracted from infected soil by floatation in water and collected on a 250 μm (no. 60) sieve. Harvested cysts were crushed gently using a drill press and the eggs were collected on a 25 μm (no. 500) sieve (Faghihi and Ferris, 2000) and further purified on a sucrose density gradient. The eggs were surface sterilized in 0.02% sodium azide for 20 minutes and washed extensively in sterile water to remove any traces of sodium azide. Parasitic J2s were isolated by hatching eggs in the presence of gentamycin at 1.5 mg/ml and nystatin at 0.05 mg/ml at 28° C on a modified Baermann pan for 2 days. Hatched juveniles were collected and surface sterilized using mercuric chloride solution (0.002% mercuric chloride, 0.001% Triton X-100, 0.02% Sodium azide) for 7 minutes followed by 5 washes with sterile water. Sterilized juveniles were re-suspended in sterile 0.1% agarose.

Nematode infection assay for *AtOPT6* promoter-GUS activity

For *AtOPT6* promoter-GUS constructs, seedlings were infected with 30 – 50 pre-parasitic J2s of SBCN and 50 – 75 pre-parasitic J2s of RKN. Samples were collected at 3dpi, 7 dpi, 10dpi, 14dpi, 18 dpi and 21 dpi. Collected samples were used to observe induction of AtOPT6-GUS in the feeding cells for both SBCN and RKN, formed as a result of infection in roots, by β-glucoronidase staining of roots, followed by acid-fuchsin staining for SBCN nematodes. At each time point, a random sample of 10 roots from infected and uninfected seedlings were stained by acid-fuschin to determine the life stage

of the juveniles as described by Dropkin et al. (1969) and by β-glucuronidase to observe induction of *AtOPT6* in the feeding cells.

Nematode infection assay for wild-type and *opt6* mutant plants

To determine the infection rate of *opt6* mutant and wild-type plants, seedlings were grown in 12-well plates. At 8-10 days post germination, 20 µl of 0.1% agarose containing 200 pre-parasitic juveniles was applied at the base of the root tip of each seedling. Seedlings were observed 3, 7, 10, 14, 19 and 21 days post infection to follow the life cycle of the nematodes at various juvenile and adult female stages. The total number of cyst were counted on each seedling as part of infection assay on day 24 to obtain an overall count. The numbers were averaged per infected seedling for each plant line and plotted on the graph. For RKN infection, seedlings were grown in 6-well plates and at 14 days post germination, 30 µl of 0.1% agarose containing 200 pre-parasitic juveniles was applied at the base of the root tip of each seedling. Seedlings were observed during the course of infection and total number of galls were counted 30 days post infection. The numbers were averaged per infected seedling for each plant line and plotted on the graph.

Nematode staining by acid fuchsin

Seedlings (roots) infected with nematodes were washed in 10% sodium hypochloride (household bleach) for 7 minutes and rinsed in tap water several times for 20 minutes. *AtOPT6*: promoter GUS seedlings were stained for β-glucuronidase prior to acid fuchsin staining. 1 ml of acid fuchsin stain (1.5 % acid fuchsin in glacial acetic acid)

was added to 50 ml boiling water. Roots were boiled in the solution for 1 minute and were cooled at root temperature for 30 minutes in the same solution. Infected roots were transferred to 100% ethanol and carefully observed using an Olympus SZX12 microscope.

Root growth assay of plants treated exogenously with synthetic CLE peptides

Wild-type and *opt6* mutant seeds were sterilized and germinated on plates containing Knop's medium with 10 μM AtCLE19p, HgCLEp or no peptide as control. Plates were incubated vertically in a growth chamber and grown under long day conditions (i.e., 14 hours/10 hours light/dark cycle at 22 °C with 60% relative humidity). Root-length was marked 48 hours post germination and every 24 hours thereafter. At day 10, total root length measurements were taken, averaged and plotted on the graph for each peptide or control treatment for all plant lines.

Microscopy of root cross-sections

Galls from *AtOPT6* promoter-GUS seedlings infected with *M. incognita* and stained for β-glucuronidase expression were excised manually and fixed in 4% para-formaldehyde for 24 hours. Samples were washed twice with 15%, 30%, 50% and 70% ethanol for 30 minutes. Samples in 70% ethanol were processed for embedding in paraffin. A microtome was used to create 5 μm thick sections that were mounted on a slide and put on a slide warmer for 42 °C overnight. The next day samples were de-paraffinized, mounted with glycerol and observed with an Olympus IX70 inverted microscope equipped with an Orca ER digital camera.

RESULTS

AtOPT6 promoter – GUS expression was induced early during cyst and root-knot nematode infection

In order to examine the expression of *AtOPT6* during cyst and root-knot nematode infection, *AtOPT6* promoter – GUS transgenic lines were analyzed during the course of infection. Mock-infected plants and those infected with sugar beet cyst nematode (SBCN) were analyzed 3, 7, 10, 14, 17 and 21 days post infection (dpi). In the roots of mock-infected samples at 3dpi, *AtOPT6* expression was strong in vascular tissues (Fig 2A). In SBCN-infected roots, *AtOPT6* expression was induced during the early stages of infection (3dpi) as parasitic juveniles (pJ2s) initiated the development of feeding sites (Fig 2B). A striking difference with *AtOPT6* expression was observed in uninfected and infected roots during the late J2 stage of nematode development. *AtOPT6* expression was very strong in developing syncytia and surrounding cells; whereas weaker expression was observed in the uninfected root vascular tissue of the same developmental stage of root tissue (Fig 2C and 2D). No *AtOPT6* expression was detected in the feeding site or surrounding cells at later life stages (Fig 2F and 2H). Mock-infected roots at a similar time point also showed no *AtOPT6* expression (Fig 2E and 2G). During the time course of cyst neamtode infection in Arabidopsis, *AtOPT6* was up-regulated during early stages of syncytia development and in surrounding cells until the late J2 stage of nematode development as compared to uninfected roots. Expression of *AtOPT6* was not detected at later stages of nematode development in syncytia or surrounding cells.

Figure 2: *AtOPT6* promoter – GUS expression analysis during cyst nematode infection.

(A, C, E and G) Mock infected root tissues of *AtOPT6* promoter – GUS plants at 3, 7, 14 and 21 dpi, respectively.

(B, D, F and H) Infected root tissues of *AtOPT6* promoter – GUS plants at 3, 7, 14 and 21 dpi, respectively.

(B) Expression of *AtOPT6* is up-regulated in the developing feeding site (syncytium) and surrounding cells during the very early parasitic J2 stages of cyst nematode development. Pictures were taken at 3dpi.

(D) Expression of *AtOPT6* was up-regulated in the developing syncytium and surrounding cells during late parasitic J2 stages of cyst nematode development. Pictures were taken at 7 dpi.

(F) *AtOPT6* was not expressed in the developing syncytium during the early J3 to late J4 stage of cyst development. Pictures were taken at 14 dpi.

(G) No alteration in *AtOPT6* expression was observed in syncytia of adult females. Pictures were taken at 21 dpi.

Arrows indicate syncytia; arrow heads indicate the cyst nematode during their course of development.

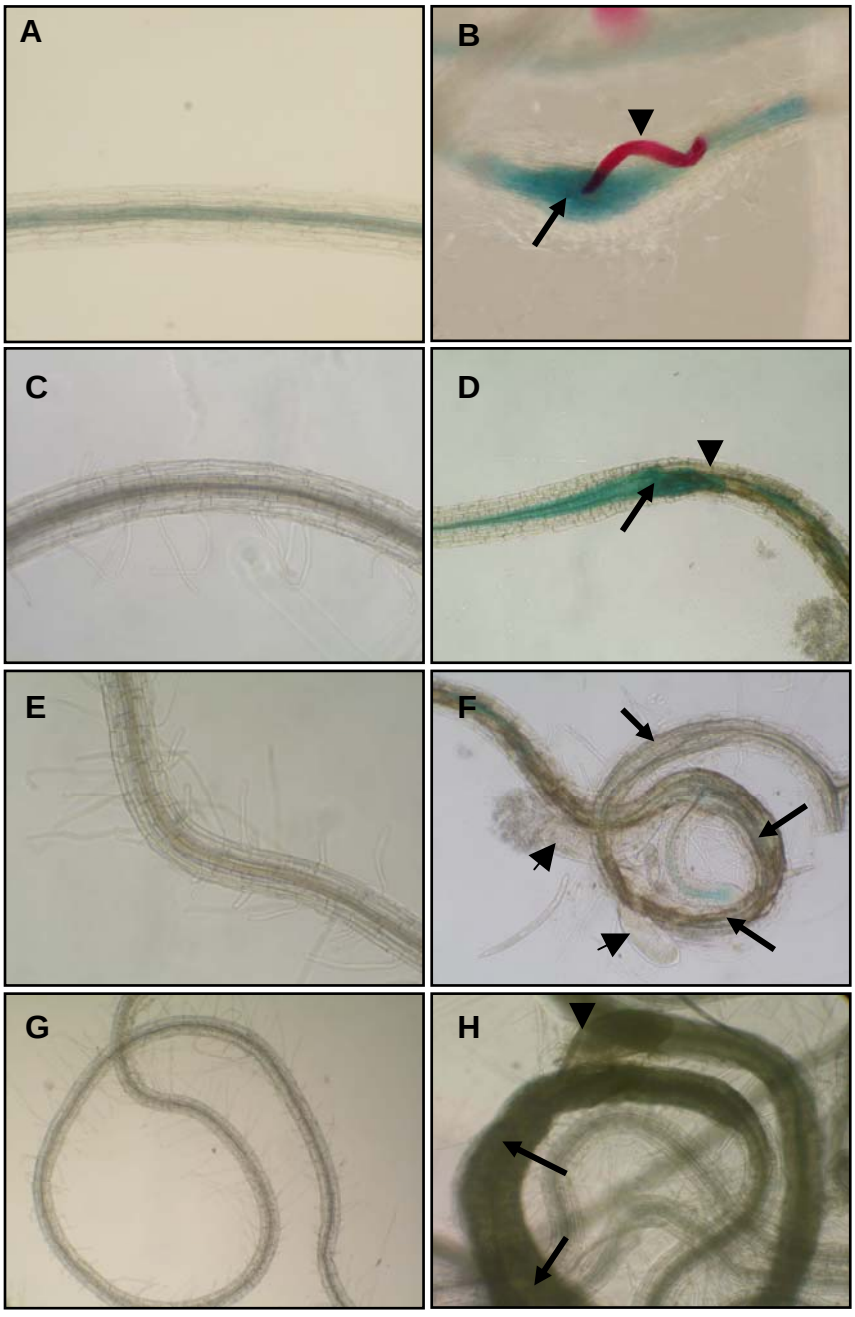
A
B
C
D
E
F
G
H

AtOPT6 expression during root-knot nematode development in infected roots revealed that *AtOPT6* was expressed during the stages of parasitism as J2 migrated through root tissue and established giant-cells. Expression of *AtOPT6* was stronger during the initial infection and remained strong during late J2 (Fig 3E and 3F) and early J3 (Fig 3H and 3I) stages of nematode development within giant-cells and surrounding, as compared with the mock-infected roots (Fig 3D and 3G). However, during the early J3 stage of nematode development, expression of *AtOPT6* was lower in giant-cells as compared with surrounding cells of developing galls (Fig 3I). During later stages of nematode development (late J3 and J4 stages), *AtOPT6* expression decreased significantly in both giant-cells and surrounding gall cells (Fig 3L) but was higher than in mock-infected roots, which showed no appreciable *AtOPT6* expression (Fig 3J). By late J4 stage of root-knot nematode development, AtOPT6 expression was no longer detected in either giant-cells or galls. Thus, *AtOPT6* expression in giant cells and surrounding cells of roots infected with root-knot nematode was slightly different than that found syncytia and surrounding cells of roots infected with the sugar beet cyst nematode (compare Fig 2 and Fig 3). In the latter case, expression of *AtOPT6* was not affected during the early J3 stage of cyst nematode development and after; whereas *AtOPT6* expression was induced in the giant cells and surrounding cells during the early J3 stage of root-knot nematode development. During the time course of root-knot nematode infection, expression of *AtOPT6* was elevated in the giant cells and surrounding cells for a longer period of time (late J3 stage).

Figure 3: *AtOPT6* promoter – GUS expression during root-knot nematode infection.

(A, D, G and J) Mock-infected root tissues of *AtOPT6* promoter – GUS plants at 3, 7, 14 and 18 dpi respectively.

(B, E, H and K) Whole-mount pictures of the various stages of gall development at 3, 7, 14 and 18 dpi, respectively.

(C, F, I and L) Longitudinal or transverse cross-sections of whole-mount tissues depicted in B, E, H and K, respectively.

(B) Whole-mount sample of a very early stage (pJ2) of root-knot nematode infection at 3dpi.

(C) Cross-section of root showing migrating J2. Picture was taken at 3 dpi.

(E) Whole-mount sample of late J2 infection at 7 dpi.

(F) Cross section of the gall in Fig 3E. Note the head of nematode as indicated by arrow-head and formation of giant cells indicated by arrows.

(H) Whole-mount sample of a developing gall at 14 dpi.

(I) Cross section of the gall in Fig 3H. Giant cells have formed at this point and the nematode has started feeding and maturing. The head and partial body of the nematode is clearly visible (arrow-head) and giant cells are indicated by arrows.

(K) Whole-mount sample of gall at 18 dpi. A gall of two different stages are present. GUS staining is still visible in the younger gall.

(L) Cross section of the gall in Fig 3K. No GUS was detected in the more mature gall. The empty spaces are visible where giant cells should be (arrows). During sample processing, giant-cell contents may have been lost. GUS staining is still visible within giant-cells of the younger gall.

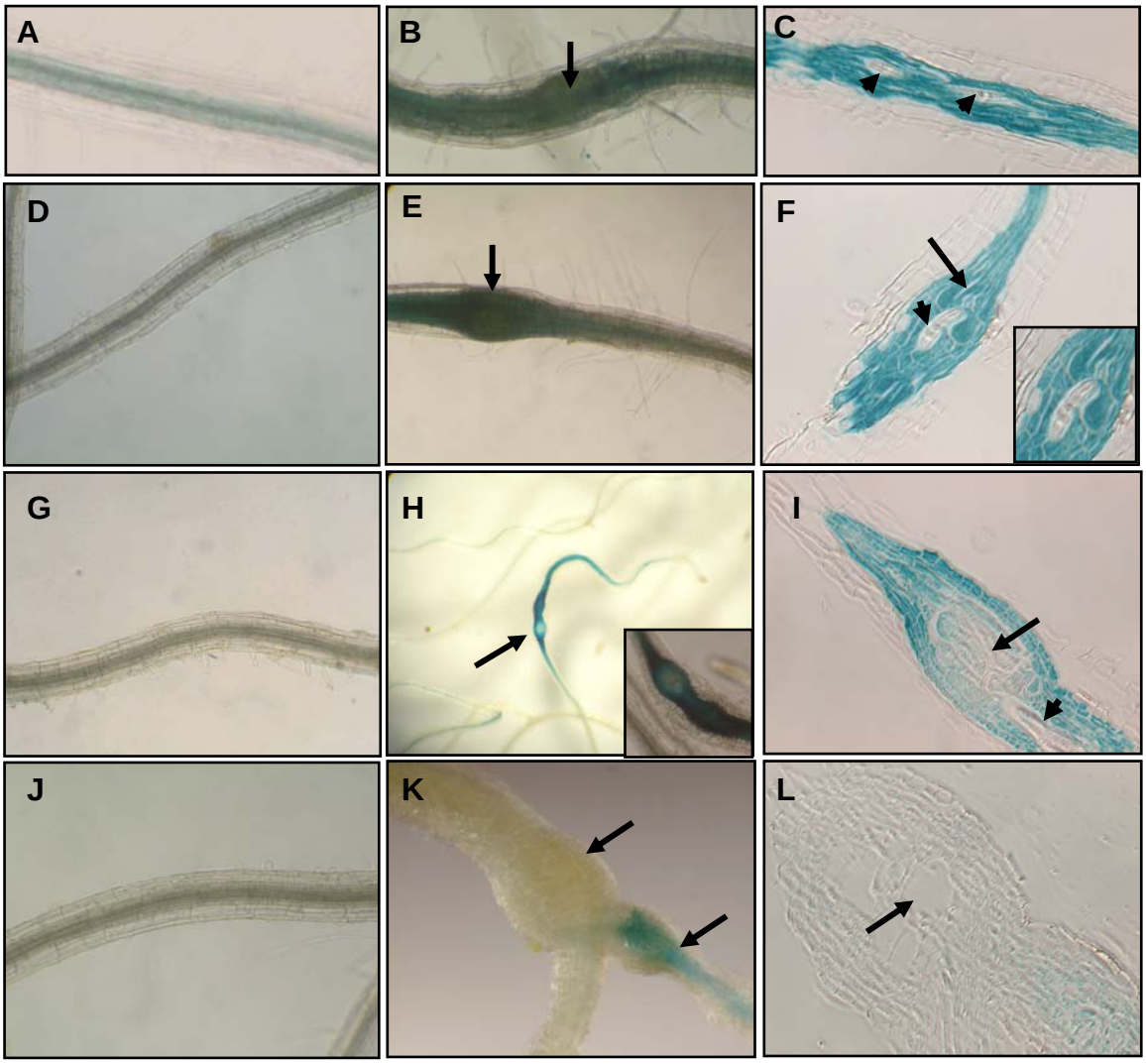
A
B
C
D
E
F
G
H
I
J
K
L

***opt6* mutant plants are less susceptible to both cyst and root-knot infection**

The OPT6-GUS results indicate that OPT6 is expressed during the early stages of syncytia and giant-cell development suggesting that OPT6 may play a role in their development. In order to obtain more insight into AtOPT6 function during cyst and root-knot infection, infection of *opt6* mutant and wild-type plants was analyzed. For the cyst infection assay, *opt6* mutant and wild-type control plants were grown in 12-well culture plates in a randomized pattern to eliminate plate effects. Seedlings were inoculated with 200 pre-parasitic second-stage juveniles (ppJ2s) of sugar beet cyst nematode and the formation of the feeding site and infection by pJ2s was observed at 3, 7, 10 and 24 days post-infection (dpi). The number of total female cysts were counted at 24 dpi for each plant and average values were plotted. Three independent biological replicates were completed for cyst nematode infection. Statistical analysis (T-test) was performed for each independent trial with a P value of 0.05. As shown in Fig 4, the average number of cysts on *opt6* mutant plants was 50% less than found on wild-type control plants. This was true for all three replicates. Observation under the light microscope revealed no difference in the size or shapes of the feeding site in either the mutant or wild type plant lines. The average number of juveniles was also counted at 24 dpi and *opt6* mutant plants showed 50% less juveniles than wild-type control plants (data not shown).

Similar infection assays were carried out using the root-knot nematode, *M. incognita*. However, this infection assay was done in 6-well culture plates. Infected plants were observed at 4, 10, 17 and 30 dpi. The total number of galls was counted at 30 dpi for the *opt6* mutant and wild-type control plants. One trial was carried out for root-knot

Figure 4: Sugar beet cyst nematode infection assay of the *opt6* mutant and wild-type plants.

Cyst counts for *opt6* mutant plants and wild-type control plants during sugar beet cyst nematode infection. Error bars represent standard deviation. This graph is a representation of three independent experiments with n=30 (n is total number of plants in each infection assay). Statistical analysis was performed using a Student T test with a P value of 0.05. Additional experiments with complemented lines still need to be done.

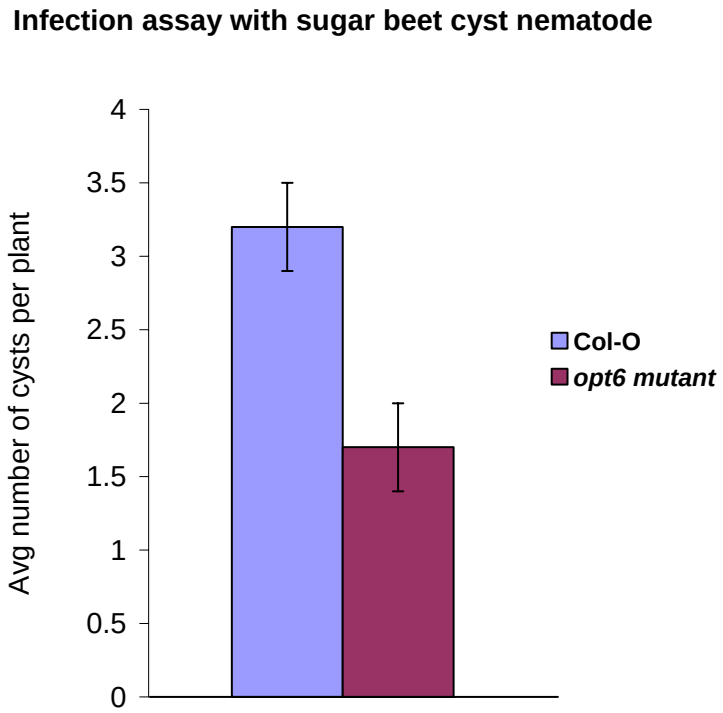

Figure 5: Root-knot nematode infection assay of *opt6* mutant and wild-type plants.

Gall counts for *opt6* mutant plants and wild-type control plants following root-knot nematode infection. Error bars represent standard deviation. This graph is a representation of one experiment with n=18 (n is total number of plants infected assay). Statistical analysis was performed using a Student T test with a P value of 0.05. Additional replicates needed for this experiment.

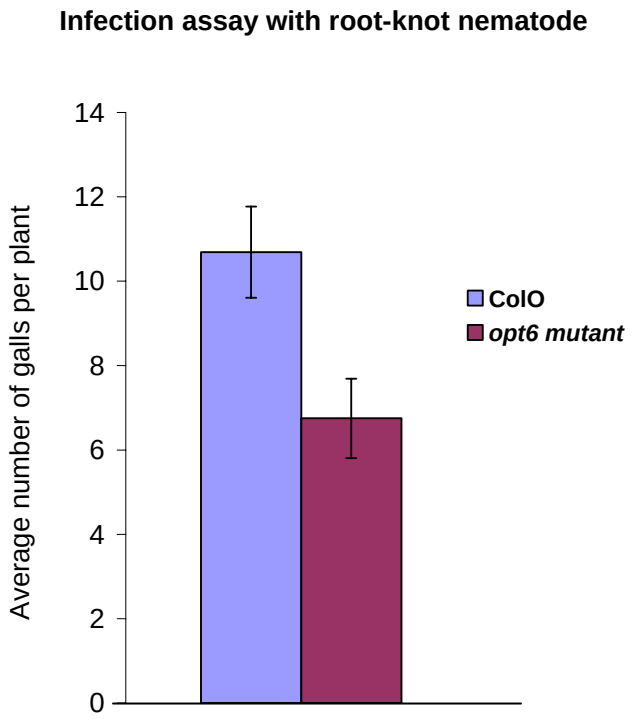

nematode infection. As shown in Fig 5, the average number of galls formed on the *opt6* mutant plants was 33% less than that formed on the wild-type control plants.

AtOPT6 mediates *Arabidopsis* and nematode CLE transport in *Xenopus laevis* oocytes

Cyst nematodes secrete CLE-like peptides that share significant similarity with the *Arabidopsis* CLEs (Wang et al., 2005). There are atleast 31 *Arabidopsis* genes in the CLE family. CLV3, the founding member of the plant CLE family, plays an important role in the maintenance of the shoot apical meristem (Schoof et al., 2000). Other members of the CLE family, including CLE19 and CLE40, are known to play a role in root meristem maintenance (Fiers et al., 2004; Hobe et al., 2003). Small peptides are also secreted by RKN. A 13-amino acid peptide, RKN 16D10, was shown to stimulate root growth when over-expressed in *Arabidopsis thaliana* (Huang et al., 2006a). The mechanism by which these nematode peptides are secreted into the plant cells is not known. Therefore, to determine the function of AtOPT6 in the transport of these peptides, transport of the plant peptides AtCLE19p, AtCLE5p and nematode peptides HgCLEp, HsCLEAp, HsCLEBp and RKN16D10p was analyzed in *Xenopus* oocytes expressing the AtOPT6 transporter. As a positive control for these studies, the transport of glutathione (GSH) and the tetrapeptide GGFL, both of which are transported by AtOPT6, was also measured. As shown in Fig 6, addition of AtCLE19p in the bath solution produced higher inward currents, as compared with positive control substrate GSH. Addition of HgCLEp in the bath solution also resulted in inward current similar to the GSH control. AtOPT6 also mediated transport of the other plant and nematode peptides AtCLE5p, HsCLEAp,

Figure 6: Transport of *Arabidopsis* CLEs, cyst CLEs and RKN 16D10 peptide by AtOPT6 expressed in *Xenopus laevis* oocytes.

A. Transport of GSH, GGFL, Arabidopsis CLEs, cyst CLEs and root-knot 16D10 peptides by AtOPT6 at 500 μM and -80mV.

B. Concentration dependent currents using AtCLE19p as a substrate. Currents were obtained from AtOPT6-expressing oocytes at pH 5.0.

A

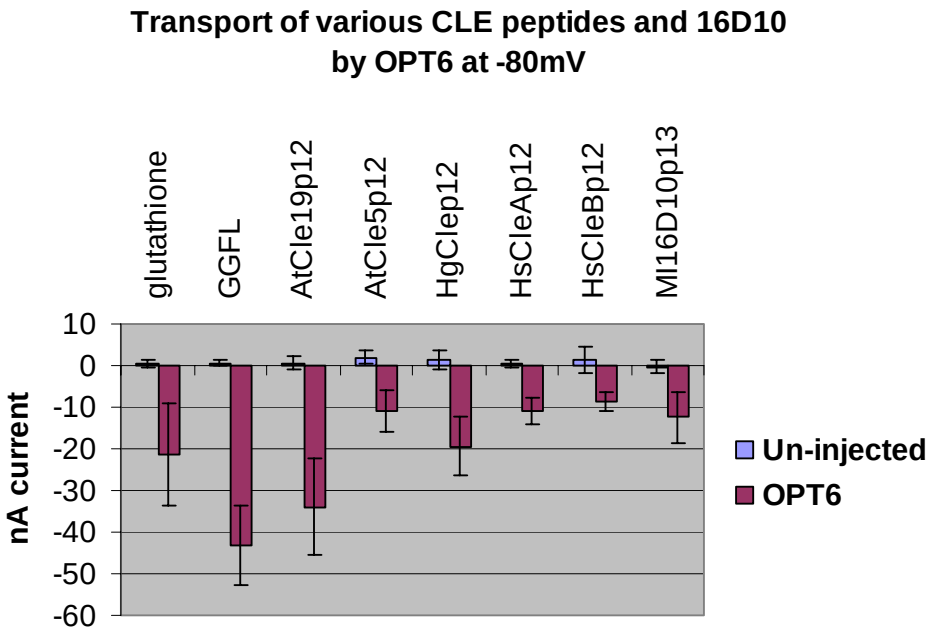

B

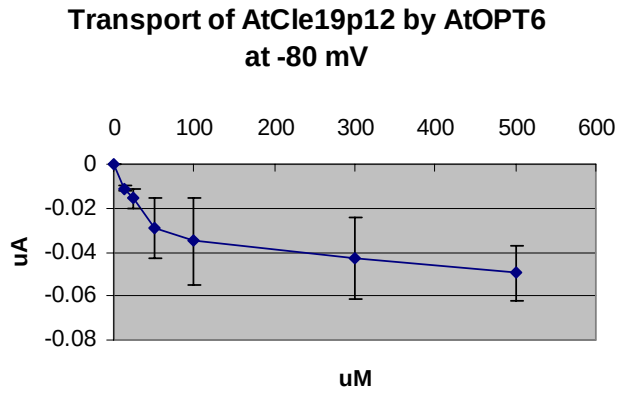

The above data was kindly provided by Sharon Pike in Dr. Walter Gassmann's laboratory.

HsCLEBp and RKN16D10. However, addition of these peptides to the bath solution produced inward currents lower than was obtained with AtCLE19p. Concentration dependent transport of AtCLE19p by AtOPT6 showed maximum inward currents at 500 μM (Fig 6B). K_m and I_{max} values for AtCLE19p were calculated by linearizing substrate concentration/current curves obtained at -80mV. The $K_{0.5}$ value was calculated as 20.7 μM and the I_{max} value was 52 nA, indicating that AtOPT6 mediated AtCLE19 transport with high affinity.

opt6 mutant and wild-type roots show similar sensitivity to exogenous application of plant and nematode peptides

Exogenous application of AtCLE19p and AtCLE40p resulted in consumption of the root meristem (Fiers et al., 2005). Earlier results demonstrated that AtOPT6 mediates transport of both plant and nematode CLE peptides in the heterologous *Xenopus* system. To determine the effect of these CLE peptides on root growth, *opt6* mutant and wild-type control plants were germinated in the presence of 10 μM AtCLE19p, HgCLEp and RKN 16D10 peptides. Root growth was marked 48 hours after germination and each 24 hours thereafter. Root growth was inhibited and numerous lateral roots were formed both in *opt6* mutant and wild-type control plants grown in presence of CLE peptides (Fig 7). These data indicate that the *opt6* mutant plants behaved in a similar manner to wild-type control plants.

Figure 7: Effect of the exogenous application of CLE peptides on *opt6* mutant and wild-type root growth.

Chemically synthesized peptides were kindly provided by Dr. Melissa Mitchum. One experiment with 15 seedlings for each plant line was carried out. Error bars represent standard error.

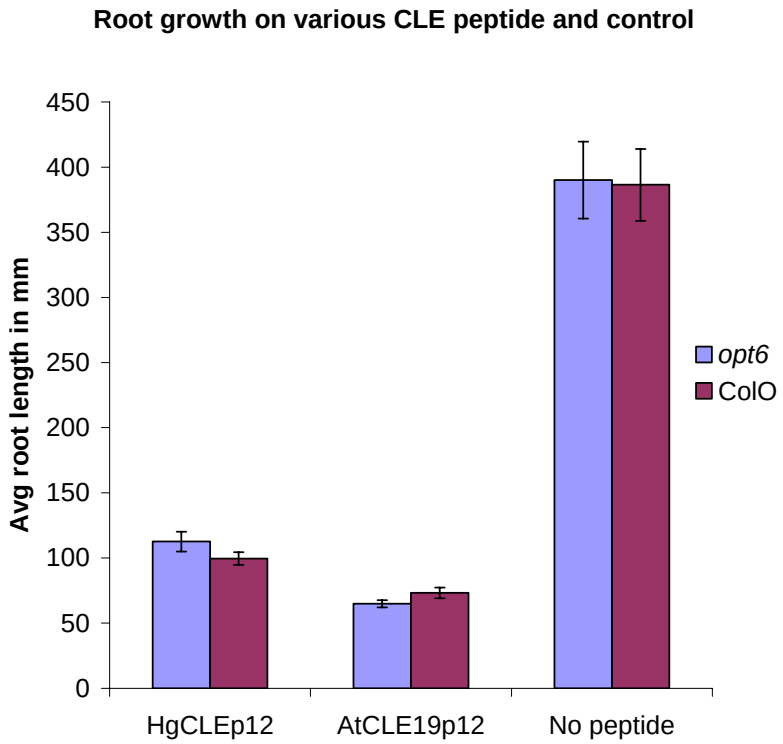

DISCUSSION

AtOPT6 is up-regulated during early stages of nematode infection

Only two transport proteins, AtSUC2 and AtCAT6, were implicated in nutrient transport during nematode feeding site formation (Hoth et al., 2005; Hammes et al., 2006). Promoter – GFP analysis revealed that *AtSUC2* was localized to the phloem companion cells. Functional plasmodesmata, connecting the phloem and syncytium, allowed transport of up to 27 KD compounds (Hoth et al., 2005). *AtSUC2* itself was not localized to the developing syncytium (Hoth et al., 2005). Promoter – GUS analysis of amino acid transporter *AtCAT6* revealed expression in giant cells, suggesting a role in providing nutrients to the developing root-knot nematode (Hammes et al., 2006). In the course of our current work, expression of the oligopeptide transport gene, *AtOPT6*, was induced during the early stages of cyst development in the syncytium and surrounding cells, but was not strongly expressed during the later stages of cyst development from the early J3 to adult female. Root-knot nematodes are known to possess an active subventral esophageal gland during parasitic J2 to third-stage juvenile (J3) developmental stage. These glands secrete the 16D10 peptide into the root cells, which may play a role in the induction of giant cell differentiation. Expression of AtOPT6 in developing giant cells correlates with the time of secretion of root-knot secreted peptides. Expression of an *AtOPT6*-green fluorescent protein in onion cells localized the transporter to the plasma membrane (data not shown). Hence, we postulate that AtOPT6 would function in the uptake of peptides from the apoplast. This role is also consistent with data obtained from the expression of *AtOPT6* in *Xenopus* oocytes. At this point, it is not clear whether the

nematode inserts the peptides directly into the plant cell, a case in which AtOPT6 transport would not be necessary. It is also possible that the nematode releases the peptide into the apoplastic space or that the peptide is subsequently released from the initially penetrated plant cell into the apoplastic space. In these scenarios, uptake of the peptide by AtOPT6 could be important. Alternatively, while AtOPT6 is capable of transporting CLE peptides, this function may not be central to nematode infection. AtOPT6 may function, as is the case of AtSUC2 and AtCAT6, in bringing nutrients to the nematode feeding site.

An unanswered question is why the expression of *AtOPT6* is reduced during the later stages of nematode parasitism? If AtOPT6 was involved in the transport of peptides as a source of nitrogen to the developing nematode, we would expect *AtOPT6* expression to remain high throughout the life cycle of nematode in feeding cells since the nutritional demands would remain. A clear explanation is that AtOPT6 may be involved in transport of peptides into the developing syncytium during early stages of infection when the phloem and syncytia are symplastically isolated (Hoth et al., 2005; Hoffmann and Grundler, 2006). There is a need of an active transport of loading nutrients from phloem into the syncytia during early stages of cyst infection (Hoffmann et al., 2007). The induction of AtOPT6 expression at the feeding site correlates with the phase of active transport that requires transporters to transport nutrients into the syncytium. At later stages of syncytium development a symplastic connection is established between syncytium and phloem via functional plasmodesmata eliminating the need for transporters to transport nutrients into the syncytium (Hoffmann et al., 2007). AtOPT6 expression remains unaltered during later stages of nematode infection after the

plasmodesmatal connection have already been established indicating a role of AtOPT6 in transport of peptides during nematode infection. However, current data does not allow us to clearly distinguish between a possible signaling role for AtOPT6, through transport of the nematode CLE peptides, or strictly a nutritional role, through the transport of nitrogen-rich peptides.

opt6 mutant plants display more resistance to nematodes than wild-type plants

During the initial stages of infection, cyst nematodes secrete CLE-like peptides (Wang et al., 2005). One of the CLE-like peptides, *Hg-SYV46* secreted by *Heterodera glycines*, shares high amino-acid similarity with CLV3, including a highly conserved glycine residue shown to be critical for CLV3 function in *Arabidopsis* (Fletcher et al., 1999; Wang et al., 2005). CLV3 is known to play a role in maintainence of floral shoot meristems in *Arabidopsis* (Schoof et al., 2000). *Hg-SYV46* was shown to complement the *clv3-1* mutant phenotype suggesting a functional similarity between the plant secreted and nematode secreted peptides (Wang et al., 2005). This molecular mimicking of plant peptides by nematode secreted peptides is thought to play a role in successful development of the feeding site and in the infection of plant roots (Wang et al., 2005; Caillaud et al., 2007). The infective and parasitic J2 to early J3 stages of root knot nematode development are those involved in the initiation and development of the giant-cell feeding sites. During these stages, which correspond to 3-11 days post infection, the 16D10 peptide is secreted by the nematode (Huang et al., 2006a). It is possible that other, unidentified peptides are also secreted during the initial stages of nematode infection and giant-cell development. Expression of AtOPT6 correlates with above mentioned stages of

nematode parasitism. The fact that AtOPT6, when expressed in *Xenopus* ooctyes, can also mediate transport of the nematode CLE peptides adds further support for a crucial role for such uptake during nematode infection. However, at this point, the data allow only this correlation. What is lacking is clear evidence that CLE uptake by AtOPT6 occurs *in planta* and is crucial for nematode virulence.

In order to provide further support of a role for AtOPT6 in nematode infection, we examined the phenotype of the *opt6* mutant and wild-type control plants when infected with the sugar beet cyst nematode and root-knot nematode. The *opt6* mutant plants showed a 50% decrease in the number of cysts formed, as compared with wild-type control plants, when infected with the sugar beet cyst nematode. The shape and size of the syncytium formed on both the mutant and wild-type plants was similar. Somewhat similar results were obtained upon infection with the root-knot nematode infection; the *opt6* mutant plants produced 33 % fewer galls than wild-type control plants. These results do not resolve the issue of whether AtOPT6 transport of the nematode CLE peptides occurs *in planta*. However, these data clearly show that AtOPT6 function, regardless of the physiological substrate, is important for successful parasitism by the nematode.

AtOPT6 mediates CLE peptide transport in a heterologous system

Until recently, AtOPT transporters were thought to mediate the movement of tetra- and pentapeptides (Koh et al., 2002; Osawa et al., 2006). However, recently, Reuss and Morschhauser, (2006) reported that the expression of CaOPT1, CaOPT2 and CaOPT3 in yeast allowed the uptake of an eight amino acid peptides. We have now expanded the size range for AtOPT uptake even further by demonstrating the uptake by

AtOPT6 of the CLE peptides. AtOPT6 transports the 12 amino acid AtCLE19p with high affinity consistent with a physiological role for such substrates. These recent results clearly show that AtOPT6 can transport a broad range of substrates from the tri-peptide GSH to the 13 amino acid RKN 16D10 peptide which is consistent with earlier studies of both plant and yeast OPT transporters (Koh et al., 2002; Osawa et al., 2006, Reuss and Morschhauser, 2006; Sharon Pike – personal communication).

The transport of such large peptides by the proton symport mechanism of the AtOPT transporters raises interesting questions about the molecular mechanism. As discussed above, these data also raise the question as to whether the AtOPT transporters play a role in the movement of plant signaling peptides. An increasing number of such peptides have been identified in plants. Phytosulfokine (PSK), a disulfated pentapeptide, isolated from asparagus mesophyll cell culture is a mitogenic factor involved in the early process of cell differentiation (Matsubayashi et al., 1996). PSK interacts with a type of LRR-RLK receptor on the plasma membrane to trigger the downstream signaling process (Matsubayashi et al., 2002). The POLARIS (*PLS*) gene encodes a predicted polypeptide of 36 amino acids and *pls* mutants exhibited a short-root phenotype, showed reduced vasculature in leaves and were hyper-responsive to exogenous cytokinins. The *PLS* gene is located within a short distance of an auxin inducible transcript. However, it is unclear whether PLS polypeptide functions directly or indirectly through auxin-cytokinin homeostatis (Casson et al., 2002). Systemin, an 18 amino acid peptide in tomato, is a key signal for the systemic activation of defense genes in response to pest attacks (Pearce et al., 1991). Therefore, there are several possible plant signaling peptides of the size to be transported by AtOPTs.

Does *AtOPT6* play a role in root differentiation during the development of nematode feeding site?

Exogenous addition of AtCLE19p and the HgCLEp peptides to *Arabidopsis* roots leads to the cessation of root growth due to consumption and premature differentiation of the apical meristem. We postulated that, if AtOPT6 mediates the uptake of these peptides, then the *opt6* mutant roots should show resistance to their inhibitory effect on root growth. However, when tested, both the mutant and wild-type roots exhibited a similar sensitivity when grown in presence of 10 μM AtCLE19p or HgCLEp. However, given that 9 *AtOPT* transporters in *Arabidopsis* and their overlapping expression patterns (Stacey et al, 2006), it is plausible that functional redundancy among these transporters prevented us from seeing a phenotype with plants lacking only the *AtOPT6* transporter.

Thus, the combined data of *AtOPT6* promoter – GUS expression analysis, infection assays using *opt6* mutant and wild-type control plants and substrate transport studies of AtOPT6 bring us to one conclusion: AtOPT6 is important during nematode parasitism and appears to play a role during the initial and critical stages of feeding site formation and infection. However, at this point, we cannot distinguish between two possible mechanisms for AtOPT6 action. That is, one, AtOPT6 may transport nutrients to the sink tissue formed by nematode infection (i.e., feeding site). AtOPT6 is not only expressed in the feeding site but also in the surrounding cells consistent with long-distance transport of peptides from source tissue to the developing feeding site. Two, it is possible that AtOPT6 is involved in the uptake of CLE peptides from the apoplast. However, this mechanism is not consistent with the model for CLE action, based on the

example of CLV3, in which the CLV peptides in the apoplast act by interaction with a plasma membrane localized receptor (i.e., CLV1/2; Hojo et al., 2003). Therefore, we can only speculate. Perhaps the nematode CLEs could be either secreted directly into the cytoplasm or CLEs act by interacting with a cytoplasmic receptor and, hence, uptake from the apoplast is essential. Alternatively, the nematode CLE peptides may be released from the cell into which they are initially injected and then transported into neighboring cells by the AtOPT6 transporter. This could expand the infection zone, enhancing cell fusion as occurs during formation of the cyst nematode syncytium. What is lacking is clear evidence for AtOPT6 uptake of nematode CLE peptides *in planta*. It would also be helpful to localize the nematode CLE peptides. Are they released by the nematode through the stylet into the plant cell cytoplasm, into the apoplast or exported from the initially injected plant cell into the apoplast? The questions of nematode CLE peptide uptake into plants is currently been addressed by Dr. Mitchum's lab (Dr. Mellissa Mitchum – personal communication).

CONCLUSION

Nine OPT genes have been identified in *Arabidopsis* and so far only AtOPT3 is well characterized in terms of its physiological role during plant growth and development (Stacey et al., 2002; Stacey et al., 2006; Stacey et al., 2007). Here, the role of AtOPT6 during plant growth and development is dissected using various genetic, molecular biology and pathology techniques. Expression analysis of *AtOPT6* during plant development gave a clue into possible function of AtOPT6 during various stages of plant growth. *AtOPT6* exhibited strong expression during germination in the seedlings, mainly in the vascular tissue of developing cotyledons and hypocotyls (Chapter I – Fig 2). All *AtOPT* promoter – GUS lines analyzed showed vascular expression in roots, hypocotyl, cotyledons and leaves (Stacey et al., 2006; this study). However, no expression was observed in root epidermis, root hairs and root tips indicating that AtOPTs are possibly not involved in peptide uptake from soil. Floral organs displayed distinct expression among the *AtOPTs*. GUS expression in developing ovules was observed only with *AtOPT6* promoter – GUS lines (Chapter I – Fig 3). Similarly, only AtOPT1 GUS expression was observed in the pollen tube and GUS expression in the developing embryo was observed only for *AtOPT3* and *AtOPT8*. There were some overlapping expression patterns in pollen grains, filaments, petals and sepals among the AtOPT members (Stacey et al., 2002; Stacey et al., 2006). Members of the sucrose transport family were localized to sieve elements or companion cells and led to the hypothesis that these transporters may interact physically to achieve sugar loading into phloem. Indeed,

by split-ubiquitin analysis in yeast, it was demonstrated that SUT2 acted as sucrose sensor and interacted with SUT4 to regulate activity of this protein (Weise et al., 2000; Reinders et al., 2002). Like sucrose transporters, it is possible that different members of the *AtOPT* gene family may interact with each other to achieve long distance peptide transport in plants. However, subcellular localization or interactions among the *AtOPT* gene family remains to be studied.

Cagnac et al., (2004) showed that AtOPT6 mediated GSH uptake when expressed in yeast. Similar results were obtained for GSH transport by AtOPT6 in *Xenopus* (Sharon Pike – personal communication). It is known that PCs are oligo-peptides and are synthesized from GSH. In addition, it was demonstrated that expression of phytochelatin synthetase (PCS), an enzyme involved in PC synthesis, is induced in the presence of cadmium. Plants sequester Cd into vacuoles and the apoplastic space in the form of PC-Cd complexes. Various ABC transport proteins are involved in sequestration of PC-Cd complexes (Lee et al., 2005; Kim et al., 2006). Indirect evidence for long distance transport of PCs was provided by Gong et al., (2003). However, the mechanism involved in transport of PC is unclear. Here, we hypothesized a role for AtOPT6 in the transport of PC or PC-Cd. *AtOPT6* over-expressing lines grown in the presence of Cd exhibited hyper-sensitivity to Cd. These plants also had higher root growth inhibition and less tissue weight as compared with *opt6* mutant and wild-type control plants (Chapter II – Fig 4, 6 and 7). Measurement of Cd and PC concentration showed higher accumulation of both Cd and PCs in roots and lower accumulation of Cd in shoots of *AtOPT6* over-expressing lines as compared with the wild-type control (Chapter II – Fig 8 and Fig 10). These data indicate that the root-inhibition phenotype is actually due to higher

accumulation of Cd and PC in roots of AtOPT6 over-expressing lines. It is possible that AtOPT6 is transporting PC or PC-Cd complex into the roots.

Public microarray analysis revealed that *AtOPT6* transcripts were up-regulated during infection with bacterial pathogen *Pst* DC3000. Therefore, to elucidate the role of AtOPT6 during bacterial pathogenesis, wild-type control, *opt6* mutant and AtOPT6 over-expressing plants were infected with *Pst* DC3000. Analysis of bacterial growth in infected plants 3 days post infection, revealed that *opt6* mutant plants showed 10-fold lower bacterial levels and significantly lower chlorosis in leaves as compared with the wild-type control and *AtOPT6* over-expressing plants (Chapter III – Fig 1 and Fig 2). In infected leaves, chlorosis is caused mainly by the presence of phytotoxins such as coronatine, phaseolotoxin and tabtoxin released by *Pst* DC3000 (Gross et a., 1991). Of these phytotoxins, coronatine (COR) is structurally similar to MeJA and is thought to manipulate jasmonate signaling to promote virulence. The lack of chlorosis and lower bacterial population in *opt6* mutant plants may be due to lack of transport of coronatine. To test this hypothesis, we examined bacterial growth and infection using *Pst* DC3000 deficient in coronatine biosynthesis (COR -). Bacterial growth was similar during the course of infection in wild-type control, *opt6* mutant and *AtOPT6* over-expressing plants when infected with the COR- *Pst* DC3000 (Chapter III – Fig 4). These data support the hypothesis that AtOPT6 may be involved in transport of coronatine into the infected cells. Transport of coronatine in oocytes expressing AtOPT6 cRNA needs to be examined to come to any definite conclusion.

The role of AtOPT6 during nematode parasitism was also tested using AtOPT6 promoter – GUS transgenic lines and *opt6* mutant plants. Promoter – GUS analysis

during the course of both cyst and root-knot nematode infection showed that expression of *AtOPT6* increases in feeding sites (both syncytia and giant cells) and surrounding cells during early stages of nematode infection in the root cells (Chapter IV – Fig 2 and Fig 3). There is no induction of *AtOPT6* expression during later stages of infection. There is a growing amount of evidence that both cyst and root-knot nematodes secrete CLE-like peptides into root cells that can mimic the plant CLE peptides and play a role in cell differentiation, possibly to promote feeding site formation (Wang et al., 2005; Huang et al., 2006a).

Based on promoter – GUS expression analysis, there is a possibility that AtOPT6 is involved in transport of either plant CLEs or nematode secreted CLEs in infected root cells. This hypothesis is supported by the fact that AtOPT6 mediates transport of various plant CLEs and nematode CLE peptides when expressed in *Xenopus* oocytes (Chapter IV – Fig 6). Moreover, *opt6* mutant plants show a 50% reduction in the number of cysts and a 33% reduction in the number of galls when infected with cyst and root-knot nematode, respectively (Chapter IV – Fig 4 and Fig 5). It may also be possible that AtOPT6 plays a role in transport of nutrients to the feeding site. This hypothesis is supported by the evidence that feeding sites are symplastically isolated during early stages of nematode infection and need transporters to transport nutrients to the feeding sites (Hoth et al., 2005; Hoffmann and Grundler, 2006). At later stages of nematode infection, symplastic connection via functional plasmodesmata eliminates the need to transporters (Hoffmann et al., 2007). The expression pattern of AtOPT6 during the course of nematode development supports the hypothesis of nutrient transport in the feeding site. AtOPT6 also transports plant and nematode CLEs opening up a possibility that AtOPT6 may be

involved in signaling processes during nematode infection. However, transport of CLEs by AtOPT6 is not established *in planta*. Whether AtOPT6 is involved in signaling or providing nutrition during nematode infection remains an open question.

REFERENCE

Adamis, P.D.B., Panek, A.D., and Eleutherio, E.C.A. (2007). Vacuolar compartmentation of the cadmium-gluathione complex protects *Saccharomyces cerevisiae* from mutagenesis. Toxicol Lett **173,** 1-7.

Ballio, A., Barra, D., Collina, A., G., M., Pucci, P., and Mimmaco, M. (1991). Syringopeptins, new phytotoxic lipodepsipeptides of *Pseudomonas syringae* pv. *syringae*. Febs Lett **291,** 109-112.

Becher, M., Talke, I.N., Krall, L., and Kramer, U. (2004). Cross-species microarray transcript profiling reveals high constitutive expression of metal homeostasis genes in shoots of the zinc hyperaccumulator *Arabidopsis halleri*. Plant J **37,** 251-268.

Bender, C. L., Alarcon-Chaidez, F., and Gross, D. C. (1999). *Psuedomonas syringae* phytotoxins: mode of action, regulation, and biosynthesis by peptide and polyketide synthetases. Microbiol Mol Biol Rev. **63**, 266-92

Bent, A.F., Kunkel, B.N., Dahlbeck, D., Brown, K.L., Schmidt, R., Giraudat, J., Leung, J., and Staskawicz, B.J. (1994). Rps2 of *Arabidopsis thaliana* - a leucine-rich repeat class of plant-disease resistance genes. Science **265,** 1856-1860.

Bernard, C., Roosens, N., Czernic, P., Lebrun, M., and Verbruggen, N. (2004). A novel CPx-ATPase from the cadmium hyperaccumulator *Thlaspi caerulescens*. Febs Lett **569,** 140-148.

Bidwai, A. P., and Takemoto, J. Y. (1987). Bacterial phytotoxins, syringomycin, induces a protein kinase-mediated phosphorylation of red beet plasma membrane polypeptides. Proc Natl Acad Sci U S A. **84**, 6755-6759.

Bird, D.M. (1996). Manipulation of host gene expression by root-knot nematodes. Journal of Parasitology **82,** 881-886.

Blaudez, D., Kohler, A., Martin, F., Sanders, D., and Chalot, M. (2003). Poplar metal tolerance protein 1 confers zinc tolerance and is an oligomeric vacuolar zinc transporter with an essential leucine zipper motif. Plant Cell **15,** 2911-2928.

Bourbouloux, A., Shahi, P., Chakladar, A., Delrot, S., and Bachhawat, A.H. (2000). Hgt1p, a high affinity glutathione transporter from the yeast *Saccharomyces cerevisiae*. J Biol Chem **275,** 13259-13265.

Bogs, J., Bourbouloux, A., Cagnac, O., Wachter, A., Rausch, T., and Delrot, S. (2003). Functional characterization and expression analysis of a glutathione transporter, BjGT1, from *Brassica juncea*: evidence for regulation by heavy metal exposure. Plant Cell Environ **26,** 1703-1711.

Borisjuk, N., Sitailo, L., Adler, K., Malysheva, L., Tewes, A., Borisjuk, L., and Manteuffel, R. (1998). Calreticulin expression in plant cells: developmental regulation, tissue specificity and intracellular distribution. Planta **206,** 504-514.

Brooks, D.M., Hernandez-Guzman, G., Kloek, A.P., Alarcon-Chaidez, F., Sreedharan, A., Rangaswamy, V., Penaloza-Vazquez, A., Bender, C.L., and Kunkel, B.N. (2004). Identification and characterization of a well-defined series of coronatine biosynthetic mutants of *Pseudomonas syringae* pv. *tomato* DC3000. Mol Plant Microbe In **17,** 162-174.

Busch, W., and Saier, M.H. (2002). The transporter classification (TC) system, 2002. Crit Rev Biochem Mol **37,** 287-337.

Cagnac, O., Bourbouloux, A., Chakrabarty, D., Zhang, M.Y., and Delrot, S. (2004). AtOPT6 transports glutathione derivatives and is induced by primisulfuron. Plant Physiol **135,** 1378-1387.

Caillaud, M.-C., Dubreuil, G., Quentin, M., Perfus-Barbeoch, L., Lecomte, P., de Almeida Engler, J., Abad, P., Rosso, M.-N., and Favery, B. (2007) Root-knot nematodes manipulate plant cell functions during a compatible interaction. Journal of Plant Physiol **In Press, Corrected Proof**.

Cairns, N.G., Pasternak, M., Wachter, A., Cobbett, C.S., and Meyer, A.J. (2006). Maturation of *Arabidopsis* seeds is dependent on glutathione biosynthesis within the embryo. Plant Physiol **141,** 446-455.

Campbell, E.J., Schenk, P.M., Kazan, K., Penninckx, I.A.M.A., Anderson, J.P., Maclean, D.J., Cammue, B.P.A., Ebert, P.R., and Manners, J.M. (2003). Pathogen-responsive expression of a putative ATP-binding cassette transporter gene conferring resistance to the diterpenoid sclareol is regulated by multiple defense signaling pathways in *Arabidopsis*. Plant Physiol **133,** 1272-1284.

Casson, S. A., Chilley, P. M., Topping, J. F., Souter, M. A., and Lindsey, K. (2002). The POLARIS gene of *Arabidopsis* encodes a predicted peptide required for correct root growth and leaf vascular patterning. Plant Cell **14**, 1705-1721

Clemens, S. (2000). Molecular mechanisms of plant metal tolerance and homeostasis. Planta. **212**, 475-86.

Chang, S. W., Lee, S. J., and Je, C. H. (2005). Phytoremediation of atrazine by poplar trees: toxicity, uptake, and transformation. J Environ Sci Health B. **40**, 801-811

Chen, A., Komives, E.A., and Schroeder, J.I. (2006). An improved grafting technique for mature *Arabidopsis* plants demonstrates long-distance shoot-to-root transport of phytochelatins in *Arabidopsis*. Plant Physiol **141,** 108-120.

Chen, S., Sanchez-Fernandez, R., Lyver, E.R., Dancis, A., and Rea, P.A. (2007). Functional characterization of AtATM1, AtATM2, and AtATM3, a subfamily of *Arabidopsis* half-molecule ATP-binding cassette transporters implicated in iron homeostasis. J Biol Chem **282,** 21561-21571.

Chiang, C.S., Stacey, G., and Tsay, Y.F. (2004). Mechanisms and functional properties of two peptide transporters, AtPTR2 and fPTR2. J Biol Chem **279,** 30150-30157.

Cobbett, C.S. (2000). Phytochelatins and their roles in heavy metal detoxification. Plant Physiol **123,** 825-832.

Cock, J.M., and McCormick, S. (2001). A large family of genes that share homology with CLAVATA3. Plant Physiol **126,** 939-942.

Curie, C., Alonso, J.M., Le Jean, M., Ecker, J.R., and Briat, J.F. (2000). Involvement of NRAMP1 from *Arabidopsis thaliana* in iron transport. Biochem J **347,** 749-755.

Curie, C., Panaviene, Z., Loulergue, C., Dellaporta, S.L., Briat, J.F., and Walker, E.L. (2001). Maize yellow stripe1 encodes a membrane protein directly involved in Fe(III) uptake. Nature **409,** 346-349.

Darvill, A. G., and Albersheim, P. (1984). Phytoalexins and their elicitors – a defense against microbial infection of plants. Annu. Rev, Plant Physiol. **35**, 243-275

Dautova, M., Rosso, M.N., Abad, P., Gommers, F.J., Bakker, J., and Smant, G. (2001). Single pass cDNA sequencing - a powerful tool to analyse gene expression in preparasitic juveniles of the southern root-knot nematode *Meloidogyne incognita*. Nematology **3,** 129-139.

Davis, E.L., Hussey, R.S., Baum, T.J., Bakker, J., and Schots, A. (2000). Nematode parasitism genes. Annu Rev Phytopathol **38,** 365-396.

Delhaize, E., Kataoka, T., Hebb, D.M., White, R.G., and Ryan, P.R. (2003). Genes encoding proteins of the cation diffusion facilitator family that confer manganese tolerance. Plant Cell **15,** 1131-1142.

Dietrich, D., Hammes, U., Thor, K., Suter-Grotemeyer, M., Fluckiger, R., Slusarenko, A.J., Ward, J.M., and Rentsch, D. (2004). AtPTR1, a plasma

membrane peptide transporter expressed during seed germination and in vascular tissue of *Arabidopsis*. Plant J **40,** 488-499.

Ding, X., Shields, J., Allen, R., and Hussey, R.S. (1998). A secretory cellulose-binding protein cDNA cloned from the root-knot nematode (*Meloidogyne incognita*). Mol Plant Microbe In **11,** 952-959.

Doares, S.H., Syrovets, T., Weiler, E.W., and Ryan, C.A. (1995). Oligogalacturonides and chitosan activate plant defensive genes through the octadecanoid pathway. Proc Natl Acad Sci USA **92,** 4095-4098.

Doyle, E.A., and Lambert, K.N. (2002). Cloning and characterization of an esophageal-gland-specific pectate lyase from the root-knot nematode *Meloidogyne javanica*. Mol Plant Microbe In **15,** 549-556.

Drews, G.N., Lee, D., and Christensen, G.A. (1998). Genetic analysis of female gametophyte development and function. Plant Cell **10,** 5-17.

Drager, D.B., Desbrosses-Fonrouge, A.G., Krach, C., Chardonnens, A.N., Meyer, R.C., Saumitou-Laprade, P., and Kramer, U. (2004). Two genes encoding *Arabidopsis halleri* MTP1 metal transport proteins co-segregate with zinc tolerance and account for high MTP1 transcript levels. Plant J **39,** 425-439.

Dropkin, V. H., Helgeson, J. P., and Upper, C. D. (1969). The hypersensitivity reaction of tomato resistant to *Meloidogyne incognita*: Reversal by cytokinins. J. Nematol. **1**, 55-61.

Faghihi, J., and Ferris, J. M. (2000). An efficient new device to release eggs from *Heterodera glycines*. J. Nematol. **32**, 411-413.

Felsenstein, J. (2000). PHYLIP (Phylogeny Inference Package). University of Washington, Seattle **Ed 3.6.** .

Feys, B.J.F., Benedetti, C.E., Penfold, C.N., and Turner, J.G. (1994). *Arabidopsis* mutants selected for resistance to the phytotoxin coronatine are male-sterile, insensitive to methyl jasmonate, and resistant to a bacterial pathogen. Plant Cell **6,** 751-759.

Fiers, M., Hause, G., Boutilier, K., Casamitjana-Martinez, E., Weijers, D., Offringa, R., van der Geest, L., Campagne, M.V., and Liu, C.M. (2004). Mis-expression of the CLV3/ESR-like gene CLE19 in *Arabidopsis* leads to a consumption of root meristem. Gene **327,** 37-49.

Fiers, M., Golemiec, E., Xu, J., van der Geest, L., Heidstra, R., Stiekema, W., and Liu, C.M. (2005). The 14-amino acid CLV3, CLE19, and CLE40 peptides trigger

consumption of the root meristem in *Arabidopsis* through a CLAVATA2-dependent pathway. Plant Cell **17,** 2542-2553.

Fletcher, J. C., Brand, U., Running, M. P., Simon, R., and Meyerowitz, E. M. (1999). Signaling of cell fate decisions by CLAVATA3 in *Arabidopsis* shoot meristems. Science. **283**, 1911-1914.

Flor, H.H. (1971). Current status of gene-for-gene concept. Annual Review of Phytopathology **9,** 275-296.

Fotopoulos, V., Gilbert, M.J., Pittman, J.K., Marvier, A.C., Buchanan, A.J., Sauer, N., Hall, J.L., and Williams, L.E. (2003). The monosaccharide transporter gene, *AtSTP4*, and the cell-wall invertase, *At beta fruct1*, are induced in *Arabidopsis* during infection with the fungal biotroph *Erysiphe cichoracearum*. Plant Physiol **132,** 821-829.

Frommer, W.B., Hummel, S., and Rentsch, D. (1994). Cloning of an *Arabidopsis* histidine transporting protein related to nitrate and peptide transporters. Febs Lett **347,** 185-189.

Fukuchi, N., Isogai, A., Nakayama, J., Takayama, S., Yamashita, S., K., S., Takemoto, J., and Suzuki, A. (1992). Structure and stereochemistry of three phytotoxins, syringomycin, syringotoxin and syringostatin, produced by *Pseudomonas syringae* pv. *syringae*. J Biol Chem**,** 1149-1157.

Gaedeke, N., Klein, M., Kolukisaoglu, U., Forestier, C., Muller, A., Ansorge, M., Becker, D., Mamnun, Y., Kuchler, K., Schulz, B., Mueller-Roeber, B., and Martinoia, E. (2001). The *Arabidopsis thaliana* ABC transporter AtMRP5 controls root development and stomata movement. Embo J **20,** 1875-1887.

Goellner, M., Smant, G., De Boer, J.M., Baum, T.J., and Davis, E.L. (2000). Isolation of beta-1,4-endoglucanase genes from *Globodera tabacum* and their expression during parasitism. J Nematol **32,** 154-165.

Goellner, M., Wang, X.H., and Davis, E.L. (2001). Endo-beta-1,4-glucanase expression in compatible plant-nematode interactions. Plant Cell **13,** 2241-2255.

Gong, J.M., Lee, D.A., and Schroeder, J.I. (2003). Long-distance root-to-shoot transport of phytochelatins and cadmium in *Arabidopsis*. Proc Natl Acad Sci USA **100,** 10118-10123.

Greulich, F., Yoshihara, T., and Ichihara, A. (1995). Coronatine, a bacterial phytotoxin, acts as a stereospecific analog of jasmonate type signals in tomato cells and potato tissues. Journal of Plant Physiol **147,** 359-366.

Gross, D. C. 1991. Molecular and genetic analysis of toxin production by pathovars of *Pseudomonas syringae*. Annu. Rev. Phytopathol. **29:**247-278

Hall, J. L., and Williams, L. E. (2003). Transition metal transporters in plants. J Exp Bot. **54**, 2601-2613

Hajdukiewicz, P., Svab, Z., and Maliga, P. (1994). The small, versatile Ppzp family of *Agrobacterium* binary vectors for plant transformation. Plant Mol Biol **25,** 989-994.

Hammes, U.Z., Nielsen, E., Honaas, L.A., Taylor, C.G., and Schachtman, D.P. (2006). AtCAT6, a sink-tissue-localized transporter for essential amino acids in *Arabidopsis*. Plant J **48,** 414-426.

Hammes, U.Z., Schachtman, D.P., Berg, R.H., Nielsen, E., Koch, W., McIntyre, L.M., and Taylor, C.G. (2005). Nematode-induced changes of transporter gene expression in *Arabidopsis* roots. Mol Plant Microbe In **18,** 1247-1257.

Hammond, J.P., Bowen, H.C., White, P.J., Mills, V., Pyke, K.A., Baker, A.J.M., Whiting, S.N., May, S.T., and Broadley, M.R. (2006). A comparison of the *Thlaspi caerulescens* and *Thlaspi arvense* shoot transcriptomes. New Phytol **170,** 239-260.

Hauser, M., Donhardt, A.M., Barnes, D., Naider, F., and Becker, J.M. (2000). Enkephalins are transported by a novel eukaryotic peptide uptake system. J Biol Chem **275,** 3037-3041.

Hauser, M., Narita, V., Donhardt, A.M., Naider, F., and Becker, J.M. (2001). Multiplicity and regulation of genes encoding peptide transporters in *Saccharomyces cerevisiae*. Mol Membr Biol **18,** 105-112.

Higgins, C.F., and Payne, J.W. (1977a). Peptide transport by germinating barely embryos. Planta **134,** 205-206.

Higgins, C.F., and Payne, J.W. (1977b). Characterization of active dipeptide transport by germinating barley embryos: effects of pH and metabolic inhibitors. Planta **136,** 71-76.

Higgins, C. F., Payne, J. W. (1978) Peptide transport by germinating barley embryo: uptake of physiological di- and oligopeptides. Planta **138:** 211-216

Higgins, C. F., Payne, J. W. (1982). Plant peptides. *In* D Boulder, B Parthier, eds, Encyclopedia of Plant Physiology, Vol. 14A. Springer Verlag, New York, pp 438-458

Higgins, C.F. (1992). ABC transporters - from microorganisms to man. Annu Rev Cell Biol **8,** 67-113.

Hilpert, B., Bohlmann, H., op den Camp, R., Przybyla, D., Miersch, O., Buchala, A., and Apel, K. (2001). Isolation and characterization of signal transduction mutants of *Arabidopsis thaliana* that constitutively activate the octadecanoid pathway and form necrotic microlesions. Plant J **26,** 435-446.

Hobe, M., Muller, R., Grunewald, M., Brand, U., and Simon, R. (2003). Loss of CLE40, a protein functionally equivalent to the stem cell restricting signal CLV3, enhances root waving in *Arabidopsis*. Dev Genes Evol **213,** 371-381.

Hoffmann, J., and Grundler, F. M. W. (2006). Females and males of root-parasitic cyst nematodes induce different symplasmic connections between their syncytial feeding cells and the phloem in *Arabidopsis thaliana*. Plant Physiol and Biochem. **44**, 430-433.

Hoffmann, J., Krzysztof, W., Andreas, B., and Grundler, F. M. W. (2007). Sucrose supply to nematode-induced syncytia depends on the apoplasmic and symplasmic pathways. J Exp Bot. **58**, 1591-1601.

Hood, E.E., Gelvin, S.B., Melchers, L.S., and Hoekema, A. (1993). New *Agrobacterium* helper plasmids for gene-transfer to plants. Transgenic Res **2,** 208-218.

Hoth, S., Schneidereit, A., Lauterbach, C., Scholz-Starke, J., and Sauer, N. (2005). Nematode infection triggers the de novo formation of unloading phloem that allows macromolecular trafficking of green fluorescent protein into syncytia. Plant Physiol **138,** 383-392.

Howden, R., Goldsbrough, P.B., Andersen, C.R., and Cobbett, C.S. (1995). Cadmium-sensitive, cad1 mutants of *Arabidopsis thaliana* are phytochelatin deficient. Plant Physiol **107,** 1059-1066.

Huang, G.Z., Dong, R.H., Allen, R., Davis, E.L., Baum, T.J., and Hussey, R.S. (2006a). A root-knot nematode secretory peptide functions as a ligand for a plant transcription factor. Mol Plant Microbe In **19,** 463-470.

Huang, G.Z., Allen, R., Davis, E.L., Baum, T.J., and Hussey, R.S. (2006b). Engineering broad root-knot resistance in transgenic plants by RNAi silencing of a conserved and essential root-knot nematode parasitism gene. Proc Natl Acad Sci USA **103,** 14302-14306.

Iacobellis, N., Lavermicocca, I., Simmaco, M., and Ballio, A. (1992). Phytotoxic properties of *Pseudomonas syringae* pv. *syringae* toxins. Physiol of Mol Plant Path **40,** 107-116.

Ichihara, A., Shiraishi, H., Sato, S., Sakamura, K., Nishiyama, R., Sakai, A., Furusaki, A., and Matsumoto, T. (1977). The structure of coronatine. J of Am Chem Soc **99,** 636-637.

Jarosz, A.M., Sheets, M., and Levy, M. (1982). Cuticle thickness in phlox and resistance to powdery mildew: an unreliable line of defense Amer J. Bot. **69**, 824-828.

Jones, H.D. (2005). Wheat transformation: current technology and applications to grain development and composition. J Cereal Sci **41,** 137-147.

Jones, M.G.K. (1981). Host cell responses to endoparasitic nematode attack: structure and function of giant cells and syncytia. Annual Applied Biology **97,** 353-372.

Karim, S., Holmstrom, K.O., Mandal, A., Dahl, P., Hohmann, S., Brader, G., Palva, E.T., and Pirhonen, M. (2007). AtPTR3, a wound-induced peptide transporter needed for defence against virulent bacterial pathogens in *Arabidopsis*. Planta **225,** 1431-1445.

Karim, S., Lundh, D., Holmstrom, K.O., Mandal, A., and Pirhonen, M. (2005). Structural and functional characterization of AtPTR3, a stress-induced peptide transporter of *Arabidopsis*. J Mol Model **11,** 226-236.

Kauss, H., and Jeblick, W. (1995). Pretreatment of parsley suspension-cultures with salicylic-acid enhances spontaneous and elicited production of H_2O_2. Plant Physiol **108,** 1171-1178.

Kauss, H., Theisingerhinkel, E., Mindermann, R., and Conrath, U. (1992). Dichloroisonicotinic and salicylic-acid, inducers of systemic acquired-resistance, enhance fungal elicitor responses in parsley cells. Plant J **2,** 655-660.

Kenyon, J.S., and Turner, J.G. (1992). The stimulation of ethylene synthesis in *Nicotiana tabacum* leaves by the phytotoxin coronatine. Plant Physiol **100,** 219-224.

Kim, D-Y., Bovet, L., Kushnir, S., Noh, E.W., Martinoia, E., and Lee, Y. (2006). AtATM3 is involved in heavy metal resistance in *Arabidopsis*. Plant Physiol **140,** 922-932.

Kim, D-Y., Bovet, L., Maeshima, M., Martinoia, E and Youngsook Lee, Y. (2007) The ABC transporter AtPDR8 is a cadmium extrusion pump conferring heavy metal resistance. Plant J. 50, 207-218.

Kim, M.G., da Cunha, L., McFall, A.J., Belkhadir, Y., DebRoy, S., Dangl, J.L., and Mackey, D. (2005). Two *Pseudomonas syringae* type III effectors inhibit RIM-regulated basal defense in *Arabidopsis*. Cell **121,** 749-759.

Klein, M., Perfus-Barbeoch, L., Frelet, A., Gaedeke, N., Reinhardt, D., Mueller-Roeber, B., Martinoia, E., and Forestier, C. (2003). The plant multidrug resistance ABC transporter AtMRP5 is involved in guard cell hormonal signalling and water use. Plant J **33,** 119-129.

Koh, S., Wiles, A.M., Sharp, J.S., Naider, F.R., Becker, J.M., and Stacey, G. (2002). An oligopeptide transporter gene family in *Arabidopsis*. Plant Physiol **128,** 21-29.

Koenning, S.R., Overstreet, C., Noling J. W., Donald, P.A., Becker, J., and Fortnum, B.A. (1999). Survey of crop losses in response to phytoparasitic nematodes in the United States for 1994. J Nematol **31,** 587-618.

Korenkov, V., Park, S., Sreevidya, C., Morris, J., Hirschi, K., and Wagner, G. (2007). Enhanced Cd-selective root-tonoplast transport in tobaccos expressing *Arabidopsis* cation exchangers. Planta **225,** 403-411.

Krumm, T., Bandemer, K., and Boland, W. (1995). Induction of volatile biosynthesis in the Lima bean (*Phaseolus lunatus*) by leucine and isoleucine conjugates of 1-oxo- and 1-hydroxyindan-4-carboxylic acid: evidence for amino acid conjugates of jasmonic acid as intermediates in the octadecanoid signaling pathway. Febs Lett **377,** 523-529.

Laurie-Berry, N., Joardar, V., Street, I.H., and Kunkel, B.N. (2006). The *Arabidopsis thaliana* JASMONATE INSENSITIVE 1 gene is required for suppression of salicylic acid-dependent defenses during infection by *Pseudomonas syringae*. Mol Plant Microbe In **19,** 789-800.

Lee, Y.H., and Tegeder, M. (2004). Selective expression of a novel high-affinity transport system for acidic and neutral amino acids in the tapetum cells of *Arabidopsis* flowers. Plant J **40,** 60-74.

Lee, D.A., Chen, A., and Schroeder, J.I. (2003). *ars1*, an *Arabidopsis* mutant exhibiting increased tolerance to arsenate and increased phosphate uptake. Plant J **35,** 637-646.

Lee, M., Lee, K., Lee, J., Noh, E.W., and Lee, Y. (2005). AtPDR12 contributes to lead resistance in *Arabidopsis*. Plant Physiol **138,** 827-836.

Li, J., Brader, G., and Palva, E.T. (2004). The WRKY70 transcription factor: A node of convergence for jasmonate-mediated and salicylate-mediated signals in plant defense. Plant Cell **16,** 319-331.

Li, Z.S., Lu, Y.P., Zhen, R.G., Szczypka, M., Thiele, D.J., and Rea, P.A. (1997). A new pathway for vacuolar cadmium sequestration in *Saccharomyces cerevisiae*: YCF1-catalyzed transport of bis(glutathionato)cadmium. Proc Natl Acad Sci USA **94,** 42-47.

Lubkowitz, M.A., Barnes, D., Breslav, M., Burchfield, A., Naider, F., and Becker, J.M. (1998). *Schizosaccharomyces pombe Isp4* encodes a transporter representing a novel family of oligopeptide transporters. Mol Microbiol **28,** 729-741.

Lubkowitz, M.A., Hauser, L., Breslav, M., Naider, F., and Becker, J.M. (1997). An oligopeptide transport gene from *Candida albicans*. Microbiol-Uk **143,** 387-396.

Martinoia, E., Klein, M., Geisler, M., Bovet, L., Forestier, C., Kolukisaoglu, U., Muller-Rober, B., and Schulz, B. (2002). Multifunctionality of plant ABC transporters - more than just detoxifiers. Planta **214,** 345-355.

Martinoia, E., Maeshima, M., and Neuhaus, H. E. (2007). Vacuolar transporters and their essential role in plant metabolism. J Exp Bot. **58**, 83-102.

Matsubayashi, Y., Ogawa, M., Morita, A., and Sakagami, Y. (2002). An LRR receptor kinase involved in perception of a peptide plant hormone, phytosulfokine. Science. **296**, 1470-1472

Matsubayashi, Y., and Sakagami, Y. (1996). Phytosulfokine, sulfated peptides that induce the proliferation of single mesophyll cells of *Asparagus officinalis* L. Proc Natl Acad Sci U S A. 93, 7623-7627

Metraux, J.P., Signer, H., Ryals, J., Ward, E., Wyssbenz, M., Gaudin, J., Raschdorf, K., Schmid, E., Blum, W., and Inverardi, B. (1990). Increase in salicylic-acid at the onset of systemic acquired-resistance in cucumber. Science **250,** 1004-1006.

Meyer, S., Lauterbach, C., Niedermeier, M., Barth, I., Sjolund, R.D., and Sauer, N. (2004). Wounding enhances expression of AtSUC3, a sucrose transporter from *Arabidopsis* sieve elements and sink tissues. Plant Physiol **134,** 684-693.

Miller, A.J., Fan, X.R., Orsel, M., Smith, S.J., and Wells, D.M. (2007). Nitrate transport and signalling. J Exp Bot **58,** 2297-2306.

Mindrinos, M., Katagiri, F., Yu, G. L., and Ausubel, F. M. (1994). The *A.thaliana* disease resistance gene RPS2 encodes a protein containing a nucleotide-binding site and leucine-rich repeats. Cell. **78**, 1089-1099.

Miranda, M., Borisjuk, L., Tewes, A., Dietrich, D., Rentsch, D., Weber, H., and Wobus, U. (2003). Peptide and amino acid transporters are differentially regulated during seed development and germination in faba bean. Plant Physiol **132,** 1950-1960.

Mitchell, R.E. (1976). Isolation and structure of a chlorosis-inducing toxin of *Pseudomonas phaseolicola*. Phytochemistry **15,** 1941-1947.

Mitchell, R.E., and Bieleski, R.L. (1977). Involvement of phaseolotoxin in halo blight of beans. Transport and conversion to functional toxin. Plant Physiol **60,** 723-729.

Muntz, K., Belozersky, M.A., Dunaevsky, Y.E., Schlereth, A., and Tiedemann, J. (2001). Stored proteinases and the initiation of storage protein mobilization in seeds during germination and seedling growth. J Exp Bot **52,** 1741-1752.

Mur, L.A.J., Naylor, G., Warner, S.A.J., Sugars, J.M., White, R.F., and Draper, J. (1996). Salicylic acid potentiates defence gene expression in tissue exhibiting acquired resistance to pathogen attack. Plant J **9,** 559-571.

Murashige, T., and Skoog, F. (1968). A revised medium for rapid growth and bioassays with tobacco tissue culture. Plant Physiol **15,** 473-497.

Nurnberger, T., and Brunner, F. (2002). Innate immunity in plants and animals: emerging parallels between the recognition of general elicitors and pathogen-associated molecular patterns. Current Opin Plant Biol. **5**, 318-324

Olsen, O.A. (2004). Nuclear endosperm development in cereals and *Arabidopsis thaliana*. Plant Cell **16,** S214-S227.

Osawa, H., Stacey, G., and Gassmann, W. (2006). ScOPT1 and AtOPT4 function as proton-coupled oligopeptide transporters with broad but distinct substrate specificities. Biochem J **393,** 267-275.

Orsel, M., Krapp, A., and Daniel-Vedele, F. (2002). Analysis of the NRT2 nitrate transporter family in *Arabidopsis*. Structure and gene expression. Plant Physiol **129,** 886-896.

Ortiz, D.F., Ruscitti, T., Mccue, K.F., and Ow, D.W. (1995). Transport of metal-binding peptides by Hmt1, a fission yeast ABC-type vacuolar membrane-protein. J Biol Chem **270,** 4721-4728.

Palmer, D.A., and Bender, C.L. (1995). Ultrastructure of tomato leaf tissue treated with the pseudomonad phytotoxin coronatine and comparison with methyl jasmonate. Mol Plant Microbe In **8,** 683-692.

Papoyan, A., and Kochian, L.V. (2004). Identification of *Thlaspi caerulescens* genes that may be involved in heavy metal hyperaccumulation and tolerance. Characterization of a novel heavy metal transporting ATPase. Plant Physiol **136,** 3814-3823.

Pearce, G., Strydom, D., Johnson, S., and Ryan, C. A. (1991). A polypeptide from tomato leaves induces wound-inducible proteinase inhibitor proteins. Science. 253, 895-897.

Perry, J.R., Basrai, M.A., Steiner, H.Y., Naider, F., and Becker, J.M. (1994). Isolation and characterization of a *Saccharomyces cerevisiae* peptide-transport gene. Mol Cell Biol **14,** 104-115.

Qu, L.J., and Zhu, Y.X. (2006). Transcription factor families in *Arabidopsis*: major progress and outstanding issues for future research - commentary. Curr Opin Plant Biol **9,** 544-549.

Rea, P.A. (1999). MRP subfamily ABC transporters from plants and yeast. J Exp Bot **50,** 895-913.

Rea, P. A., Li, Z-S., Lu, Y-P., and Drozdowicz, Y. M. (1998). From vacuolar pumps to multispecific ABC transporters. Annu Rev Plant Physiol. **49,** 727-760.

Reinders, A., Schulze, W., Kuhn, C., Barker, L., Schulz, A., Ward, J. M., and Frommer, W. B. (2002). Protein-protein interactions between sucrose transporters of different affinities colocalized in the same enucleate sieve element. Plant Cell. 14, 1567-1577.

Reits, E.A.J., Vos, J.C., Gromme, M., and Neefjes, J. (2000). The major substrates for TAP in vivo are derived from newly synthesized proteins. Nature **404,** 774-778.

Rentsch, D., Laloi, M., Rouhara, I., Schmelzer, E., Delrot, S., and Frommer, W.B. (1995). Ntr1 encodes a high-affinity oligopeptide transporter in *Arabidopsis*. Febs Lett **370,** 264-268.

Rentsch, D., Schmidt, S., and Tegeder, M. (2007). Transporters for uptake and allocation of organic nitrogen compounds in plants. Febs Lett **581,** 2281-2289.

Reuss, O., and Morschhauser, J. (2006). A family of oligopeptide transporters is required for growth of *Candida albicans* on proteins. Mol Microbiol **62,** 916-916.

Rojo, E., Sharma, V.K., Kovaleva, V., Raikhel, N.V., and Fletcher, J.C. (2002). CLV3 is localized to the extracellular space, where it activates the *Arabidopsis* CLAVATA stem cell signaling pathway. Plant Cell **14,** 969-977.

Rosso, M.N., Favery, B., Piotte, C., Arthaud, L., De Boer, J.M., Hussey, R.S., Bakker, J., Baum, T.J., and Abad, P. (1999). Isolation of a cDNA encoding a beta-1,4-endoglucanase in the root-knot nematode *Meloidogyne incognita* and expression analysis during plant parasitism. Mol Plant Microbe In **12,** 585-591.

Rosso, M.G., Li, Y., Strizhov, N., Reiss, B., Dekker, K., and Weisshaar, B. (2003). An *Arabidopsis thaliana* T-DNA mutagenized population (GABI-Kat) for flanking sequence tag-based reverse genetics. Plant Mol Biol **53,** 247-259.

Salt, D.E., and Wagner, G.J. (1993). Cadmium transport across tonoplast of vesicles from oat roots - evidence for a Cd2+/H+ antiport activity. J Biol Chem **268,** 12297-12302.

Salt, D.E., Prince, R.C., Pickering, I.J., and Raskin, I. (1995). Mechanisms of cadmium mobility and accumulation in Indian mustard. Plant Physiol **109,** 1427-1433.

Sambrook, J., Fritsch, E.F., and Maniatis, T.C.S.H.L.P., Plainview, NY), 2nd edition. ((1989)). Molecular Cloning: A laboratory manual. Cold Spring Harbor Lab. Press, Plainview, NY **2nd edition**.

Sanchez-Fernandez, R., Davies, T.G.E., Coleman, J.O.D., and Rea, P.A. (2001). The *Arabidopsis thaliana* ABC protein superfamily, a complete inventory. J Biol Chem **276,** 30231-30244.

Sato, S., Suzuki, H., Widyastuti, U., Hotta, Y., and Tabata, S. (1994). Identification and characterization of genes induced during sexual-differentiation in *Schizosaccharomyces pombe*. Curr Genet **26,** 31-37.

Schaaf, G., Schikora, A., Haberle, J., Vert, G., Ludewig, U., Briat, J.F., Curie, C., and von Wiren, N. (2005). A putative function for the *Arabidopsis* Fe-phytosiderophore transporter homolog AtYSL2 in Fe and Zn homeostasis. Plant Cell Physiol **46,** 762-774.

Schmitt, L., and Tampe, R. (2002). Structure and mechanism of ABC transporters. Current Opinion Structure Biology **12,** 756-760.

Schoof, H., Lenhard, M., Haecker, A., Mayer, K.F.X., Jurgens, G., and Laux, T. (2000). The stem cell population of *Arabidopsis* shoot meristem is maintained by a regulatory loop between the *CLAVATA* and *WUSCHEL* genes. Cell **100,** 635-644.

Sidler, M., Hassa, P., Hasan, S., Ringli, C., and Dudler, R. (1998). Involvement of an ABC transporter in a developmental pathway regulating hypocotyl cell elongation in the light. Plant Cell **10,** 1623-1636.

Smant, G., Stokkermans, J.P.W.G., Yan, Y.T., de Boer, J.M., Baum, T.J., Wang, X.H., Hussey, R.S., Gommers, F.J., Henrissat, B., Davis, E.L., Helder, J., Schots, A., and Bakker, J. (1998). Endogenous cellulases in animals: Isolation of beta-1,4-endoglucanase genes from two species of plant-parasitic cyst nematodes. Proc Natl Acad Sci USA **95,** 4906-4911.

Song, W., Steiner, H.Y., Zhang, L., Naider, F., Stacey, G., and Becker, J.M. (1996). Cloning of a second *Arabidopsis* peptide transport gene. Plant Physiol **110,** 171-178.

Song, W., Koh, S., Czako, M., Marton, L., Drenkard, E., Becker, J.M., and Stacey, G. (1997). Antisense expression of the peptide transport gene *AtPTR2-B* delays flowering and arrests seed development in transgenic *Arabidopsis* plants. Plant Physiol **114,** 927-935.

Stacey, M. G., Patel, A., McClain, W. E., Mathieu, M., Remley, M., Rogers, E. E., Gassmann, W., Blevins, D. G., and Stacey, G. (2007). The *Arabidopsis* AtOPT3 protein functions in metal homeostatis and movement of iron to developing seeds. In press - Plant Physiol.

Stacey, M.G., Koh, S., Becker, J., and Stacey, G. (2002a). AtOPT3, a member of the oligopeptide transporter family, is essential for embryo development in *Arabidopsis*. Plant Cell **14,** 2799-2811.

Stacey, G., Koh, S., Granger, C., and Becker, J. M. (2002b). Peptide transport in plants. Trends Plant Sci. **7**, 257-63

Stacey, M.G., Osawa, H., Patel, A., Gassmann, W., and Stacey, G. (2006). Expression analyses of *Arabidopsis* oligopeptide transporters during seed germination, vegetative growth and reproduction. Planta **223,** 291-305.

Stein, M., Dittgen, J., Sanchez-Rodriguez, C., Hou, B.H., Molina, A., Schulze-Lefert, P., Lipka, V., and Somerville, S. (2006). *Arabidopsis* PEN3/PDR8, an ATP binding cassette transporter, contributes to nonhost resistance to inappropriate pathogens that enter by direct penetration. Plant Cell **18,** 731-746.

Steiner, H.Y., Song, W., Zhang, L., Naider, F., Becker, J.M., and Stacey, G. (1994). An *Arabidopsis* peptide transporter is a member of a new class of membrane-transport proteins. Plant Cell **6,** 1289-1299.

Steiner, H.Y., Naider, F., and Becker, J.M. (1995). The PTR Family - a new group of peptide transporters. Mol Microbiol **16,** 825-834.

Suresh, B., and Ravishankar, G. A. (2004). Phytoremediation – a novel and promising approach for environmental clean-up. Crit Rev Biotechnol. **24**, 97-124

Talke, I.N., Hanikenne, M., and Kramer, U. (2006). Zinc-dependent global transcriptional control, transcriptional deregulation, and higher gene copy number for genes in metal homeostasis of the hyperaccumulator *Arabidopsis halleri*. Plant Physiol **142,** 148-167.

Thompson, J.D., Gibson, T.J., Plewniak, F., Jeanmougin, F., and Higgins, D.G. (1997). The CLUSTAL_X windows interface: flexible strategies for multiple sequence alignment aided by quality analysis tools. Nucleic Acids Res **25,** 4876-4882.

Tommasini, R., Vogt, E., Fromenteau, M., Hortensteiner, S., Matile, P., Amrhein, N., and Martinoia, E. (1998). An ABC-transporter of *Arabidopsis thaliana* has both glutathione-conjugate and chlorophyll catabolite transport activity. Plant J **13,** 773-780.

Tsay, Y.F., Schroeder, J.I., Feldmann, K.A., and Crawford, N.M. (1993). The herbicide sensitivity gene chl1 of *Arabidopsis* encodes a nitrate-inducible nitrate transporter. Cell **72,** 705-713.

Tsay, Y.F., Chiu, C.C., Tsai, C.B., Ho, C.H., and Hsu, P.K. (2007). Nitrate transporters and peptide transporters. Febs Lett **581,** 2290-2300.

Turner, J.G., and Debbage, J.M. (1982). Tabtoxin-induced symptoms are associated with accumulation of ammonia formed during photorespiration. Physiology Plant Pathology **20,** 223-233.

Uppalapati, S.R., Ayoubi, P., Weng, H., Palmer, D.A., Mitchell, R.E., Jones, W., and Bender, C.L. (2005). The phytotoxin coronatine and methyl jasmonate impact multiple phytohormone pathways in tomato. Plant J **42,** 201-217.

van de Mortel, J.E., Villanueva, L.A., Schat, H., Kwekkeboom, J., Coughlan, S., Moerland, P.D., van Themaat, E.V.L., Koornneef, M., and Aarts, M.G.M. (2006). Large expression differences in genes for iron and zinc homeostasis, stress response, and lignin biosynthesis distinguish roots of *Arabidopsis thaliana* and the related metal hyperaccumulator *Thlaspi caerulescens*. Plant Physiol **142,** 1127-1147.

Vanholme, B., De Meutter, J., Tytgat, T., Van Montagu, M., Coomans, A., and Gheysen, G. (2004). Secretions of plant-parasitic nematodes: a molecular update. Gene **332,** 13-27.

Vatamaniuk, O.K., Mari, S., Lu, Y.P., and Rea, P.A. (1999). AtPCS1, a phytochelatin synthase from *Arabidopsis*: Isolation and in vitro reconstitution. Proc Natl Acad Sci USA **96,** 7110-7115.

Verret, F., Gravot, A., Auroy, P., Leonhardt, N., David, P., Nussaume, L., Vavasseur, A., and Richaud, P. (2004). Overexpression of AtHMA4 enhances root-to-shoot translocation of zinc and cadmium and plant metal tolerance. Febs Lett **576,** 306-312.

Wang, X.H., Mitchum, M.G., Gao, B.L., Li, C.Y., Diab, H., Baum, T.J., Hussey, R.S., and Davis, E.L. (2005). A parasitism gene from a plant-parasitic nematode with function similar to CLAVATA3/ESR (CLE) of *Arabidopsis thaliana*. Mol Plant Pathol **6,** 187-191.

Wasternack, C., and Parthier, B. (1997). Jasmonate signalled plant gene expression. Trends Plant Sci **2,** 302-307.

Waterworth, W.M., West, C.E., and Bray, C.M. (2000). The barley scutellar peptide transporter: biochemical characterization and localization to the plasma membrane. J Exp Bot **51,** 1201-1209.

Waterworth, W.M., Ashley, M.K., West, C.E., Sunderland, P.A., and Bray, C.M. (2005). A role for phosphorylation in the regulation of the barley scutellar peptide transporter HvPTR1 by amino acids. J Exp Bot **56,** 1545-1552.

Weber, M., Harada, E., Vess, C., von Roepenack-Lahaye, E., and Clemens, S. (2004). Comparative microarray analysis of Arabidopsis thaliana and *Arabidopsis halleri* roots identifies nicotianamine synthase, a ZIP transporter and other genes as potential metal hyperaccumulation factors. Plant J **37,** 269-281.

Weinberg, M.V., and Maier, R.J. (2007). Peptide transport in *Helicobacter pylori*: Roles of dpp and opp systems and evidence for additional peptide transporters. J Bacteriol **189,** 3392-3402.

Weise, S.E., Schrader, S.M., Kleinbeck, K.R., and Sharkey, T.D. (2006). Carbon balance and circadian regulation of hydrolytic and phosphorolytic breakdown of transitory starch. Plant Physiol **141,** 879-886.

West, C.E., Waterworth, W.M., Stephens, S.M., Smith, C.P., and Bray, C.M. (1998). Cloning and functional characterization of a peptide transporter expressed in the scutellum of barley grain during the early stages of germination. Plant J **15,** 221-229.

Wiggers, R.J., Starr, J.L., and Price, H.J. (1990). DNA content and variation in chromosome number in plant cells affected by *Meloidogyne incognita* and *M. Arenaria*. Phytopathology **80,** 1391-1395.

Williamson, V. M., and Gleason, C. A. (2003). Plant-nematode interactions. Curr Opin Plant Biol. **6**, 327-333.

Wintz, H., Fox, T., Wu, Y.Y., Feng, V., Chen, W.Q., Chang, H.S., Zhu, T., and Vulpe, C. (2003). Expression profiles of *Arabidopsis thaliana* in mineral deficiencies reveal novel transporters involved in metal homeostasis. J Biol Chem **278,** 47644-47653.

Yen, M.R., Tseng, Y.H., and Saier, M.H. (2001). Maize Yellow Stripe1, an iron-phytosiderophore uptake transporter, is a member of the oligopeptide transporter (OPT) family. Microbiol **147,** 2881-2883.

Yeung, A.K., Basu, S.K., Wu, S.K., Chu, C., Okamoto, C.T., Hamm-Alvarez, S.F., von Grafenstein, H., Shen, W.C., Kim, K.J., Bolger, M.B., Haworth, I.S., Ann, D.K., and Lee, V.H.L. (1998). Molecular identification of a role for tyrosine 167 in the function of the human intestinal proton-coupled dipeptide transporter (hPepT1). Biochem Bioph Res Co **250,** 103-107.

Yu, B., Wakao, S., Fan, J., and Benning, C. (2004). Loss of plastidic lysophosphatidic acid acyltransferase causes embryo-lethality in *Arabidopsis*. Plant Cell Physiol. **45,** 503-510.

Zhang, M.Y., Bourbouloux, A., Cagnac, O., Srikanth, C.V., Rentsch, D., Bachhawat, A.K., and Delrot, S. (2004). A novel family of transporters mediating the transport of glutathione derivatives in plants. Plant Physiol **134,** 482-491.

Zimmerli, L., Jakab, G., Metraux, J. P., and Mauch-Mani, B. (2000). Potentiation of pathogen-specific defense mechanisms in *Arabidopsis* by beta-aminobutyric acid. Proc Natl Acad Aci U S A. **97**, 12920-12925.

Zmasek, C.M., and Eddy, S.R. (2001). ATV: display and manipulation of annotated phylogenetic trees. Bioinformatics **17,** 383-384.

VITA

Ami Patel was born on Dec 5th in Baroda, India. She is one of the three children of Sharda and Jash Patel and she currently lives in Columbia, Missouri with husband Akshay Patel and son Krishang Patel.

She graduated from Sardar Patel University with B.Sc in Microbiology (Major) and Music (Minor) in 1997 with cum Laude. She completed her M.Sc in Microbiology in 1999 and joined Alembic Pharmaceutical Inc, as a Research Associate. She came to United States in Jan 2000 to Clemson University and completed her MS in Microbiology and Molecular Medicine in June 2002. She joined University of Missouri-Columbia in Dr. Gary Stacey's lab in June 2002 and finished her doctorate degree in Dec 2007 in Plant Microbiology and Pathology.

Her hobbies include canoeing, hiking and biking. She loves to go camping in her free time. She will join as a post-doctorate in Dr. Debra Anderson's lab at University of Missouri-Columbia and work in bacterial pathogenesis. She plans to continue her career in microbial pathogenesis for some time and later move into finance field in biotechnology industry.